**University of South-Eastern Norway**
Faculty of Technology, Natural Sciences and Maritime Studies
—
Doctoral dissertation no. 56
**2020**

Fasil Ayelegn Tassew

# Capabilities of anaerobic granular sludge bed process for the treatment of particle-rich substrates

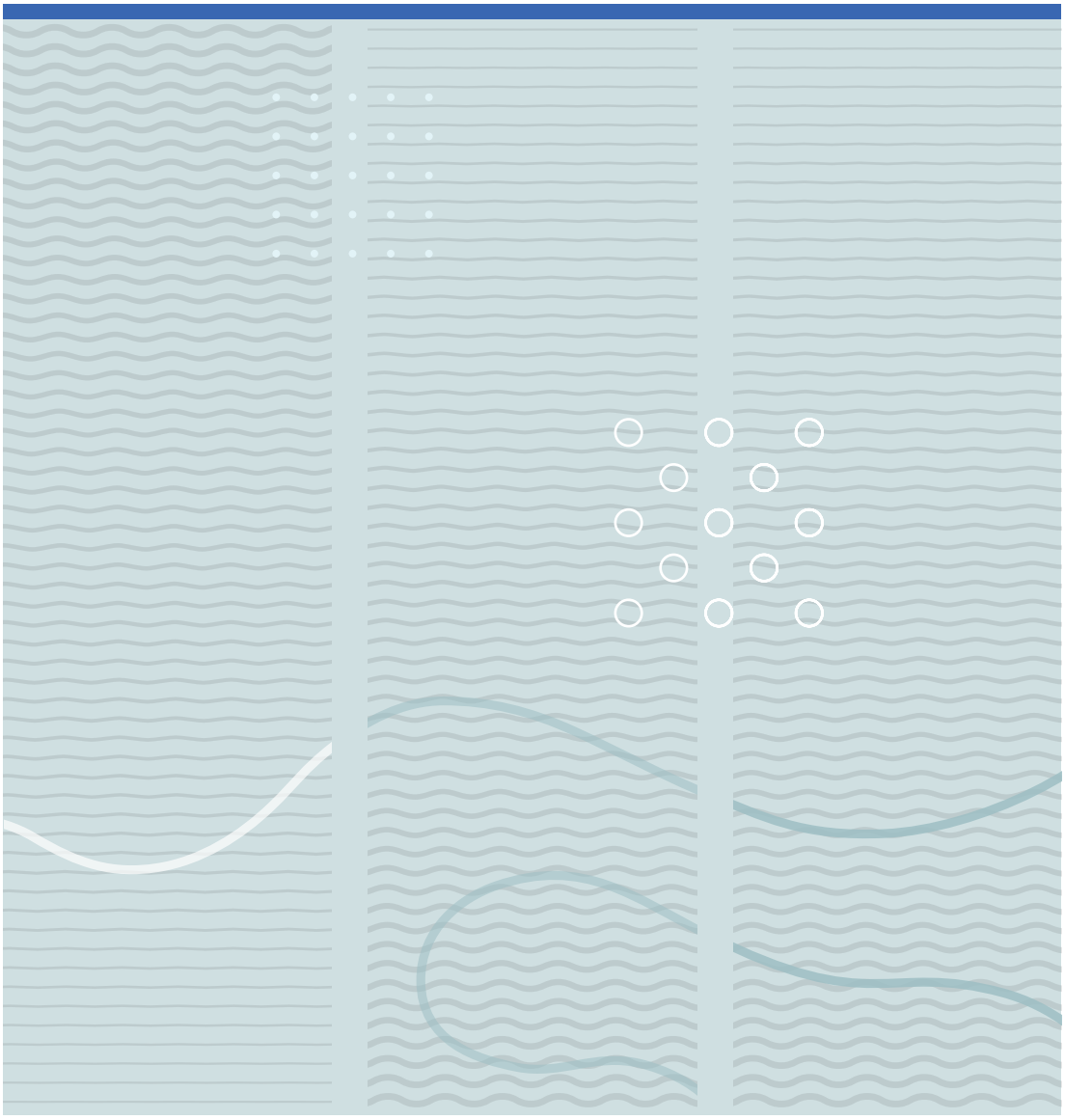

Fasil Ayelegn Tassew

# Capabilities of anaerobic granular sludge bed process for the treatment of particle-rich substrates

A PhD dissertation in
**Process, Energy and Automation Engineering**

© 2020 Fasil Ayelegn Tassew
Faculty of Technology, Natural Sciences and Maritime Studies
University of South-Eastern Norway
Porsgrunn, 2020

**Doctoral dissertations at the University of South-Eastern Norway no. 56**

ISSN: 2535-5244 (print)
ISSN: 2535-5252 (online)

ISBN: 978-82-7206-542-2 (print)
ISBN: 978-82-7206-543-9 (online)


This publication is, except otherwise stated, licenced under Creative Commons. You may copy and redistribute the material in any medium or format. You must give appropriate credit provide a link to the license, and indicate if changes were made.
http://creativecommons.org/licenses/by-nc-sa/4.0/deed.en

Print: University of South-Eastern Norway

# Preface

I wrote this dissertation in partial fulfilment of the requirements for the degree of Doctor of Philosophy in Process, Energy and Automation Engineering at the University of South-Eastern Norway (USN). I have carried out the PhD project at USN Porsgrunn campus from January 2016 to December 2019. My main supervisor was professor Rune Bakke and co-supervisor was associate professor Wenche Hennie Bergland. The PhD was funded through Biogas2020 project under the European regional development fund. Partial contribution was obtained from the Norwegian research council's Bærekraftig biogass, EnergiX project. Laboratory works that resulted in published articles were carried out at USN laboratories at the Department of process, energy and environmental technology. Experimental works related to pilot biogas reactor was carried out at Bjorkedalen pilot reactor at a farm in Porsgrunn. As part of the PhD project, I also attended courses with a total of 31 ECTS.

- Water Treatment and Environmental Biotechnology (EET2110), USN
- Matrix Methods (D0308), USN
- Production and application of biogas (D0116), (Perolofgården, Sweden)
- Theory of Science and Ethics (D0611), USN (Lesvos, Greece)
- Advanced Biofilm Course (Karlsruher Institut für Technologie, Germany)
- Advanced Course Environmental Biotechnology
  (Technische Universiteit Delft, the Netherlands)
- Anaerobic Digestion for the Production of Biogas and Biochemicals
  (Aalborg Universitet, Denmark)

This dissertation is organised into five chapters where introduction, literature review, methods used, results and conclusions are discussed followed by a presentation of references used in those chapters. Published as well as submitted articles and conference presentations are provided as attachments. In the appendix section, Matlab codes used during image processing are provided.

Fasil Ayelegn Tassew

Porsgrunn, September 2019.

# Acknowledgements

First and foremost, I would like to thank my main supervisor professor Rune Bakke for his invaluable support and supervision throughout this project. I am very grateful for the opportunities I was provided and the advice and support I was given. I would also like to thank co-supervisor associate professor Wenche Hennie Bergland for her contribution and supervision. I want to extend a special thanks to associate professor Carlos Dinamarca for his advice, contribution and insightful comments.

I would like to thank Dr Eshetu Janka who has been very supportive and friendly throughout the PhD project. I will never forget the amazing discussions we always had during lunchtimes at work as well as outside of work. Fellow PhD candidates: Samee, Anirudh, and many more thank you for all the memorable and fun times we have had.

Finally, thank you to my parents Ayelegn Tassew (Gashe) and Yeshi Teshager (Eyiwa) who have been unbelievably supportive and understanding. In addition, thank you to my sisters Frehiwot and Tanawork and my brothers Samuel and Kidus, I miss you every day and I am looking forward to seeing you again.

# Abstract

High-rate anaerobic reactors have qualities that make them more attractive for anaerobic digestion of organic substrates compared to traditional reactors such as Continuous Stirred Tank Reactor (CSTR). These qualities include high organic loading rate (OLR), short hydraulic retention time (HRT) and efficient conversion of organic matter into biogas. However, their use has been largely restricted to organic wastes that are low in suspended solids. Application of high-rate granular sludge bed reactors to particle-rich substrates is limited due to problems that stem from slow particle disintegration and solid accumulation. Since some of the largest renewable biomass resources are particle-rich, it is important to find remedies to the slow particle disintegration and solid accumulation so that such resources can be efficiently utilized in high-rate reactors and transformed into a source of renewable energy. In order to accomplish this, a thorough understanding of the interaction of granular sludge bed with particles is essential.

A review of the current state of application of granular sludge beds for anaerobic digestion of particle-rich substrates was carried out in order to establish how and to what extent substrate particles influence granular sludge beds and vice versa. It was found that successful high-rate digestion of particle-rich substrates with solid contents as high as 35% was possible in dry anaerobic digestion processes but in conventional high-rate reactors such as UASB, the TS limit seemed to be around 10%. Pretreatment of substrates has been used to improve the anaerobic digestion process. Economically sustainable methods of pretreatment are, however, limited. Several methods have been tried to improve the disintegration and hydrolysis of solid particulates with varying degree of success. Enzymatic pretreatment and co-digestion are often used. In addition, various reactor modifications have been implemented to deal with the increased solid accumulation associated with particle-rich substrates. Factors that affect disintegration and hydrolysis of particulates were investigated along with the kinetics used to model them. When the solid particulates contain recalcitrant lignocellulosic compounds, it is advantageous to classify them into easily and slowly disintegrating fractions.

The success of high-rate reactors depends on the formation and sustenance of granular sludge with high settling characteristics so that they resist being washed out of the

reactor. The settling characteristic of granules is crucial and needs to be monitored regularly. In this dissertation, settling velocity and size distribution of granules were studied using image analysis and settling column experiments with the aim to establish a method that uses image data generated using Matlab as a tool to determine the theoretical (calculated) size distribution and settling velocity of granules and compare them with experimental values. Comparable theoretical and experimental mean settling velocity values were obtained. Settling velocities increased with Reynolds number (Re). Significant size differences were found in granules collected at different heights of the lab-scale reactor.

Particle disintegration was studied in batch anaerobic reactors at 35 °C using particle-rich substrate from manure supernatant. Two types of samples were applied, one high in suspended particles and another low in suspended particle content. Both feeds were digested with and without cellulase enzyme addition to obtain a better understanding of particle degradation mechanisms, kinetics and stoichiometry. Higher biomethane potential was found in the substrates with high–particle content but with a lower conversion rate. The addition of cellulase increased biomethane production rates in both high– and low–particle content samples enhancing yield by 54% and 40%, respectively and converting 69% and 87% of feed chemical oxygen demand (COD), respectively. Disintegration was modelled by classifying the solid particulates into fast and slow disintegrating fractions resulting in a good fit between experimental and simulated values. Particle disintegration was also studied in continuous reactors at 25–35 °C.

Particulate contents ranging from 3.0–9.4 gTSS/L were fed into a 1.3 L lab-scale up-flow anaerobic sludge bed reactor (UASB). Biogas production was monitored while changing the temperature and particle content of the substrates. Biogas production increased with temperature in both high and low particle content substrates, however, the temperature effect was strongest on the high–particle substrate. Both the high– and low–particle samples produced a comparable amount of biogas at 25 °C, suggesting that biogas at this temperature came mainly from the digestion of small particles and soluble components present in similar quantities in both substrates. At 35 °C, the high–particle sample showed significantly higher biogas production than the low–particle sample,

which was attributed to increased (temperature-dependent) disintegration of larger solid particulates. Simulation of disintegration was carried out using a similar scheme as in the batch reactors. Classifying the solid particulates into fast and slow disintegrating fractions resulted in comparable results between the simulated and experimental values.

Keywords: Particle-rich substrate; Disintegration; Hydrolysis; Settling velocity; Temperature; Biogas;

# List of papers

## Article 1

Tassew, F.A., Bergland, W.H., Dinamarca, C. and Bakke, R., 2019. Settling velocity and size distribution measurement of anaerobic granular sludge using microscopic image analysis. Journal of microbiological methods, 159, pp.81–90. https://doi.org/10.1016/j.mimet.2019.02.013

## Article 2

Tassew FA, Bergland WH, Dinamarca C, Kommedal R, Bakke R. Granular sludge bed processes in anaerobic digestion of particle-rich substrates. *Energies*. 2019; 12(15):2940. https://doi.org/10.3390/en12152940

## Article 3

Tassew FA, Bergland WH, Dinamarca C, Bakke R. Effect of Particulate Disintegration on Biomethane Potential of Particle-rich Substrates in Batch Anaerobic Reactor. *Applied Sciences*. 2019; 9(14):2880. https://doi.org/10.3390/app9142880

## Article 4

Tassew FA, Bergland WH, Dinamarca C, Bakke R. Influences of temperature and feed particle content on granular sludge bed anaerobic digestion. Submitted to the journal: Biomass and bioenergy.

## Conference poster

Tassew F.A, Bergland W.H, Dinamarca C, Bakke R. Image analysis to measure settling characteristics of granular sludge. Presented to Granular sludge conference, IWA Biofilms specialist group, Delft, Netherlands (2018)

# Abbreviations and nomenclature

ABR – Anaerobic Baffled Reactor

ACP – Anaerobic Contact Process

AD – Anaerobic Digestion

ADM1 – Anaerobic Digestion Model No.1

ADP – Adenosine Diphosphate

AF – Anaerobic Filter

AMP – Adenosine Monophosphate

AMPTS – Automatic Methane Potential Test System

APHA – American Public Health Association

ATP – Adenosine Triphosphate

C – Elemental Carbon

C/N – Carbon to Nitrogen ratio

$C_2H_4O_2$ – Average Chemical Composition of Volatile Fatty Acids

$C_{57}H_{104}O_6$ – Average Chemical Composition of Lipids

$C_5H_7O_2N$ – Average Chemical Composition of Proteins

$C_6H_{10}O_5$ – Average Chemical Composition of Carbohydrates

$C_6H_{10}O_5$ – Average Chemical Composition of Lignins

Cd – Cadmium

CF – Centrifuged Feed

$CH_4$ – Methane

Co – Cobalt

$CO_2$ – Carbon dioxide

COD – Chemical Oxygen Demand

CSTR – Continuous Stirred Tank Reactor

EGSB – Expanded Granular Sludge Bed

EPS – Extracellular Polymeric Substances

FAO – Food And Agriculture Organization

Fe – Iron

FISH – Fluorescence Insitu Hybridization

GC–FID – Gas Chromatography Flame Ionization Detector

$H_2$ – Hydrogen

$H_2O$ – Water

$H_2S$ – Hydrogen sulfide

HLR– Hydraulic Loading Rate

HRT – Hydraulic Retention Time

LCFA – Long Chain Fatty Acids

MF – Milled Feed

N – Elemental nitrogen

$NH_3$ – Ammonia gas

$NH_4^+$ – Ammonium ion

Ni – Nickel

$O_2$ – Oxygen gas

OFMSW – Organic Fraction Of Municipal Solid Waste

OLR – Organic Loading Rate

P – Phosphorus

PF – Pumped Feed

pH – Hydrogen ion concentration

POME – Palm Oil Mill Effluent

Re – Reynolds number

RF – Raw Feed

RPM – Revolution Per Minute

S – Sulfur

SRT – Sludge Retention Time

TS – Total Solids

TSS – Total Suspended Solids

UASB – Upflow Anaerobic Sludge Blanket

UASR – Upflow Anaerobic Solid Removal

VFA – Volatile Fatty Acids

VS – Volatile Solids

VSS – Volatile Suspended Solids

Zn – Zink

$ZrO_2$ – Zirconium Oxide

# Table of contents

# 1 Introduction

In this chapter, an introductory overview of anaerobic digestion as a biochemical process is provided. Factors that affect its applications are laid out and discussed. Common examples of high-rate reactors and challenges associated with them, specifically for particle-rich substrates, are provided. The chapter concludes by setting the objectives, approaches and scopes of the dissertation.

## 1.1 Background

Global energy consumption has been heavily dependent on fossil fuels for the past century. However, fossil fuels are limited resources that are projected to be depleted in the coming decades [1]. An alarming increase in atmospheric $CO_2$ concentration due to the use of fossil fuels is causing climate change whose catastrophic effects are being felt across the world [2]. In addition, rapid population growth and improved living conditions across the world increase the demand for energy considerably. Governments and various interest groups are focused on finding alternative energy sources that are renewable and environmentally friendly. An energy resource is considered renewable if it is harnessed from natural processes that are replenished continually such as by sunshine and wind [3]. Most renewable energy resources come from the sun directly or indirectly. Solar energy technologies such as Photovoltaic solar panels directly use sunlight to generate renewable energy. Wind energy, hydropower, and biomass energy are examples of renewable energies that come indirectly from the sun. New and efficient technologies that made it possible to harness various alternative energy sources have been developed over the years. Solar energy technologies have been using solar energy to convert sunlight into electricity [4]. Wind energy is also being used to generate electricity through wind turbines [5]. A large number of hydropower dams are being built across the developing world in addition to the already large number of hydropower dams found in the developed world [6]. Biofuels such as biodiesel, bioethanol, and biogas are being produced from biomass through various processes [7]. Global renewable energy consumption is growing rapidly (Figure 1.1) however so there is still a long way to go to end fossil fuel dependence. According to a report by REN21

[8] (Renewables 2018 global status report), as of 2016, the global renewable energy consumption accounts for 18.2% of the global energy consumption. Relatively high cost and technological limitations contribute to the low share of renewables in the energy market.

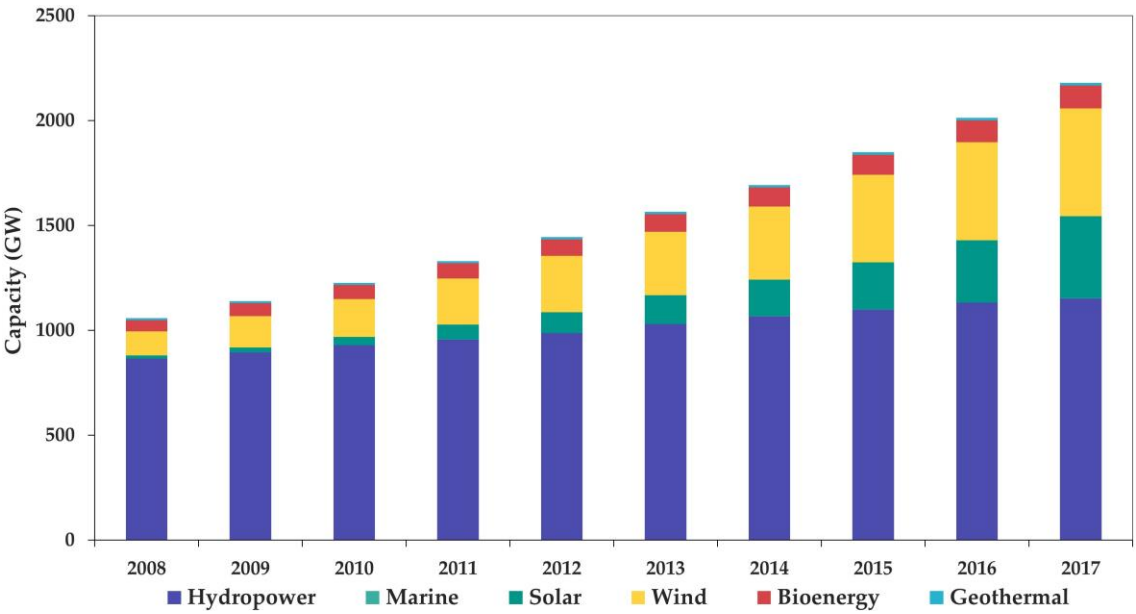


**Figure 1.1: Global increase in renewable energy capacity in the last decade** [9]**.**

Biomass is one of the most promising and abundantly available renewable energy resources on earth. The food and agriculture organization of the United Nations, FAO, defines biomass as "Material of biological origin excluding material embedded in geological formations and transformed to fossil" [10]. The energy recovered from biomass is called bioenergy. Bioenergy is considered renewable because the energy contained in the biomass is harvested from the sun through the process of photosynthesis [11]. There are different kinds of biomass that are composed of various proportions of carbohydrates, proteins, and lipids. The largest source of biomass is forest wood, which is rich in carbohydrates such as cellulose, hemicellulose, and lignin. Other sources of biomass such as energy crops tend to contain higher proportions of proteins and lipids. Most of the biomass that is used for bioenergy recovery come from forestry, agricultural residues, waste, energy crops, parks and gardens, and industry. Conversion of biomass into bioenergy has been going on since humans discovered fire. Solid biomass such as wood and solid wastes are burned to generate heat energy. A large part

of the world still uses this method to heat houses, cook food and carry out other activities. Modern biomass–to–bioenergy conversion technologies are wide-ranging but they are classified into two broad categories called thermochemical and biochemical processes [12]. Thermochemical processes include combustion, gasification and pyrolysis whereas biochemical processes include fermentation, mechanical extraction, and anaerobic digestion. A significant section of biomass is produced because of human activity. Industrial, domestic, agricultural, leisure and other human activities produce a vast amount of wastewater that contains an array of biodegradable organic compounds, of which, only a small part is being utilised to recover renewable energy [13]. This shows that there is a huge potential for renewable energy in wastewater treatment. If the right treatment is used, not only does it contribute to the need for renewable energy but also contributes to environmentally friendly waste management. Whether humans are involved or not, natural decomposition of organic compounds occurs. When the decomposition is carried out in an environment where there is oxygen, it is aerobic decomposition; in the absence of oxygen, the decomposition is anaerobic and produces a mixture of gases. The main product of anaerobic decomposition is $CH_4$, which is a potent greenhouse gas but also an energy carrier (Eq. 1). The need for wastewater treatment and resource recovery is paramount considering that $CH_4$ emission from untreated wastewater contributes nearly 500 million tons of $CO_2$ equivalent to the global emission of greenhouse gases [14]. With increasing consciousness for resource recovery and environmental friendliness, governments and interest groups are noticing the potential of renewable energy from anaerobic treatment of wastewater, resulting in a rapid increase in installation of anaerobic treatment plants across the world. The energy economy of methane produced by anaerobic treatment of wastewater indicates that sustainable renewable energy recovery is possible.

$$CH_4 + 2O_2 \rightarrow CO_2 + 2H_2O \quad (1)$$

$\Delta H$ = –890 kJ/mol $CH_4$ = 39.7 kJ/L $CH_4$ (at standard conditions)

1kJ = 2.78 x $10^{-4}$ kWh

1 $m^3$ $CH_4$ = 11 kWh

Recoverable energy from biogas (assuming 65% $CH_4$ in biogas) = 7.2 kWh/$m^3$ biogas

The recovered energy is used for heating, electricity and combined heat and power. A more advanced way of using the recovered energy is to upgrade the $CH_4$ content above 95% and inject it into natural gas grids. Upgraded and liquified biogas is also being used as a transportation fuel. The number of vehicles that operate on compressed/liquified biogas is increasing.

### 1.1.1 Overview of Anaerobic digestion process

Anaerobic digestion (AD) is a biochemical process that is carried out by microorganisms in the absence of oxygen. During anaerobic digestion, organic compounds are broken down into simple molecules of $CH_4$ and $CO_2$. However, small amounts of $H_2S$, $H_2O$, and other trace gases are also produced. The produced gases are collectively called Biogas. Microorganisms need a source of carbon and energy for maintenance and reproduction. They obtain carbon source and energy through anaerobic oxidation of organic compounds. In order to achieve this, microorganisms are evolved to be capable of metabolizing a wide range of organic compounds resulting in a complex set of biochemical reactions that are generally grouped into disintegration, hydrolysis, acidogenesis, acetogenesis and methanogenesis steps [15]. Organic compounds (substrates) must be in a soluble form to be taken in and metabolised intracellularly by microorganisms. Prior to intracellular metabolism, extracellular conversion of organic compounds into soluble forms must take place [15]. This is carried out by the disintegration and hydrolysis steps. During disintegration, macromolecules such as carbohydrates, proteins, and lipids are released from a complex composite form of substrates. Disintegration also produces soluble and particulate forms of inert compounds that are not possible to hydrolyse. Disintegration is sometimes lumped together with Hydrolysis and other times it is altogether overlooked, but it is nevertheless an important step of anaerobic digestion. Hydrolysis of the macromolecules follows disintegration. During hydrolysis, extracellular enzymes secreted by microorganisms are used to hydrolyse and produce soluble forms of the

macromolecules. Carbohydrates are converted into simple sugars, proteins are converted to amino acids and lipids are converted to long-chain fatty acids (LCFA).

After hydrolysis, the soluble compounds are taken inside microbial cells and undergo further breakdown. What follows is the acidogenesis step where the soluble compounds are transformed into organic acids by acidogenetic bacteria. The organic acids are collectively called volatile fatty acids (VFA), which are comprised mainly of acetic, butyric and propionic acids. $CO_2$ and $H_2$ are also produced during the acidogenesis step. Acetic acid formed during acidogenesis is a substrate for methanogenesis and proceeds directly to the methanogenesis step but other organic acids undergo additional step called acetogenesis. Acetogenesis is carried out by acetogens which are obligate anaerobic bacteria that use the acetyl-CoA pathway to produce acetate through $CO_2$ reduction [16]. The last step is methanogenesis which is carried out by archaea, not bacteria. Archaea generally have a slower growth rate than bacteria. During methanogenesis, $CH_4$ is produced through two pathways by different types of archaea. The first one, known as aceticlastic methanogenesis, is carried out by heterotrophic organisms that use acetic acid to produce $CH_4$ and $CO_2$. Whereas the second pathway is called hydrogenotropic methanogenesis and is performed by autotrophic organisms that use $CO_2$ and $H_2$ to produce $CH_4$. The rate-limiting step of anaerobic digestion process varies depending on the nature of the substrate used. For substrates with high particle content, disintegration and hydrolysis are considered rate-limiting, whereas, in substrates where soluble compounds dominate, methanogenesis is often the rate-limiting step. The above-described set of AD reactions are illustrated in Figure 1.2. Biochemical reactions carried out during anaerobic oxidation of organic compounds must be exergonic in order to maintain life and reproduction of microorganisms. Exergonic reactions have a negative Gibbs free energy i.e. the reaction results in a net release of free energy that is used by microorganisms [17]. Microbial cells store the energy in the form of Adenosine Triphosphate (ATP). ATP contains high–energy phosphoanhydride bonds that are used to "fuel" maintenance of the microbe and new cell formation which is an energy-intensive anabolic process. When ATP is used, it is converted to Adenosine Diphosphate (ADP) or Adenosine Monophosphate (AMP).

Conversely, when an organic compound is broken down by microorganisms, the net free energy is used to convert ADP to ATP in a process known as ADP phosphorylation.

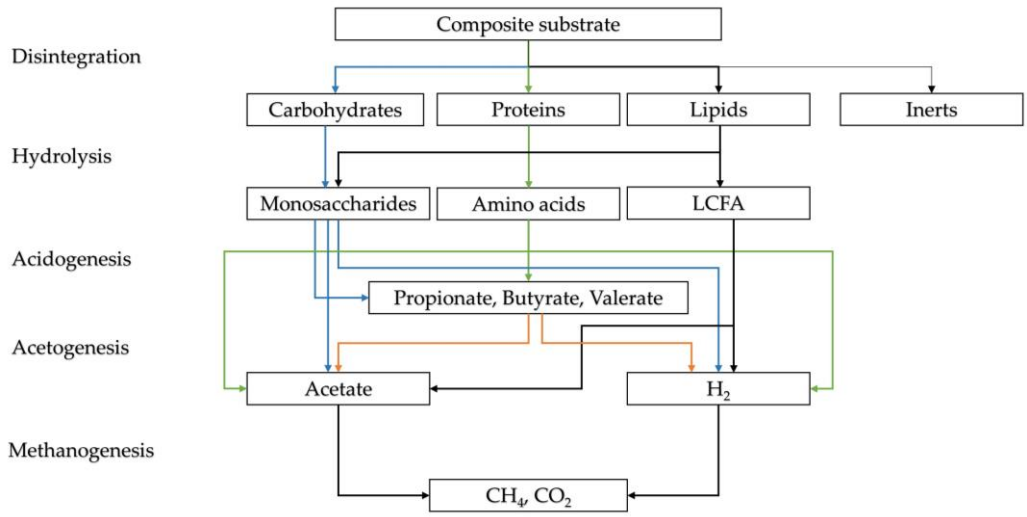


**Figure 1.2: Biochemical reactions and steps in anaerobic digestion process (adapted from Batstone et al. (2002) [15])**

## 1.1.2 Factors affecting anaerobic digestion

Anaerobic digestion is affected by several physical, biochemical and operational factors. The temperature in which anaerobic digestion is carried out is one of the most important factors to consider. Anaerobic reactions that produce methane are known to take place at widely varying temperatures in nature [18]. Anaerobic digestion is classified as psychrophilic (< 20 °C), mesophilic (20–42 °C), thermophilic (42–60 °C) and hyperthermophilic (< 60 °C) based on the temperature in which the digestion takes place (see Article 4). The influence of temperature on anaerobic digestion is extensive. It affects various aspects of the digestion process including microbial growth, nutrient uptake, gas solubility, chemical equilibriums and enzymatic activity. Optimum growth and metabolic rates of microorganisms are achieved in a specific temperature range. Deviation from this temperature may result in disturbance of microbial composition and adaptation to the new temperature can take long time. Microorganisms with faster growth rates such as acidogens adapt to temperature changes relatively faster than slow growers like methanogens. Temperature has a direct and indirect influence on the

availability of nutrients to microorganisms. The rate of hydrolysis of complex particulates depends on temperature. Higher temperature generally leads to faster hydrolysis and relative abundance of nutrients (both macro and micro). Many Biochemical reactions that take place during anaerobic digestion are catalysed by enzymes whose activity are highly dependent on temperature.

In anaerobic reactors, physical factors such as hydraulic retention time (HRT) and organic loading rate (OLR) have influences on the digestion process. Hydraulic retention time is the average time the feed liquid phase remains in an anaerobic reactor, whereas organic loading rate is the amount of organic substrate added per unit volume of the reactor per day (kg $m^{-3}$ $d^{-1}$). It is assumed that the longer a substrate stays in a reactor the higher the probability of digestion, as a result, longer HRT is associated with more extensive digestion. HRT of AD varies depending on the nature of substrates, type of reactor, the temperature of digestion and other factors. HRT values range from over a hundred days such as in floating drum and fixed dome reactors (used in households in developing countries) to a few hours in modern high-rate reactors [19]. OLR of the reactor is an important factor as it is linked to the stability of the digestion process. The right OLR has to be maintained in order to maintain a stable process. If excess organics are loaded especially those that are easily degradable, there is a risk of accumulation of volatile fatty acids which can lead to process inhibition directly or through pH drop. Appropriate OLR values vary depending on factors such as feed composition, temperature, reactor volume, reactor type, etc. Traditional low-rate reactors have, by definition, low OLR (2–3 kgVS $m^{-3}$ $d^{-1}$ ) whereas high-rate reactors are capable of loading rates up to 40 kg $m^{-3}$ $d^{-1}$ [20][21] or more [22].

The organic composition of the substrates is also an important factor in anaerobic digestion. Anaerobic microorganisms require balanced nutrients to grow and reproduce. Macronutrients (carbohydrate, protein, and lipid), micronutrients such as trace metals (Fe, Co, Ni), P, N, and vitamins are required. Nutrient balance is usually assessed as a ratio of the total mass of carbon (g) and nitrogen (g) in the substrate (C/N ratio). Low C/N ratios of substrates such as manure are known to sometimes lead to ammonia inhibition. Whereas, high C/N ratios of substrates such as rice straw and

cassava peel lead to a decline in biogas production as a result of a decline in consumption of available C due to lack of nitrogen. The optimum C/N ratio range is considered to be 25–30 [23].

The pH in which anaerobic digestion takes place is another important factor that needs close monitoring. Anaerobic microorganisms have strict pH ranges where they grow and metabolize optimally. Deviations from these ranges can result in digestion failure from which recovery is difficult. Methanogens are especially sensitive to pH changes. The most favourable pH range for anaerobic digestion is 6.8–7.2, however, efficient digestion can take place up to pH 8.0. Anaerobic digestion is susceptible to process failure due to the presence of inhibitory substances. Due to inherent differences in nutrient requirement, growth rate and sensitivity to reactor conditions among various microbial communities, it can be difficult to maintain stable anaerobic digestion. The inhibition is often observed by the gradual decrease in biogas production [23]. Another common manifestation of inhibition is decline in pH. This is an indication that the methanogenesis step is inhibited and volatile fatty acids are being accumulated. The most common example is ammonia inhibition. Koster and Lettinga (1988) [23] reported that when the concentration increased above 4 g $NH_3$–N/L more than half of the methanogen population was lost but acidogens did not seem to be affected. Anaerobic digestion of substrates that contain elevated concentration of ammonia, such as pig manure slurry should monitor and take precautionary steps to avoid inhibition. Sulfide is another common source of inhibition in anaerobic digestion. Sulfates are reduced to sulfide by sulfate-reducing bacteria. Sulfide is toxic to methanogens. In addition, sulfate-reducing bacteria compete with methanogens and other microorganisms for resources, contributing to the overall inhibiting effect and loss of methane yield. Various reports show sulfide concentrations above 100–800 mg/L cause inhibition [24]. Some metal ions are also known to inhibit anaerobic digestion. Heavy metal ions such as Cd, Fe, Co, and Zn can accumulate over time and may reach inhibitory levels since they are not biodegradable. Some organic compounds especially halogenated benzenes and phenols are also reported to show inhibitory tendencies [25].

### 1.1.3 Anaerobic reactors and models

One of the most attractive features of anaerobic digestion is its simplicity of design and high versatility. There are several types of anaerobic reactors ranging in simplicity from fixed dome biogas reactor to modern high-rate reactors such as up-flow anaerobic sludge blanket (UASB). In its most basic form, the design of anaerobic reactor remains simple, as it includes a reactor vessel, inlet, and outlet chambers and gas collection system. This made it possible to develop low–cost anaerobic reactors, which are being installed in large numbers in developing countries to satisfy energy demand and manage waste. At the same time, developed countries are also installing modern high–tech anaerobic reactors to treat industrial, municipal and agricultural waste. Simplicity and versatility mean anaerobic reactors are being adopted in developed and developing countries to fulfil various demands.

Various models have been proposed for anaerobic digestion. The earliest models were simple and did not include complex phenomena such as microbial growth rate and reaction kinetics. They simply estimated how much methane could be produced from a given organic substrate. An example of such models is the Buswell's formula and its derivatives (Eq. 2–4). Buswell and Symons (1933) [26] formulated a stoichiometric equation for the anaerobic reaction of organic compounds that contain C, H and O.

$$C_nH_aO_b + \left(n - {}^{a}/_{4} - {}^{b}/_{2}\right)H_2O \rightarrow \left({}^{n}/_{2} - {}^{a}/_{8} - {}^{b}/_{4}\right)CO_2 + \left({}^{n}/_{2} - {}^{a}/_{8} - {}^{b}/_{4}\right)CH_4 \quad (2)$$

For organic compounds that contain C, H, O, and N the equation is given as [27]:

$$C_nH_aO_bN_d + \left(n - {}^{a}/_{4} - {}^{b}/_{2} + {}^{3d}/_{4}\right)H_2O \rightarrow$$

$$\left({}^{n}/_{2} - {}^{a}/_{8} + {}^{b}/_{4} + {}^{3d}/_{8}\right)CO_2 + \left({}^{n}/_{2} + {}^{a}/_{8} - {}^{b}/_{4} - {}^{3d}/_{8}\right)CH_4 + dNH_3 \quad (3)$$

For organic compounds that contain C, H, O, N and S an equation based on [26] is derived as:

$$C_nH_aO_bN_dS_s + \frac{1}{4}(4n - a - 2b + 3d + 2s)H_2O \rightarrow$$

$$\frac{1}{8}(4n - a + 2b + 3d + 2s)\ CO_2 + \frac{1}{8}(4n + a - 2b - 3d - 2s)CH_4 + dNH_3 + sH_2S \qquad (4)$$

Since Buswell equation assumes all the reactant is consumed during the reaction, which is rarely the case during anaerobic digestion, it can only be used to estimate the theoretical maximum production of $CH_4$, $CO_2$ and other products. The actual amount of $CH_4$ and $CO_2$ produced depends on how much of the reactant is degraded. In addition, due to the higher solubility of $CO_2$ in water than that of $CH_4$, the equations predict a significantly higher quantity of $CO_2$ than what is recovered in the biogas produced in anaerobic reactors [27]. Later anaerobic digestion models improved from the work of Buswell and Symons by classifying the organic substrates as carbohydrates, lipids and proteins, improving estimations of methane production [28]. Modern anaerobic digestion models consider rates of biochemical reactions, microorganism growth, enzymatic activity, and reactor conditions to accurately simulate the digestion process. The most widely used anaerobic digestion model is ADM1 (Anaerobic Digestion Model no. 1) [15]. It was published in 2002 by the international water association (IWA) anaerobic digestion modelling task group to establish a generalised model for anaerobic digestion. The resulting model includes a description of each step including disintegration and formulation of rate and kinetic equations for major biochemical pathways and physicochemical processes [15].

### 1.1.4 Anaerobic granular sludge

Under favourable conditions, flocculent microorganisms are observed to coalesce around each other and form dense and stable aggregates that are roughly spherical in shape and sizes that are usually larger than 0.5 mm. Such aggregates are known as granular sludge. The earliest known observation of granular sludge was in the late 1960s by Young and McCarty in an anaerobic filter that treats low strength soluble organic wastes [29]. In the following years, several studies were carried out to understand what their characteristics are, how they are formed, and how they can be used in biological treatment processes. Microbial aggregation occurs through self–immobilization without a carrier material, resulting in granules that are composed mostly of active biomass with high specific activity [30]. Granular sludge density is higher than the surrounding fluid;

as a result, granules have good settling characteristics. Good settling and high biological activity are the two most important characteristics at the centre of the success of anaerobic granular sludge technology. There are several theories that try to explain the phenomenon of granule formation. Lens et al. (2004) [31] classified such theories into three broad categories:

- Physical theories: They explain granule formation in terms of an interaction between physical conditions such as flow velocity and suspended solids concentration and microorganisms (e.g.: Selection pressure theory).
- Microbial theories: They consider microbial characteristics such as physiology, secretion of extracellular polymeric substances (EPS), presence of filamentous microorganisms, etc. to explain granule formation. (e.g.: bridging microflocs theory).
- Thermodynamics theories: Such theories give importance to microbial cell surface interactions and adhesive forces in the aggregation of cells during granule formation (e.g.: surface tension model).

Regardless of how they are formed, granules are comprised of a diverse microbial ecosystem. The structure of granular sludge consists of a wide range of microorganisms that are in syntrophic and competitive relationships [32]. Microorganisms aggregate in such a way to ensure effective transport of resources (substrate) and by-products. Composition and distribution of microorganisms are important qualities of the granule. MacLeod et al. (1990) [33] proposed a granular structure that is layered with different groups of microorganisms forming layers (Figure 1.3). In anaerobic granular sludge, the inner layer is thought to consist of various types of Methanogens. The Methanogenic layer is surrounded by a layer of bacteria that consume and produce $H_2$. The outer most layer consists of various Acidogenic bacteria and some $H_2$ consuming bacteria.

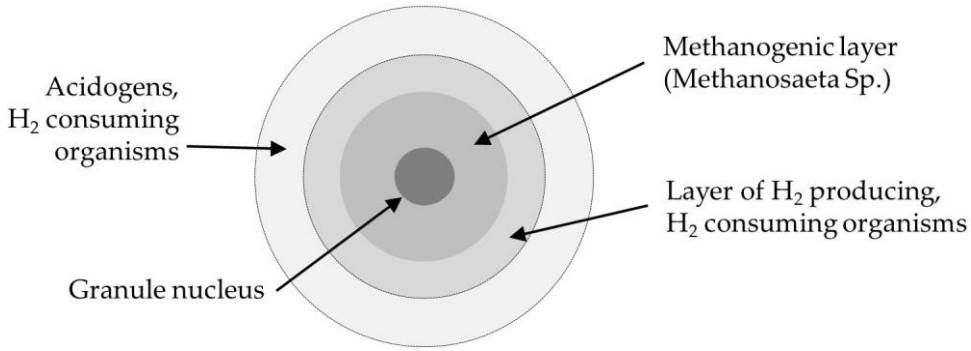


**Figure 1.3: Internal structure of anaerobic granular sludge (adapted from O'Flaherty et al. (2003) [32])**

Discovery and subsequent research on granular sludge in the early 1970s have led to a rapid rise in the adoption of anaerobic digestion for treatment of waste [21]. Previously, anaerobic systems were considered unsuitable for various waste treatment methods due to slow growth and activity of microorganisms in anaerobic environments. In addition, anaerobic systems used to require large area and volume of reactors. Granular sludge provides high specific biological activity as well as high microbial concentration because of sludge retention. With granular sludge, high loading rates and small reactor volumes are possible. This has led to the emergence of high-rate reactor systems that can efficiently treat both high- and low-strength wastes.

### 1.1.5 Anaerobic granule characteristics

The quality of anaerobic granular sludge depends on its physical and microbiological characteristics [30]. Physical characteristics of good quality granules are high settling velocity, high density and high mechanical strength. When it comes to microbiological characteristics, the most important quality of granules is containing a well–balanced microbial community that ensures high metabolic activity (conversion rate). There are proposals to define properties of a good quality granule. The following are suggested by Van Lier et al. (2015) [21].

- Settling velocity: 2–100 m/h ; typically: 30–75 m/h
- Size: 0.1–8 mm ; typically: 0.15–4 mm
- Density: 1000 kg/m$^3$–1050 kg/m$^3$

- Shape: Spherical, well–defined
- Specific methanogenic activity: 0.1–2 gCOD–$CH_4$/gVSS day

Some researchers regard other physical characteristics such as granule porosity to be an important parameter in granule quality determination because it is linked to the transport of substrates and digestion products to and from the granules. Pore size and mass transfer limitation are interlinked characteristics in anaerobic granules [30]. There are physical, chemical, biological and mechanical methods to determine various granule characteristics. Settling velocity is usually determined by using settling column tests [34]. There are microscopic and image analysis techniques that are used to determine granule size distribution and shape (more in Article 1). The density of granules can be measured using a pycnometer but methods that are more sophisticated are also available. There are standard methods that are used to determine the total solids (TS) and volatile solids (VS) contents of granules [35]. Batch test experiments are used to determine the microbiological activity of granules (see Article 3). A known concentration of substrate is used to determine the specific methanogenic activity of microorganisms and rate of reaction. Sophisticated methods such as Fluorescence In Situ Hybridization technique (FISH) are used to assess the content and distribution of microbial community in granules. Porosity and related granule properties can be determined by using size exclusion chromatography [30]. Whereas methods based on compression and abrasion resistance are available to determine the mechanical strength of granules [30].

### 1.1.6 High-rate anaerobic digestion

Continuous Stirred Tank Reactor (CSTR) systems are the most common anaerobic treatment processes while high-rate anaerobic digestion is becoming popular [21]. In CSTR, hydraulic retention time (HRT) and solids retention time (SRT) are identical. As a result, the rate of bioconversion in such systems is linked to the growth rate of anaerobic microorganisms, which is significantly slower than the growth rate of aerobic microorganisms. In order to sustain enough biomass concentration in the reactor, long HRT is required, implying large reactor volume is required and this has put traditional low-rate anaerobic systems at a disadvantage [21]. Discovery and development of

anaerobic granular sludge that are dense and have high settling characteristics introduced an important concept: HRT and SRT can be decoupled. In high-rate reactors, high concentration of biomass can be kept in a relatively small volume of a reactor. This makes it possible to undergo bioconversion in short HRT, high loading rates and the need for large reactor volume is eliminated. Compact high-rate reactors with high loading rates are now common. Since the 1970's several types of high-rate reactors have been developed. Early high-rate reactors such as Anaerobic Contact Process (ACP) faced problems such as difficulty separating sludge from treated fluid or inadequate sludge granulation [21]. The difficulty of separating sludge from treated fluid was solved in Anaerobic Filter (AF) by using support material for granular sludge [21]. Similarly, other first-generation high-rate reactors had to deal with problems that are often associated with new technologies. As high-rate technology matured, a new generation of reactors that address problems of earlier reactors started to emerge. The new generation of reactors are highly dependent on the formation of stable granules. Some of such reactors are briefly discussed below.

#### *1.1.6.1 Up-flow anaerobic sludge blanket (UASB)*

UASB was first developed by Lettinga et al. in the early 1970s [36]. UASB has been the most widely used high-rate AD reactors in the world [21]. Its simple design, low cost, low sludge production, and high removal efficiency makes it an attractive reactor. The design incorporates substrate inlet and effluent outlet at the bottom and top of the reactor, respectively. Influent is pushed upward through a blanket of granular sludge for effective contact. Three-phase separator (Gas–Liquid–Solid separator) near the top of the reactor separates the biogas, effluent and granular sludge that may have been washed out due to the hydraulic up-flow force. In UASB, the up-flow velocity of the inlet fluid is an important parameter to consider during reactor design and operation as it affects the settling velocity of the granules, the organic loading rate, and HRT. Too high up-flow velocity will result in granule to be washed out from the reactor and too low will result in inefficient contact between inlet fluid and granules. UASB has been widely used for the treatment of high strength industrial wastewater with low suspended solids content but applications for other types of substrates are also known [32].

#### *1.1.6.2 Expanded granular sludge bed (EGSB)*

Expanded granular sludge bed is a variety of the UASB reactor. It is considered a cross between UASB and fluidized bed reactors. It allows a higher up-flow velocity than that of UASB, resulting in more expanded sludge bed. While typical UASB up-flow velocities are 1–3 m/h, EGSB can have up-flow velocities of up to 10 m/h [37]. In order to accommodate high up-flow velocity, the reactor tends to be tall (7–25 m height) and/or there is a recycling of effluent. EGSB accomplishes a higher level of substrate–granule contact, which enables high organic loading rates. The resulting removal efficiency is very high. Most applications of EGSB are for the treatment of low strength industrial wastewater. It is considered especially beneficial for the degradation of highly toxic chemical compounds that are not suitable for UASB treatment [21].

#### *1.1.6.3 Anaerobic baffled reactor (ABR)*

The ABR configuration allows substrates to undergo different steps of anaerobic digestion separately. Acidogenesis and methanogenesis phases of the digestion are separated by vertical or horizontal baffles in the reactor. The separation allows both acidogens and methanogens to grow with relative independence in their respective favourable conditions. This results in a faster growth rate for both acidogens and methanogens in ABR (up to four times faster growth rates are observed [38]). There are several advantages of ABR such as simple design, few moving parts, good process control, no need for mechanical mixing since the up-and-down flow of the wastewater inside the reactor is self–mixing, high microbial growth rate, etc. Despite these advantages, ABR may be susceptible to sludge retention time limitation since high flow velocity in the reactor may push granular sludge along/across the reactor to be lost in the effluent. As a result, ABR reactors are not as widely used as UASB and EGSB. (More details regarding advantages/disadvantages of various AD reactors are presented in Article 2).

### 1.1.7 Bottlenecks in high-rate anaerobic digestion

High-rate anaerobic digestion is primarily used for the treatment of industrial wastewater, which is characterised by low suspended solids content. Both UASB and

EGSB are thought to be suitable for industrial wastewaters that are low in suspended solids. Even though there have been attempts to use high-rate reactors for wastewater with high suspended solids content, for the most part, they are restricted to low suspended solids wastewater. Some promising results have been obtained by applying UASB for particle-rich substrates such as manure supernatant [22] and co-digestion of manure and olive oil mill effluent (POME) [39] (more regarding this is presented in Article 2). Substrates that contain high suspended solids and those that contain a high concentration of lipids and protein may pose operational problems. High suspended solids in high-rate reactors may create mechanical problems such as pipe blockage, channelling and mixing problems. Accumulation of suspended matter in the granular sludge bed is often observed when substrates rich in particulate matter are used, however, the fate and interaction of such particulates are not clearly understood. Lack of clear understanding of the interaction of granular sludge with particulates in high-rate reactors seems to be a recurring bottleneck that holds high-rate anaerobic digesters from being fully applied for particle-rich substrates. Some of the most abundant resources are particle-rich. It is important to understand how such resources can be used to recover renewable energy. If the bottlenecks are removed, there is a huge potential for biogas production from agricultural wastes.

## 1.2 Objectives

Particle-rich substrates are abundant resources but they have not been used effectively in biogas production, especially in high-rate anaerobic digestion systems. One of the main reasons for this has been a lack of deeper understanding of how anaerobic granular sludge interacts with solid particulates in particle-rich substrates. Gaining knowledge of what their characteristics are leads to understanding the manner of their interaction and improved possibilities to control and optimize such processes. Understanding the interaction patterns, how solid particulates disintegrate, how influent, effluent and other reactor properties affect them is an important effort in increasing the use of high-rate anaerobic digestion for particle-rich substrates. This work aims to contribute to this

effort. The primary objectives of this work are to gain a deeper understanding of the following topics:

- Understanding anaerobic granular sludge characteristics and how reactor conditions affect their formation, size, density and settling properties.
- Developing a method that can be used to measure important granular sludge characteristics such as size and settling properties.
- How different parameters such as substrate composition and temperature affect anaerobic digestion of particle-rich substrates.
- Interaction between suspended particles and anaerobic granular sludge.
- How granular sludge respond to changes in feed properties and other process parameters.
- The implication of particulate–granule interaction on the overall biogas production.

## 1.3 Approaches

In order to achieve the objectives mentioned in the earlier section, various approaches have been used. Small-scale laboratory reactors have been built and experimental work has been carried out. A pilot anaerobic reactor was also used. In addition, modelling of anaerobic digestion was performed for various reactor conditions.

- Laboratory-scale continuous flow reactors: Two lab-scale UASB reactors that are identical in dimension and operation were used. In addition, a separate single reactor with similar but not identical dimensions was used.
- Laboratory scale batch reactors: Automatic biomethane potential test system (AMPTS) was used.
- Pilot reactor: Pilot anaerobic digester located at a farm in Bjorkedalen, Porsgrunn, Norway. Samples were regularly collected and experimental analyses were carried out.
- Laboratory experimental analysis: Influent and effluent samples, as well as granular sludge samples, were regularly collected from the lab-scale reactors and the pilot reactor for analysis. Experimental analysis of Chemical Oxygen Demand (COD), total solids, suspended solids, and other sample characteristics were measured.

- ADM1 modelling: Modelling and computer simulation of experimental conditions were carried out using ADM1 in its original version and with modifications to obtain more accurate modelling of particulates disintegration, implemented using Aquasim software.

## 1.4 Scope of the dissertation

The scopes of this PhD work are the following:

- Conduct experiments using lab-scale and pilot anaerobic digestion reactors to investigate particle-rich substrates in granular sludge bed AD
- Analysis and characterisation of influent, effluent and granular sludge samples collected from the reactors.
- Assess applicability of findings from the experiments to full-scale reactors
- Conduct anaerobic digestion modelling to understand particulate-granule interaction and its effects on the disintegration of suspended solids.
- Establish implications of experimental and theoretical results on process control and monitoring of high-rate anaerobic digestion of particle-rich substrates.

# 2 Literature review

This chapter presents a review of articles, books, scientific data and other works related to high-rate digestion of particle-rich substrates. Practical remedies suggested by various authors and their suitability in achieving the objectives of this dissertation are discussed.

## 2.1 Particle-rich substrates

One of the parameters used to characterise wastewater is the amount of solids it contains. Solid content is measured as total solids, volatile solids, suspended solids or dissolved solids. The total solids (TS) is the sum of dissolved and suspended solids. Even though there is no precise definition for dissolved solids, conventionally, many authors consider particles with diameters less than 0.45 μm to be dissolved [40].

The term "particulate" is often used to refer to suspended solids. The total solids content of substrates can be used to classify substrates, such as particle-rich and particle free. Many industrial wastewaters are considered particle-free because they contain little to no suspended solids. On the other hand, many other wastewaters, such as municipal and agricultural wastewater, contain a substantial amount of suspended solids and thus, are considered particle-rich. Some studies classify anaerobic digestion based on the total solids content of the substrates [41]. Dry, semi-dry and wet digestion are types of anaerobic digestions that are carried out using substrates with a total solids content of > 20%, 10–20% and < 10% respectively [41]. Agricultural wastes such as manure are considered particle-rich because they contain high levels of suspended solids. Animal manure is one of the most abundant resources containing nutrients and organic matter and it has the potential to be a reliable source of renewable energy as a substrate for biogas production.

### 2.1.1 Biogas production from particle-rich substrates

Particle-rich substrates contain high energy density, which gives them a high potential for biogas production. In practice, the potential is limited by how much of the particles are degraded. Chemical composition of particle-rich substrates plays an important role

in determining the extent of biodegradability. Low disintegration and hydrolysis rates are often encountered during anaerobic digestion of solid particulates. As a result, only a fraction of the solid particles is actually converted into biogas. The biogas potential of particle-rich substrates can be determined by estimating the average chemical composition of the volatile solids (VS) of the substrate. When solids are heated to 500 ± 50 °C, a fraction of them will be volatilized, these solids are called volatile solids and they are generally presumed to be organic matter even though some organic components may not be completely volatilized and certain inorganic matter may be volatilized [42]. Using Buswell's formulas in equations 2 & 3, the maximum theoretical methane potential is estimated for each compound per unit mass of VS (Eq. 5).

Buswell's methane potential in terms of volume of $CH_4$/kgVS is given as [43]:

$$\frac{CH_4 \text{ produced (mole)} \times \text{Molar gas volume (22.4 L/mole)}}{\text{Substrate used (kgVS)}} \quad (5)$$

For example, the average chemical composition of VS of manure is estimated by Møller et al. (2004) [43] as follows:

$VS_{Carbohydrate} = C_6H_{10}O_5$ (415 L $CH_4$/kgVS)

$VS_{Protein} = C_5H_7O_2N$ (496 L$CH_4$/kgVS)

$VS_{Lipid} = C_{57}H_{104}O_6$ (1014 L $CH_4$/kgVS)

$VS_{Lignin} = C_6H_{10}O_5$ (415 L $CH_4$/kgVS)

$VS_{VFA} = C_2H_4O_2$ (370 L $CH_4$/kgVS)

Chemical composition of manure from different animals shows differences. This affects the degree to which these manures are degraded and the amount of methane that can be produced. Biodegradability of manure waste is determined using biodegradability constant, which is defined as a ratio of consumed volatile solids and added volatile solids assuming infinite retention time. Biodegradability constants of animal manure were estimated to be 0.9 for swine, 0.56–0.65 for cattle (beef), 0.36 for cattle (dairy) and 0.7–0.87 for poultry [44]. Møller et al. (2004) [43] studied methane potential of manure from pigs, sows and cattle and found values of 516 L $CH_4$/kgVS, 530 L $CH_4$/kgVS and 469 L

$CH_4$/kgVS, respectively. The organic fraction of municipal solid waste (OFMSW) is also a particle-rich substrate. Organic solid waste is composed of food waste, garden waste, paper, and other degradable wastes. The physical and chemical characteristics of OFMSW varies depending on the region it is generated. Different countries produce different waste based on their cultures and food habits. As a result, the VS content in OFMSW also varies considerably. In a review carried out by Campuzano et al. (2016) [45], it was revealed that the VS from OFMSW from various countries ranges from 7% to 36% with an average at 22% (Figure 2.1). The elemental composition of OFMSW also varies depending on which study one looks at. However, average values reported by authors [45] who studied the composition of wastes in various countries seems to indicate that the C, H, N and S composition on a dry weight basis to be 46%, 6%, 3%, and 0.3%, respectively. Brown and Murphy (2013) [46] derived an average chemical formula for OFMSW that is $C_{16.4}H_{29}O_{9.8}N$ (the derivation was mainly based on food waste), while Fongsatitkul et al. (2010) [47] suggested a formula of $C_{25}H_{42.5}O_{20}N$. Application of Buswell's methane potential equations on the above stoichiometric formulas suggests a maximum theoretical methane potential of 510 L $CH_4$ /kgVS for $C_{16.4}H_{29}O_{9.8}N$ and 412 L $CH_4$ /kgVS for $C_{25}H_{42.5}O_{20}N$.

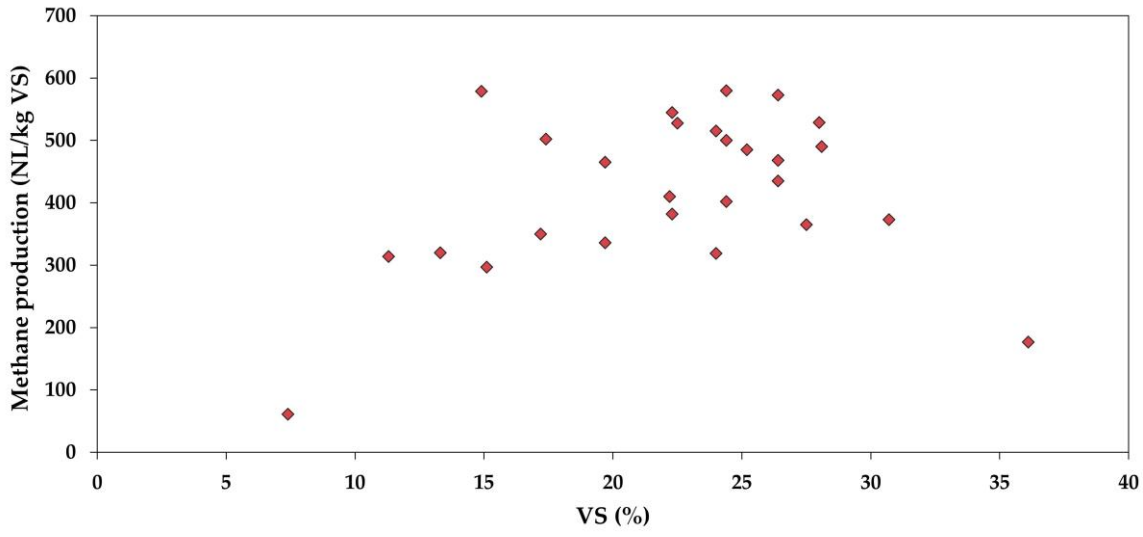


**Figure 2.1: Methane production based on VS (%) from various authors (Adapted from Campuzano et al. (2016)** [45]**)**

Some industrial effluents such as palm oil mill effluent (POME) contain high organic content, of which a substantial amount is as suspended solids. The reported COD, total, suspended and volatile solids contents of raw POME are 44–103 g/L, 40–72 g/L, 18–46 g/L and 34–49 g/L, respectively [48]. Since POME contains a high amount of oil and grease (lipids), which have a high energy density, the theoretical maximum methane potential is high. The main chemical constituents and their estimates in raw POME are crude protein (13%), crude lipid (10%) carbohydrate (30%), nitrogen-free extract (26%) the rest is ash and moisture [49]. Buswell's equations can be applied to estimate the methane potential of POME. Alternatively, COD can be used to calculate the theoretical methane potential of POME. Since the maximum amount of $CH_4$ produced from a gram of COD at standard conditions (273 K and 1 atm pressure) is 0.35 L $CH_4$ [42], the expected methane potential for raw POME with COD of 44–103 g/L would be 15–36 L $CH_4$/L raw POME. Assuming an average VS of 42 g/L, the Maximum methane potential would be 370–860 L $CH_4$/kgVS.

Another group of substrates that are considered particle-rich are energy crops, which are being increasingly used for biogas production [50]. There are several types of energy crops used as substrates in anaerobic reactors. The most common one is maize, however; wheat, potato, sugar beet, grass and other types of crops are also used. Energy crops contain high total and volatile solids contents. Typical TS values are 20–40% [50]. Methane potentials of energy crops depend on the nature and composition of energy crop as well as the part of the crop used and the season of harvest. A literature review indicates that theoretical methane potential values in L $CH_4$/kgVS are; 205–450 for Maize, 384–426 for Wheat, 276–400 for Potatoes, 236–381 for sugar beets and 298–467 for grass [50]. Overall, it is clear that the biogas potential of particle-rich substrates is high. The challenge is to achieve a high degree of biodegradation. In many cases, significant portions of organic substances remain undigested. This is especially the case if substrates contain a relatively high level of suspended solids, high lignocellulosic substances, and inhibitory compounds. Various steps are already available to increase the methane potential of particle-rich substrates. Some of the most important methods used to realise the potential of particle-rich substrates are discussed in section 2.2.

## 2.2 Anaerobic digestion of particle-rich substrates

Topics that are often associated with anaerobic digestion of particle-rich substrates are discussed. Some of the most common topics are substrate pretreatment, the need for co-digestion and commonly encountered problems during particle-rich substrate digestion.

### 2.2.1 Pretreatment methods

Particle-rich substrates are often pretreated prior to anaerobic digestion. The main objectives of pretreatment are increasing rate of anaerobic digestion and biogas yield. Various methods of pretreatment are developed over the years. They are classified as physical, chemical, biological and combined pretreatment methods. Physical pretreatment method usually involves some form of particle size reduction or attrition such as milling, leading to an increase in the surface area of substrates available for microbial action. Thermal pretreatment is carried out at high temperatures (> 50 $^{o}$C), leading to an increase in organic compound solubility. Reports from various authors show that thermal pretreatment increases biogas yield [51][52][53]. However, pretreatment at very high temperatures (> 120 °C) may lead to the formation of complex compounds that are hard to degrade (e.g. Maillard reaction between amino acids and carbohydrate products may occur [53]). Thermal pretreatment has the added benefits of pathogen removal, moisture reduction (dewatering) and reduction of substrate viscosity [53]. Chemical pretreatment is often used for substrates with significant lignocellulosic content. It involves using acidic, alkali or oxidative compounds to breakdown bonds in the lignocellulosic matrix. Compounds such as NaOH are used for alkali pretreatment. Acidic pretreatment is often carried out in combination with thermal pretreatment (thermochemical pretreatment). For oxidative pretreatment, $H_2O_2$ is used [54]. Biological pretreatment methods use microorganisms, enzymes or biological processes to treat substrates. Reports indicate that some fungi (brown-rot, white-rot, and soft-rot fungi) are capable of degrading lignocellulosic substances [55][56]. Direct hydrolytic enzyme addition is also used as a biological pretreatment method with some success [57]. Combined pretreatment processes such as steam explosion, extrusion, and

thermochemical pretreatment use a combination of physical, chemical and biological methods discussed above.

### 2.2.2 Co–digestion

Anaerobic digestion of a single substrate may face challenges due to nutrient imbalance, high concentration of inhibitory compounds, high or low C/N ratio, etc. One of the methods to solve such challenges is to co–digest two or more complementary substrates together. Carefully selected substrates and mixing ratios lead to increased biogas production as well as improved reactor stability. Co-digestion of agricultural waste (manure in particular) with other substrates is of special interest due to several advantages. Despite their abundant availability, the methane potential of animal manure is relatively low. Using co-digestion will increase methane production and increase the economic feasibility of reactors. Manure anaerobic digestion is susceptible to ammonia inhibition due to the high concentration of nitrogen-containing compounds [58]. Co-digestion with compounds high in carbon content would counter the inhibiting effect of ammonia by balancing the C/N ratio [58]. The recommended C/N ratio for anaerobic digestion varies but many authors report 20–30 is an optimal range. For manure, the ratio is usually less than 10, which is considered too low [59][60]. It is reasonable to co–digest manure with substrates high on C/N ratio so that the resulting mixture has an optimum C/N ratio. Since substrates such as energy crops, industrial wastewaters, and certain municipal waste are high in C/N ratio, they are frequently used in co-digestion of manures with encouraging results [59][60].

### 2.2.3 High-rate anaerobic digestion of particle-rich substrates

As described in section 1.1, high-rate anaerobic digestion is often used for substrates of low suspended particulate content. Attempts have been made to adapt high-rate technology for substrates with high–suspended solids content. This section summarizes the current trends and developments in the use of high-rate reactors for digestion of particle-rich substrates. Even though high-rate reactors are considered unsuitable for substrates with a high concentration of suspended solids, tests to adapt it to particle-rich substrates were started early in the development of high-rate reactors.

One of the first attempts was made by Lettinga et al. (1984) [61] where the feasibility of UASB for digestion of slaughterhouse waste with 50% insoluble suspended COD was tested. They achieved 70% treatment efficiency based on total COD and 90% based on soluble COD. Boari et al. (1984) [62] also achieved 70% total COD removal using UASB on diluted olive oil mill wastewater. Similar other attempts were also made, but in many of these attempts, there were accumulations of suspended solids in the sludge bed especially when the HRT was short and the OLR was high (see Article 2). Solid accumulation in the sludge bed is known to affect the digestion process by shortening the sludge retention time and limiting methanogenic activity. As a result, solid removal in high-rate reactors was not considerable. However, Zeeman et al. (1996) [63] used an up-flow anaerobic solid removal (UASR), a two-phase UASB type reactor, to achieve high-rate removal of suspended solids from raw domestic sewage with high suspended and colloidal COD (65% suspended solids COD removal at 3 hr HRT).

### 2.2.4 The fate of suspended particles in high-rate reactors

Suspended solids accumulation in the granular sludge bed is a common occurrence during high-rate digestion of particle-rich substrates. Accumulation of suspended solids in the sludge bed affects the digestion process by causing granular sludge washout and inhibiting methanogens [64]. Understanding how and why suspended solids accumulate is vital for the application of high-rate anaerobic digestion to particle-rich substrates. In order to understand the fate of accumulated solids, it is important to identify what factors play a role in the accumulation. Mahmoud et al. (2003) [64] reviewed the main factors that play a role in solid removal in UASB reactors. The review classified such factors into reactor operational conditions, substrate characteristics and granular sludge bed characteristics. Particular importance for this section is factors that affect the rate of conversion of entrapped solids. Solids accumulate because they have a slow rate of disintegration and hydrolysis. Temperature, size of entrapped particles, pretreatment, etc. have various effects on the rate of disintegration and hydrolysis. Higher digestion temperature leads to faster hydrolysis and efficient solid removal. The kinetics of hydrolysis is assumed to be first-order [15] where the hydrolysis rate constant follows the Arrhenius equation for temperature effect.

$$\frac{dX}{dt} = K_h X \quad (6)$$

$$K_h = Ae^{-E_a/RT} \quad (7)$$

Where dx/dt is the rate of hydrolysis, $K_h$ is hydrolysis rate constant, X particulate component, A is Arrhenius constant, $E_a$ is activation energy, R is gas constant and T is temperature. Size of the entrapped solids influences disintegration and hydrolysis rates, with smaller solids having faster rates than larger ones. Sharma et al. (1988) [65] studied the influence of particle size on biogas production by carrying out batch tests on various solid biomass residues and found out that smaller particles generate more biogas than larger ones. Interaction of accumulated solids and granular sludge involves the release of hydrolysing enzymes by microorganisms that facilitate solubilisation of accumulated solids. Accumulated solids that contain a significant amount of lignocellulosic substances (cellulose, hemicellulose, and lignin) tend to take a relatively longer time to solubilize [57] than solids that contain other biopolymers such as protein.

The difficulty of breaking down lignocellulosic substances is due to the strong and reinforced nature of their chemical structure. In the case of cellulose, its monomers (glucose molecules) are bonded by strong beta–(1,4) glycosidic bonds that are difficult to break. Lignin has a complex structure made up of phenolic monomers that are difficult to degrade. Even when degraded in small amount, the resulting phenols have an inhibitory effect on anaerobic digestion (see Article 3 for more.). Enzymatic breakdown of chemical bonds in the lignocellulosic substances takes place at a slow rate because their complex structure makes it difficult for enzymes to have easy access to such bonds. As a result, high-rate digestion that involves substrates with lignocellulosic matter such as animal manure, straw, grass, and other plant biomass tend to have solid accumulation.

### 2.2.5 Problems during digestion of particle-rich substrates

The methane potential of particle-rich substrates is high but the presence of lignocellulosic biomass and other slowly degradable substances makes it difficult to realise this potential. Pretreatment of particle-rich substrates are used to help realise

methane potential but the energy demand and cost for pretreatment is not always sustainable [66].

Digestion of particle-rich substrates often encounters problems that are related to particle accumulation. Presence of solid particles in reactors that contain various interlocking pipes, pumps, mixers and vessels often results in physical clogging due to particle embedding in pipes and pumps. When the accumulated particles become dense enough, efficient mixing becomes impossible and the digestion process is severely limited, requiring regular clean–up of reactor parts. Accumulation of solids also leads to alteration of the microbial composition and density in the sludge bed, which eventually can result in digestion failure. Accumulating solids reduce the effective volume of the reactor leading to alteration of the effective HRT and OLR values [67]. In reactors that use internal heating systems, solid particulates can be accumulated on heaters and heat exchangers, greatly reducing the efficiency of heat transfer [68]. Prolonged presence of accumulated solids can also be a cause for granular sludge washout [69]. Laboratory and full-scale experiments performed by Lettinga et al. (1991) [69] showed signs of granular washout due to the accumulation of solids in reactors. When less dense solid particulates are present, a floating layer of solids may also appear at the top of reactors (inverted solid profile) either due to the formation of foam and/or due to upward moving gases pushing/lifting the solids up.

# 3 Materials and methods

This section provides descriptions of laboratory and pilot reactors used for anaerobic digestion experiments. In addition, descriptions of analytical methods for influent, effluent and granule samples are also provided.

## 3.1 Strategy

In order to accomplish the objectives presented in section 1.2, lab-scale and full-scale (pilot) anaerobic digestion experiments were carried out. Various strategies were used depending on the specific objectives. In order to analyse granular sludge characteristics such as size and settling property, granular sludge samples were taken out from various locations in lab-scale reactors and compared with granular sludge obtained from large-scale reactors. Correlation of granular sludge characteristics with flow conditions such as up-flow velocity, organic loading rate and hydraulic retention time was assessed.

In order to understand the effect of suspended solids content of particle-rich substrates on anaerobic digestion, laboratory experiments were carried out where; one reactor was fed a substrate with high suspended solids content while the other was fed a substrate with low suspended solids content with all other controllable variables equal. Suspended solid reduction of the feed was carried out by centrifugation. Effects of temperature were studied by varying digestion temperature. Most of the laboratory experiments were carried out at 25 and 35 ˚C.

The combined effect of temperature and particulate content of the substrate was studied by using a single reactor and changing the substrates particle content and temperature at various phases during the experiment. Batch experiments were also used to determine the methane potential of substrates with high and low particulate content and with/without the addition of enzyme. In addition, kinetic parameters were determined and used in modelling of the digestion processes.

### 3.1.1 Pilot reactor

Feed, effluent, and granule samples were taken from a pilot ABR reactor (Figure 3.1) located in Porsgrunn, Norway. The reactor treats swine manure supernatant. Various temperature ranges were used during the experiments. HRT and OLR values were also varied. The basic dimensions of the reactor are provided in Table 3.1.

**Table 3.1: Dimensions and tested operational parameters of the pilot reactor**

| Reactor property | Pilot reactor |
|---|---|
| Total volume ($m^3$) | 10 |
| Single Intermittent Feed (L) | 70 |
| Intermittent Feed frequency ($d^{-1}$) | 47 |
| HLR (L/d) | 3300 |
| HRT (d) | 1–5 |
| OLR ($g.L^{-1}\,d^{-1}$) | Various |
| Up-flow velocity (m/d) | Various |
| Temperature (°C) | 20–35 |


**Figure 3.1: Pilot ABR reactor where samples were regularly investigated and reactor conditions monitored.**

### 3.1.2 Lab-scale reactors

Three lab-scale reactors were built. Two of them were used as identical parallel reactors whereas the third one was a standalone reactor with similar dimensions as the two identical. The basic set up of all three reactors are given in Figure 3.2 and dimensions in Table 3.2.

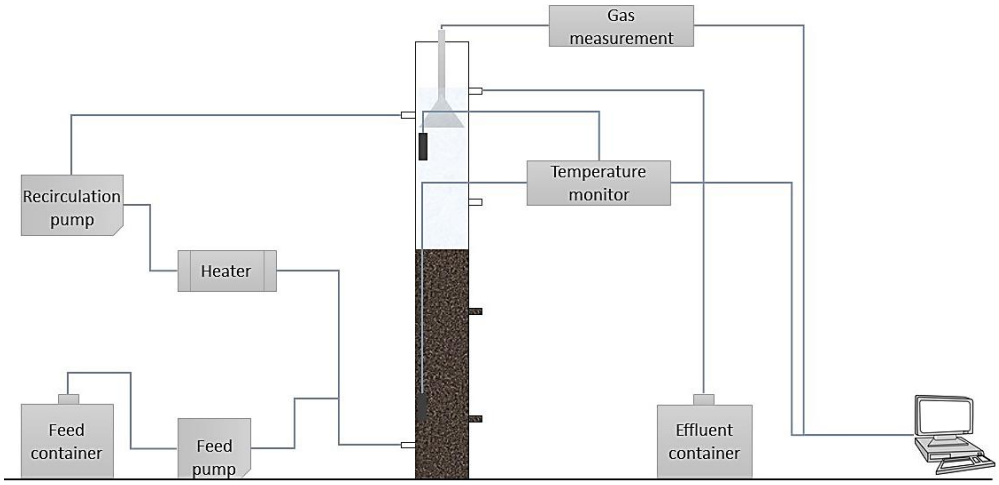


**Figure 3.2: UASB reactor set up and system description.**

**Table 3.2: Dimensions of lab-scale reactors**

| Reactor property | Standalone reactor | Parallel reactors |
|---|---|---|
| Height (m) | 0.85 | 0.52 |
| Internal diameter (m) | 0.044 | 0.054 |
| Cross–sectional area ($m^2$) | 0.0015 | 0.0023 |
| Total volume (L) | 1.3 | 1.2 |
| HRT (d) | 1–5 | Various |
| OLR ($g.L^{-1}\,d^{-1}$) | 3–21 | Various |
| Up-flow velocity (m/d) | 40–42 | 40–42 |
| Temperature (°C) | 25–38 | 25–38 |

### 3.1.3 Batch reactor

Various batch reactor experiments were carried out. Preliminary batch tests using syringes and bottles as reactor vessels were used. However, most of the data collected from batch experiments were from batch experiments using automatic methane potential test system instrument (AMPTS II, Bioprocess Control, Sweden). AMPTS is equipped with a temperature adjustable heat bath, automatic stirrer motors, a $CO_2$ removal unit, a methane volume measurement unit and software to monitor the system (Figure 3.3). For samples that require mechanical pretreatment (size reduction by milling), milling was carried out using a milling machine using $ZrO_2$ mill balls (Szegvari Attritor system, Union process from Ohio, USA). Centrifugation of samples was carried out using a Centrifuge (Beckman J–25, with JA–10 rotor).

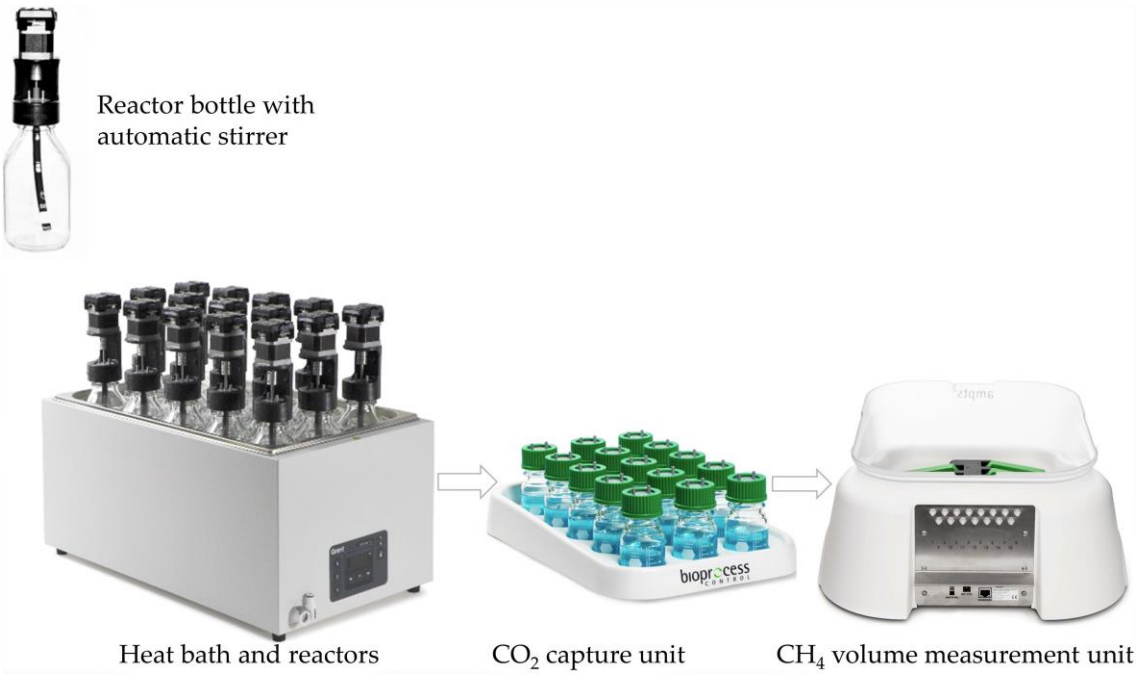


**Figure 3.3: Batch experiment reactor set up and equipment description (figure from Bioprocess control's homepage)**

## 3.2 Experimental analysis

### 3.2.1 Microscopic image analysis

Granule image analysis was carried out using a Nikon SMZ745T microscope (Figure 3.4). The microscope was calibrated using a standard ruler with a known distance so that the pixel size of the images generated by the microscope is correlated with the size of the granules. The granules were rinsed with distilled water then 10–15 granules were scooped with a spatula and placed on a microscope slide. Since data about granule perimeter is crucial, individual granules were separated so that they do not overlap and interfere with each other's perimeter measurements. The settings for image quality were adjusted and images were taken. The image files were saved as JPEG files. Each image file was then preprocessed and its data collected using Matlab codes (Appendix A and B).

**Figure 3.4: Nikon SMZ745T microscope was used to take 2D–images (2 dimensional) of granules.**

### 3.2.2 Pilot reactor experiments

Periodical monitoring of the performance of the pilot anaerobic reactor was carried out. During the monitoring, influent and effluent samples were analysed, gas flow rate and composition analysis were undertaken and granular characterization carried out. The analytical methods used for influent and effluent characterization are described in the following section. On-site biogas composition analysis was carried out using a portable gas composition analyser, Biogas 5000 (bought from Geotech UK).

### 3.2.3 Lab-scale reactor experiments

Influent and effluent samples were taken from the lab-scale reactors and analysed using various analytical methods. Sample characteristics such as total solids, total suspended solids, volatile solids, and volatile suspended solids were determined according to American public health association standard method APHA 2540 [35]. The organic content of samples was determined as total and soluble COD values using COD kits and Spectrophotometric method in accordance with APHA standard method 5220 D. Beckman 300 pH meter equipped with Sentix–82 pH electrode was used to determine sample pH. Ammonium–Nitrogen content ($NH_4^+$–N) was measured according to APHA 4500–$NH_3$. Both COD and $NH_4^+$–N concentrations were measured using commercially available test kits and Spectroquant Pharo 300 spectrophotometer (Darmstadt, Germany). Volatile fatty acid (VFA) content of samples was measured using Agilent gas chromatography–flame ionization detector (GC–FID). Standard VFA samples were used for each experiment to establish a calibration curve. Biogas compositions of samples from lab-scale reactors were analysed using SRI 8610C Gas chromatograph. A standard mixture of 60% of $CH_4$ and 38% of $CO_2$ was used for calibration.

### 3.2.4 Batch reactor experiments

Influent samples used in batch experiments were also characterised using the same methods described in section 3.2.2. In addition, granular sludge characteristics such as size, settling velocity and density were measured according to methods described in Article 1. Milling of samples was carried out using a milling machine at 400 RPM for 15

minutes. Centrifugation of feed samples was carried out for 15 minutes at 10,000 RPM using Beckman J–25 Centrifuge.

### 3.2.5 Experiments on the effects of substrate milling

In addition to the above–mentioned experiments, various others were also carried out for various purposes. One such experiment was a batch anaerobic digestion to understand the effect of milling on substrate particle size, rate of hydrolysis and biomethane potential. Even though the experiment did not produce publishable results, it is included here as it gave us insight into the effect of particle size in biomethane potential. For the experiment, pig manure slurry samples were collected from Bjorkedalen farm where a pilot anaerobic baffled reactor (ABR) reactor treats manure waste. Three main sample groups were used in the experiment.

- Raw feed (RF): Raw manure collected directly from barn manure storage.
- Milled feed (MF): Raw manure milled using 5 mm $ZrO_2$ balls at 400 RPM for 15 minutes.
- Pump feed (PF): Manure collected after raw manure passed through a rotary 'grinder' pump.

Each sample group was divided into two samples (Table 3.3). The first sample was made by sieving each sample group through a 0.85 mm sieve. The second sample was used without sieving. An additional sample was prepared by adding Cellulase enzyme into the unsieved milled feed. In total, seven feed samples were prepared. RF was directly collected from a storage tank whereas the pump feed was collected from the upper section of the pump. Apart from sieving, no further sample processing was conducted on raw and pump feeds. However, the milled feed was prepared by milling the raw feed at 400 RPM for 15 minutes. A szegvari Attritor System milling/grinding machine from Union Process was used. 3 L of raw feed was added into a vessel that contained nearly 8,000 $ZrO_2$ balls whose total volume add up to 3 L. The motor was adjusted to a speed of 400 RPM. The milling process was carried out for 15 minutes, after which, the milled sample was carefully separated from the balls and collected. Feed and granule

characterizations were carried out as described in section 3.2.3. Batch reactor experiments were performed using an AMPTS II instrument.

**Table 3.3: Samples and descriptions for milling experiment. (O: Original feed and S: Sieved feed).**

| Sample | Description |
|---|---|
| RF–O | Raw manure feed without sieving |
| RF–S | Raw manure feed after sieving through 0.85 mm sieve |
| MF–O | Milled feed without sieving |
| MF–S | Milled feed after sieving through 0.85 mm sieve |
| PF–O | Pump feed without sieving |
| PF–S | Pump feed after sieving through 0.85 mm sieve |
| MF–C | Milled feed and Cellulase enzyme without sieving |

# 4 Overview of results and discussion

In this chapter, a brief overview of results obtained from performing lab-scale and pilot reactor experiments as well as a review of published articles are presented. Results from unpublished works are also presented and discussed. The implications of the results for anaerobic digestion of particle-rich substrates in granular sludge beds are presented. Section 4.1 briefly presents results and discusses the implication of using image analysis to determine the size and settling velocity of granules. Section 4.2 discusses to what extent high-rate reactors have been used and what to do to employ successfully such reactors for particle-rich substrates. Discussion of experimental results and their significance is provided in section 4.3 for batch reactor results and section 4.4 for continuous flow reactor results.

## 4.1 Settling velocity and size distribution measurement of anaerobic granular sludge using microscopic image analysis

The development and rapid adoption of high-rate anaerobic reactors are strongly linked to the discovery of anaerobic granular sludge. Since physical characteristics such as size, settling velocity, and density of anaerobic granules are crucial parameters of a stable high-rate reactor, it is important to monitor such granular characteristics regularly. Granules in high-rate reactors are in a dynamic system where they experience physical and biological changes. Granular size changes during the anaerobic digestion process due to microbial growth and decay, granular shear–off, granule–granule collision, and granule–wall collisions. In order to monitor changes in granule size and settling velocity, we developed a method that uses microscopic image analysis, shape factor of granules and settling column experiments to determine the size distribution and settling velocity of anaerobic granules. Three samples were collected at the top, middle and bottom sections of a lab-scale UASB reactor. Two other samples were obtained from industries. Image analysis technique was used to calculate the shape factor and equivalent diameter of granules. The equivalent diameter was then used to calculate the theoretical settling

velocities and estimate size distributions. The results showed that there was a good agreement between the calculated and experimental mean settling velocity values. Both measured and calculated settling velocities increased with increasing Reynolds number (Re). However, the agreement between measured and calculated values was found to be weaker at higher Re values. Size distribution analyses of the granules have revealed that there was a significant difference in the size distribution of granule samples collected at different heights of the lab-scale reactor (Figure 4.1). Overall, granules from the bottom section of the reactor had a larger mean diameter, settling velocity and shape factor than those at the middle and the top sections. The granules collected from the top section exhibited the smallest granular diameter, settling velocity and shape factor (Figure 4.2). A more detailed data are provided in the attached Article 1.

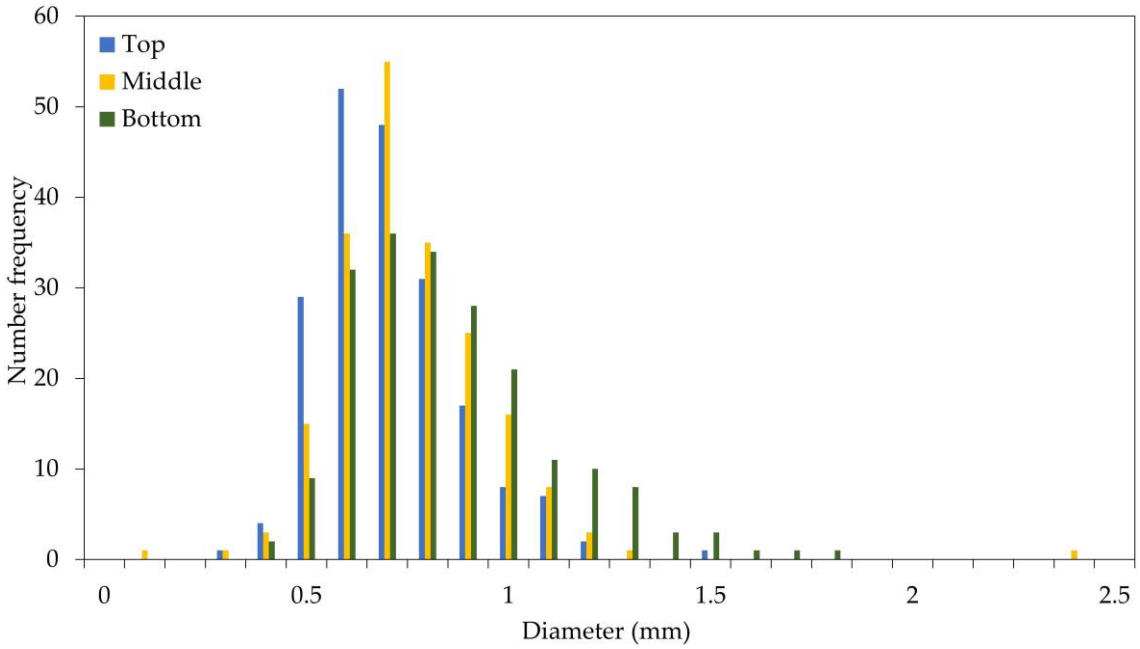


**Figure 4.1: Size distribution of granules in a Lab-scale UASB reactor.**

Use of particle-rich substrates in high-rate reactors tend to cause the accumulation of particles in the sludge bed. Accumulated solids affect the size, density and settling properties of the granular sludge. In the pilot reactor that we have monitored during the course of the PhD project, one of the recurring problem was the formation of floating particles as a top layer of the reactor, constituted mostly of scum, straw and other light suspended solids that are not entrapped in the sludge bed. We noticed presence of small

granules in the floating layer that seemed to be sheared–off from larger granules and pushed out of the sludge bed and floated to the top layer, suggesting size and settling velocity of granules are affected not just through "regular" microbial growth/decay cycle of granules but also through physical and mechanical interactions of granules with suspended solids.

We have shown that the size and shape influence the settling velocity of granules and that image analysis is an effective way to measure such properties. The method can be used for both aerobic and anaerobic granules in the intermediate flow regime (the Reynolds number value, Re, should be between 1 and 500). We also demonstrated that the method can be used on samples obtained from lab-scale and industrial reactors.

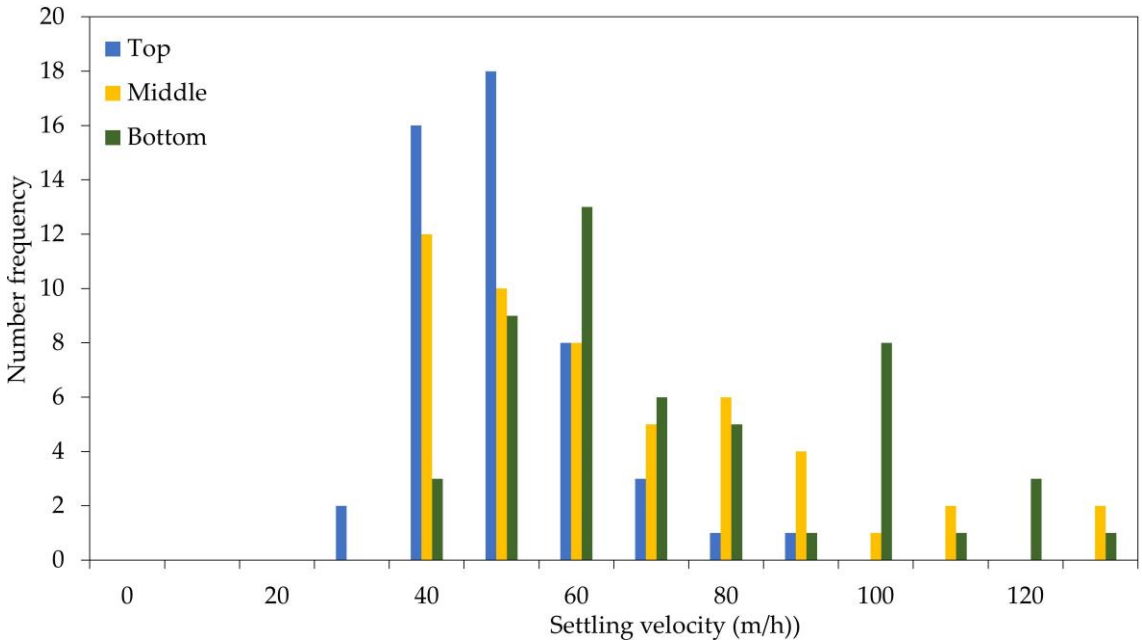


**Figure 4.2: Settling velocity distribution of granules in a Lab-scale UASB reactor.**

## 4.2 Granular sludge bed processes in anaerobic digestion of particle-rich substrates

In attached article 2, we have conducted a review of published articles, books, and reports to investigate how and to what extent feed particles influence granular sludge bed, with the aim to expand the applicability of granular sludge bed reactors to various types of slurries that are abundantly available. Granular sludge bed anaerobic digestion is well established as a method for very efficient wastewater treatment. However, it is limited by the wastewater particle content. The article shows that there are attempts, with various degrees of success, to use high-rate anaerobic digestion for particle-rich substrates. Nevertheless, the use of high-rate reactors for particle-rich substrates still face hurdles related to the slow rate of particulate disintegration that results in solid accumulation and sometimes reactor failure. Attempts ranging from the use of pretreatment methods to reactor design modifications to circumvent possible solid accumulations in reactors have been used. However, many of such methods may not be economically sustainable. Increasing disintegration and hydrolysis of solid particulates in high-rate reactors seemed to be more promising.

Applications, advantages and disadvantages of commonly used high-rate anaerobic reactors are presented in Article 2, with UASB and its variant EGSB selected for a more detailed evaluation. The review pointed out that there is a large quantity of particle-rich substrates that can be used as a feed in high-rate AD reactors, manure being such a substrate. Co-digestion of manure with other substrates such as food wastes and municipal organic wastes was found to be increasingly common, with various papers showing promising results related to the reduction of ammonia inhibition, optimum C/N ratio, increased methane yield etc.

Review of reaction kinetics involved in the digestion of particle-rich substrates was also carried out with emphasis on disintegration and hydrolysis steps. Disintegration and hydrolysis of solid particulates in such high-rate reactors and factors that affect these processes are studied especially, as rate-limiting steps. The review shows that disintegration and hydrolysis are sometimes lumped together as a single step but for

particle-rich substrates, it is advantageous to treat them as distinct steps. For practical purposes, use of first-order disintegration kinetics that classifies solid particulates into slow disintegrating and fast disintegrating fractions was found to be a workable solution. How particles may influence other key processes within granular sludge beds is also discussed. Based on this, strategies for effective digestion of particle-rich substrates in high-rate anaerobic digestion reactors are proposed. More detail is given in the attachment section for Article 2.

## 4.3 Effect of particulate disintegration on biomethane potential of particle-rich substrates in batch anaerobic reactor

The objective of this article 3 is to understand the effect of particulate disintegration on biomethane potential. We used anaerobic batch reactors to accomplish this. Two classes of samples, one rich in particles (Raw feed) and another poor in particle content (Centrifuged feed) were prepared from a pig manure supernatant. The experiments were carried out with and without cellulase enzyme addition to obtain a better understanding of particle degradation mechanisms. Automatic methane potential test system (AMPTS) was used to carry out batch reactions at 35 °C.

The investigation showed that substrates with high-suspended solids (RF) had higher biomethane potential than substrates with low-suspended solids (CF) but the conversion rate and methane yield were lower. As shown in Figure 4.3, the comparison of the biomethane potential of RF and CF revealed three distinctive stages. In the first stage (0–8 days), the rate of biomethane production was higher for CF but later overtaken by RF in the second stage (8–17 days). A maximum biomethane volume was reached at around 17 days for both RF and CF samples and remained relatively stable in the third stage (17–40 days) with no significant biomethane production for both RF and CF. However, the total volume of biomethane produced in the last stage appeared to decline slightly, which was attributed to a gradual (but small) increase in biomethane production from blank samples (in anaerobic digestion dead microbes are “recycled” and used by the rest

of microbes as a substrate leading to slight increase in the amount of biomethane produced from blank samples at the later stage of the batch test). Presence of suspended solids in higher quantities in RF contributed to its lower rate of biomethane production in the early stage of the batch test. Even if RF did not overtake CF until day 8, it is noticeable that the rate started to increase drastically from day 5. This suggests the presence of a ”lag phase” during which the disintegration of solids into hydrolysable components occurs. Such a lag phase was not observed in the sample with low suspended solids (CF). In fact, the biggest difference in the rate of biomethane production between RF and CF occurred in the first 2–3 days of the batch test where RF produced no net biomethane whereas CF produced about 50 ml.

Enzyme addition increased methane production in both types of substrates (Figure 4.4) but the increase was more pronounced in particle-rich substrates presumably due to higher cellulose content. The rate of methane production was also affected by enzyme addition. Highest biomethane production rates were achieved faster in substrates with cellulase addition compared to those without addition.

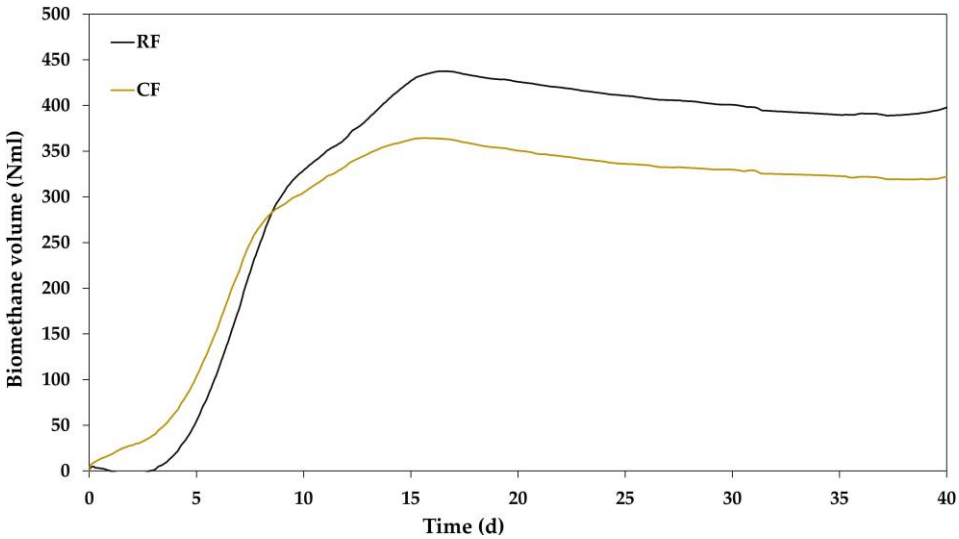


**Figure 4.3: Blank adjusted biomethane potential of samples with high suspended solids (RF) and low suspended solids (CF).**

The amount of methane produced at peak production rate was also higher in cellulase added substrates. A sharp peak was observed for both RF–CEL and CF–CEL samples on

the first day of the digestion. Digestion of easily degradable components that are consumed rapidly and released as biomethane may have temporarily spiked the total volume but this was quickly countered by an increase in biomethane production from the blank samples.

Simulation of the reactors without cellulase addition was carried out in two modes. Mode 1 was similar with standard ADM1 simulation where composite particulate (Xc) was not classified into fast and slow disintegrating fractions. Whereas, in Mode 2 simulation, particulates were classified as Xc1 and Xc2 (fast and slow fractions respectively). The result of the simulation indicated that Mode 2 simulation fit the experimental data better than Mode 1 simulation (Figure 4.5). However, substrates with low particle content (Centrifuged feed) show a marginal difference between Mode 1 and Mode 2 simulations. Substrates with high particle content (Raw feed), on the other hand, showed greatly improved fit with experimental data from Mode 1 to Mode 2 simulations, implying that Mode 2 simulation may be well suited for particle-rich substrates. Further description of experimental and simulation results and discussion can be found in Article 3 in the attachment section.

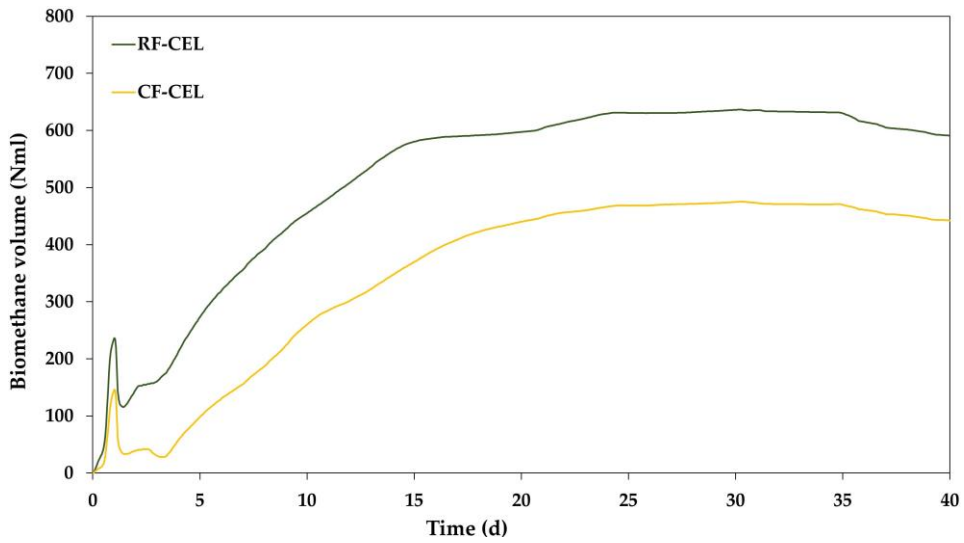


**Figure 4.4: Blank adjusted biomethane potential of cellulase–added samples with high suspended solids (RF–CEL) and low suspended solids (CF–CEL).**

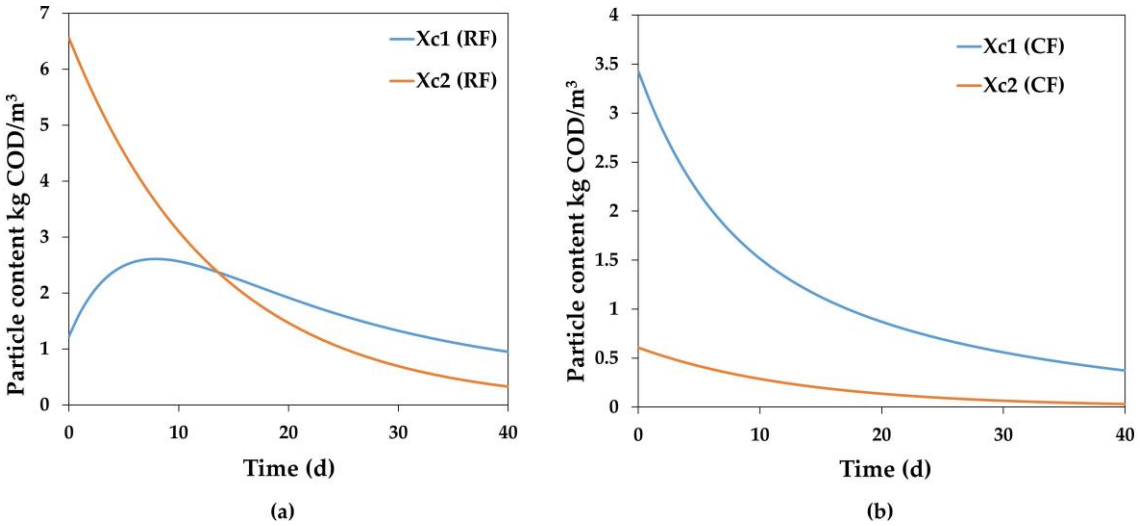


**Figure 4.5: Mode 2 simulation for particulate degradation of samples with high suspended solids: RF (a) and low suspended solids: CF (b).**

## 4.4 Influences of temperature and feed particle content on granular sludge bed anaerobic digestion

This article investigates the influences of temperature and particle content on anaerobic digestion in a continuous flow lab-scale reactor using manure supernatant as a substrate. The experiment was carried out in four phases by varying reaction temperature (25–35 °C) and substrate particle content (low–high particle content). The results show that biogas production increased with temperature in both high and low particle content substrates, however, the temperature effect was stronger on high particle content substrate (Figure 4.6).

At 25 °C, both high and low particle content substrates produced a comparable amount of biogas suggesting that biogas at this temperature came mainly from the digestion of small particles and soluble components present in similar quantities in both substrates (Table 4.1). At 35 °C, substrates with high particle content (RF) showed significantly higher biogas production than those with low particle content (CF), which was attributed to increased (temperature-dependent) disintegration of larger solid particulates.

**Table 4.1: Biogas flow rate and methane yield of samples at 25 °C and 35 °C.**

| | Average biogas flow rate (L/d) | | | | | | Methane yield (L $CH_4$/gVSS) | |
|---|---|---|---|---|---|---|---|---|
| | Experimental | | Simulation | | | | | |
| | | | Mode 1 | | Mode 2 | | | |
| **Substrate** | **25 °C** | **35 °C** | **25 °C** | **35 °C** | **25 °C** | **35 °C** | **25 °C** | **35 °C** |
| RF | 2.1±0.5 | 3.7±0.2 | 2.7±0.3 | 2.6±0.6 | 2.5±0.4 | 3.0±0.9 | 0.41 | 0.71 |
| CF | 2.4±0.2 | 3.3±0.9 | 2.4±0.1 | 2.5±0.1 | 2.8±0.0 | 4.7±0.8 | 0.76 | 1.06 |

N.B. The average biogas flow rate of RF at 35 °C (Phase 1) was calculated after the flow rate was stabilized, hence flow rates from the first 5 days were not included in the calculation.

In Phase 1, with RF at 35 °C, biogas production reached a maximum of 3.9 L/d, which immediately dropped to 1.4 L/d when the temperature was decreased to 25 °C in Phase 2. However, biogas production gradually increased to 2.5 L/d during Phase 2. Transition from Phase 2 to 3 did not result in a noticeable decrease in biogas production even if CF was used instead of RF, suggesting that the biogas production in both RF and CF at 25 °C was primarily from soluble components (i.e RF particulates are underutilized which otherwise would have achieved a much higher biogas production than CF as expected based on the much higher COD content of RF). The transition from Phase 3 to 4 was carried out by increasing the temperature from 25 °C to 35 °C while CF remains the substrate. Increased biogas production, characterized also by larger fluctuations, was observed. However, the average biogas production was 11% less than the average production observed in Phase 1.

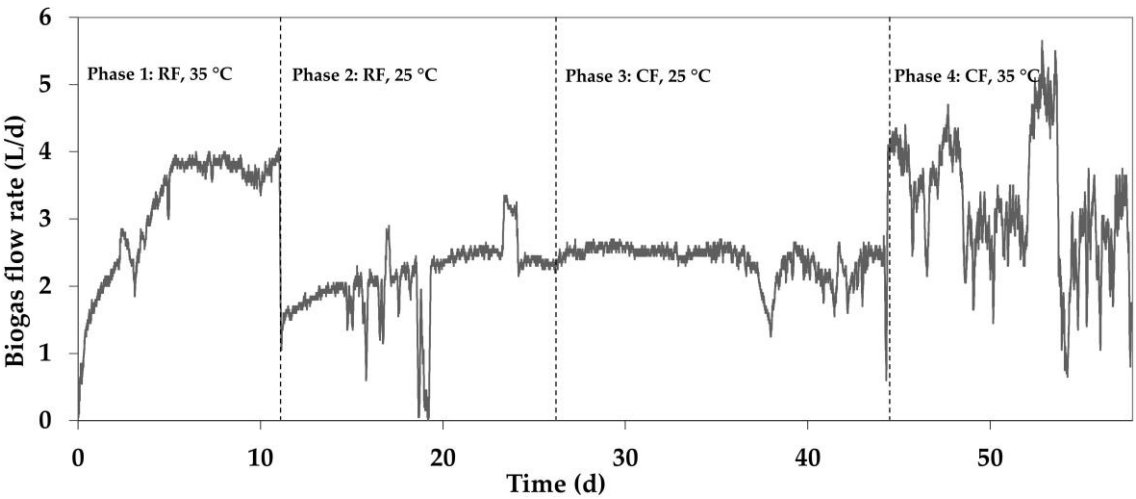


**Figure 4.6: Biogas flow rate in four phases of the experiment.**

Mode 1 and Mode 2 simulations described in section 4.3 were applied to this case also. Comparison of the two modes of simulations revealed that classification of particles into fast and slow disintegrating fractions (Mode 2) leads to a better representation of the experimental data compared to Mode 1 simulation across all four phases of the experiment (Figure 4.7). Mode 2 simulation showed a more efficient particulate removal and sensitivity to changes in temperature and particulate content than Mode 1 simulation.

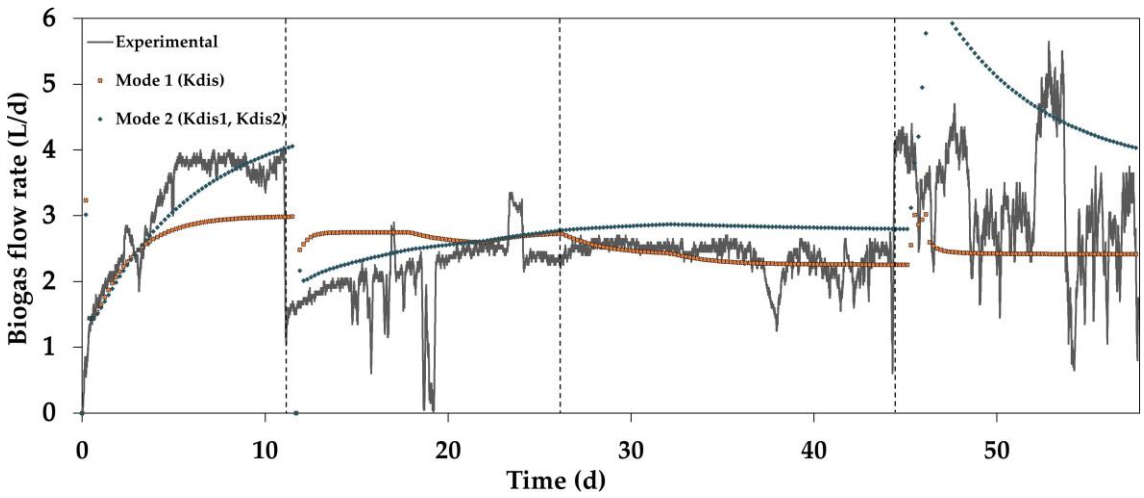


**Figure 4.7: Comparison of Mode 1 and Mode 2 simulations with the experimental data.**

## 4.5 Results from milling experiments

Milling experiment described in section 3.2.5 revealed that the total volume of methane produced from each sample groups varies (Figure 4.8). The methane volume from the blank sample was subtracted from the volume of methane produced by other samples. The specific methane production of each sample was calculated as normal volume in millilitres (Nml, volume at 0 °C and 1 atm) per gram of volatile solids (VS). The total solid content of the original and sieved feed samples was compared. Unsurprisingly, the total solid content of sieved samples was lower than the original samples. However, the extent of decrease in TS content varies from sample to sample.

The largest decrease was found in pump feed samples whereas the smallest decrease was observed in milled samples. The total solid content decreased by 30.1% from PF–O to PF–S, by 20.6% from RF–O to RF–S and by 8.3% from MF–O to MF–S. Milling reduced particle sizes considerably and allowed over 91% of the solid particles to pass through a sieve of 0.85 mm size. Minimal increase in VS content was observed from original to sieved samples and in each case, the increase is less than 6%. The decrease in the total solid content seemed to be reflected on the total COD content of the samples, particularly in the milled samples. The total COD decreased 63.4% from RF–O to RF–S, 6.0% from MF–O to MF–S and 41.2% from PF–O to PF–S. The ratio of VS to TS was also compared for all samples. Sieved samples were found to have higher VS/TS ratios than the original samples. The values were 28% (RF–O), 37% (RF–S), 22% (MF–O), 25% (MF–S), 29% (PF–O) and 42% (PF–S). The ultimate biomethane volume produced (in ml) after 40 days was 1063 for RF-O, 1158 for MF-O and 1055 for PF-O. For the sieved samples, it was 1134, 1052 and 1100 ml for RF-S, MF-S and PF-S respectively.

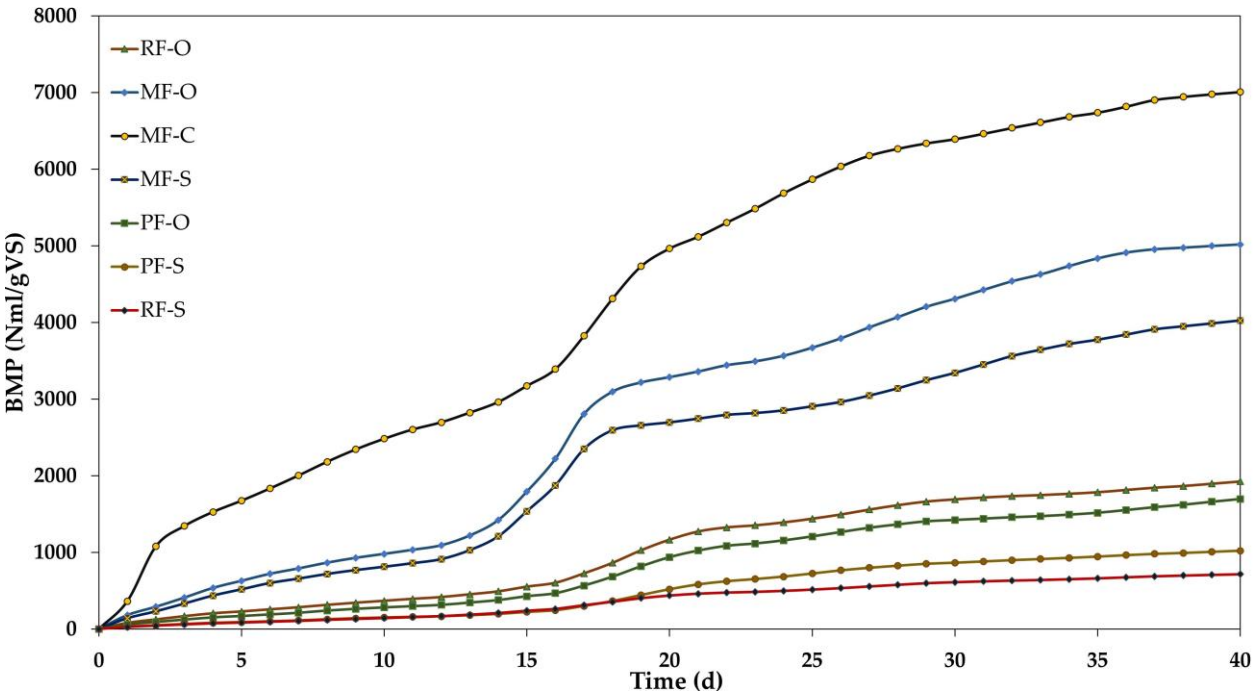


**Figure 4.8: Biomethane potential from the Milling experiment (not published).**

# 5 Conclusions

In this chapter, a summary of conclusions drawn from published articles and experiments from unpublished works are presented. It was shown that size distribution and settling velocity of granules in anaerobic reactors can be effectively measured based on image analysis. High-rate anaerobic digestion of particle-rich substrates has been considered challenging due to slow particle disintegration and hydrolysis which often lead to solid accumulation and eventual process failure. Based on literature review, reactor simulations, batch and continuous reactor experiments, this work showed that particle-rich substrates can be processed in anaerobic sludge bed reactors without process failure. Experiments carried out on the effect of substrate milling on biomethane production (unpublished work) showed that milling was an effective pretreatment method to reduce substrate particle sizes. It was also shown that the ultimate biomethane production was improved in terms of volume of biomethane. However, the high energy input required to mill the substrate may limit its economic feasibility. Altogether the work presented here demonstrates that it is possible to improve energy recovery from particle-rich slurries by high-rate sludge bed AD treatment. The conclusions made from each published article is presented below:

## 5.1 Article 1: Settling velocity and size distribution measurement of anaerobic granular sludge using microscopic image analysis

In this article, size distribution and settling velocity of granules from a lab-scale reactor and industry reactors were studied and the following conclusions were made:

- The shape factor and equivalent diameter used in this article are demonstrated to be a good way to quantify size distribution and settling velocity of granules from granular sludge bed reactors.
- Size and shape of UASB granules vary across a reactor height. Both size and shape factor increases from the top section to the bottom section of a reactor.

- Settling velocity of UASB granules depend not only on their size and density but also on the shape of the granules, which varies significantly between reactors.

## 5.2 Article 2: Granular sludge bed processes in anaerobic digestion of particle-rich substrates

This review paper assesses the state of high-rate digestion of particle-rich substrates. Successful high-rate AD of particle-rich substrates with TS content as high as 35% is possible in dry digestion processes as demonstrated by various authors. In conventional high-rate reactors such as UASB, the TS limit seemed to be around 10% TS, above which mass transfer limitation becomes a problem. Some forms of reactor modification are usually applied for high TS cases and there may be HRT or OLR restrictions due to the high solid content of the substrates. We further conclude that:

- High-rate anaerobic digestion of particle-rich substrates has the potential to increase biogas production significantly due to the abundance of such substrates.
- Economically sustainable methods of pretreatment are limited and several methods have been tried to improve the hydrolysis of solid particulates with varying degree of success (e.g., use of hydrolytic enzymes).
- Slow disintegration and hydrolysis of particulates is the main bottleneck in fully achieving the biogas potential of particle-rich substrates in high-rate sludge bed processes.
- Disintegration and hydrolysis of particulates within high-rate AD appear more promising than feed pretreatment.
- High-rate AD is traditionally assumed to only handle low particulate levels such as in industrial wastewater while newer studies show that high-rate reactors, especially hybrid types, may handle high levels of particulates.
- The degree of particle degradation within AD depends mainly on retention time so the challenge is to obtain long SRT in reactors with low HRT (SRT > HRT).
- Feed particles have typically much lower density than granular sludge and may therefore not be retained by the same mechanisms and reactor configurations as the granules. They may float when associated with biogas bubbles.

- Devices to retain floating sludge may, therefore, be required to obtain efficient disintegration and hydrolysis of particulates.
- There is evidence that the bacteria in the outer layer of granules can use extracellular polymeric structures to attach particles for the purpose of retaining and digesting feed particles.
- Disintegration and hydrolysis are treated as a single step in some models when they are both assumed to have first-order kinetics and this works well for non-complex substrates. Most particle-rich substrates are however quite complex and a wide range of models are proposed to handle such but more research is needed to find the best modeling approach. The relevance is emphasized by the fact that these are often the rate-limiting steps of the entire AD process on particle-rich substrates. Modified first-order kinetics that classifies solid particles into fast and slow disintegrating fractions may be a good approach for particle-rich substrates since it retains the simplicity of first-order kinetics and improves simulation accuracy.

## 5.3 Article 3: Effect of particulate disintegration on biomethane potential of particle-rich substrates in batch anaerobic reactor

After conducting batch reactor tests and analyzing results from substrates with high– and low suspended particle contents with and without enzyme addition, the following was concluded:

- High biomethane production was observed in samples with higher particle content however, specific biomethane yield was low compared to samples with low particle contents.
- Centrifugation of feed to remove particles decreased the volume of methane produced but increased the rate of methane production regardless of the addition of cellulase.

- Cellulase addition improved overall and specific methane productions both in raw and centrifuged samples but the improvement was higher in raw samples that contained higher suspended solids.
- Simulation results revealed that classifying complex particulates into fast and slow disintegrating fractions led to more accurate modeling of digestion of particle-rich substrates.

## 5.4 Article 4: Influences of temperature and feed particle content on granular sludge bed anaerobic digestion

Anaerobic digestion experiments using lab-scale UASB reactor on two sets of feed samples with varying level of suspended solids and digestion temperature revealed influences of temperature and particulate content on sludge bed anaerobic digestion. The experiments and simulations carried out and the results obtained led to the following conclusions:

- Increase in temperature increased the overall biogas production in both high and low particulate content substrates but the temperature effect was stronger on high particle content substrates.
- Disintegration and hydrolysis of suspended solids were significantly enhanced by temperature increase from 25 to 35 °C.
- Methane yields were significantly higher for the low particulate sample (CF) than the high particulate sample (RF) both at 25 and 35 °C.
- Particulate and COD removal efficiencies were improved at the higher temperature. $COD_{total}$ removal efficiency improved from 44% at 25 °C to 73% at 35 °C for the high particulate substrate and from 43% at 25 °C to 54% at 35 °C for the low particulate substrate. $COD_{soluble}$ removal efficiencies were also improved at higher temperatures but they were approximately similar for both high and low particulate substrates.
- Classifying particulates into fast and slow disintegrating and applying temperature-dependent disintegration constant values ($K_{dis}$) fit the experimental data better than the traditional ADM1 method of simulation.

## 5.5 Suggestions for future work

In this dissertation, the experimental work and the results presented are carried out in batch and continuous lab-scale reactors with limited volumes and their applicability to large-scale reactors may be somewhat limited. Application of the experimental and simulation methods to investigate the disintegration of particulates in full-scale reactors is suggested for future works. The intention was to carry out such work on the farm scale pilot ABR mentioned under methods (Section 3.1.1) but this was not achieved due to technical problems beyond my control. As a result, I specifically suggest the investigation of disintegration and hydrolysis of suspended particles as well as their interaction with granular sludge beds in full-scale reactors. The effect of temperature and particle size/content on disintegration and hydrolysis of particle-rich substrates has been addressed in this dissertation. Other factors that affect disintegration and hydrolysis especially the influence of physical parameters and reactor conditions have not been included in this work. I, especially, suggest future investigations on the influence of loading and flow rates on disintegration and hydrolysis of particle-rich substrates in full-scale reactors. The economic feasibility of measures to enhance particle utilization by methods investigated here (enzymes and milling), in full-scale reactors should also be further investigated, given the large biogas potential of such substrates.

# References

[1] S. Shafiee and E. Topal, "When will fossil fuel reserves be diminished?," *Energy Policy*, vol. 37, no. 1, pp. 181–189, 2009.

[2] Karl. R. T. and Trenberth. E. K., "Modern global climate change," *Science (80-. ).*, vol. 302, no. 5651, pp. 1719–1723, 2003.

[3] O. Ellabban, H. Abu-Rub, and F. Blaabjerg, "Renewable energy resources: Current status, future prospects and their enabling technology," *Renew. Sustain. Energy Rev.*, vol. 39, pp. 748–764, 2014.

[4] C.-J. Winter, R. L. Sizmann, and L. L. Vant-Hull, *Solar power plants: fundamentals, technology, systems, economics*. Springer Science & Business Media, 2012.

[5] S. Mathew, *Wind energy: fundamentals, resource analysis and economics*, vol. 1. Springer, 2006.

[6] C. Zarfl, A. E. Lumsdon, J. Berlekamp, L. Tydecks, and K. Tockner, "A global boom in hydropower dam construction," *Aquat. Sci.*, vol. 77, no. 1, pp. 161–170, 2014.

[7] D. Rutz and J. Rainer, "Biofuel Technology Handbook," pp. 1–149, 2007.

[8] REN21 2018, "Renewables 2018 Global status report," Paris, 2018.

[9] IRENA (2018), *Renewable capacity statistics 2018*. Abh Dhabi: International Renewable Energy Agency (IRENA), 2018.

[10] Food and Agriculture Organization of the United Nations, "Definitions | Energy | Food and Agriculture Organization of the United Nations." [Online]. Available: http://www.fao.org/energy/home/definitions/en/. [Accessed: 04-Jan-2019].

[11] A. Dahiya, *Bioenergy : biomass to biofuels*. Elsevier Inc., 2015.

[12] P. McKendry, "Energy production from biomass (part 2): conversion technologies," *Bioresour. Technol.*, vol. 83, no. July 2001, pp. 47–54, 2002.

[13] S. M. Tauseef, T. Abbasi, and S. A. Abbasi, "Energy recovery from wastewaters with high-rate anaerobic digesters," *Renew. Sustain. Energy Rev.*, vol. 19, pp. 704–741, 2013.

[14] USEPA, "Global Anthropogenic Non-CO2 Greenhouse Gas Emissions : 1990 - 2030," Washington DC, 2011.

[15] D. J. Batstone *et al.*, "The IWA Anaerobic Digestion Model No 1 (ADM1).," *Water Sci. Technol.*, vol. 45, no. 10, pp. 65–73, 2002.

[16] K. Küsel and H. L. Drake, "Acetogens BT - Encyclopedia of Geobiology," J. Reitner and V. Thiel, Eds. Dordrecht: Springer Netherlands, 2011, pp. 1–5.

[17] R. Kleerebezem, L. W. Hulshoff Pol, and G. Lettinga, "Energetics of product formation during anaerobic degradation of phthalate isomers and benzoate," *FEMS Microbiol. Ecol.*, vol. 29, no. 3, pp. 273–282, 1999.

[18] C. H. Burton and C. Turner, *Manure management: Treatment strategies for sustainable agriculture*. Editions Quae, 2003.

[19] T. Bond and M. R. Templeton, "History and future of domestic biogas plants in the developing world," *Energy Sustain. Dev.*, vol. 15, no. 4, pp. 347–354, 2011.

[20] K. Rajendran, S. Aslanzadeh, and M. J. Taherzadeh, "Household biogas digesters—A review," *Energies*, vol. 5, no. 8, pp. 2911–2942, 2012.

[21] J. B. van Lier, F. P. van der Zee, C. T. M. J. Frijters, and M. E. Ersahin, "Celebrating 40 years anaerobic sludge bed reactors for industrial wastewater treatment," *Rev. Environ. Sci. Biotechnol.*, vol. 14, no. 4, pp. 681–702, 2015.

[22] W. H. Bergland, C. Dinamarca, M. Toradzadegan, A. S. R. Nordgård, I. Bakke, and R. Bakke, "High rate manure supernatant digestion," *water Res.*, vol. 76, pp.

1–9, 2015.

[23] I. W. Koster and G. Lettinga, "Anaerobic digestion at extreme ammonia concentrations," *Biol. Wastes*, vol. 25, no. 1, pp. 51–59, 1988.

[24] Y. Chen, J. J. Cheng, and K. S. Creamer, "Inhibition of anaerobic digestion process: a review," *Bioresour. Technol.*, vol. 99, no. 10, pp. 4044–4064, 2008.

[25] S. K. Bhattacharya, M. Qu, and R. L. Madura, "Effects of nitrobenzene and zinc on acetate utilizing methanogens," *Water Res.*, vol. 30, no. 12, pp. 3099–3105, 1996.

[26] G. E. Symons and A. M. Buswell, "The Methane Fermentation of Carbohydrates," *J. Am. Chem. Soc.*, vol. 55, no. 5, pp. 2028–2036, 1933.

[27] T. Z. D. De Mes, A. J. M. Stams, J. H. Reith, and G. Zeeman, "Methane production by anaerobic digestion of wastewater and solid wastes," *Bio-methane & Bio-hydrogen*, pp. 58–102, 2003.

[28] N. Kythreotou, G. Florides, and S. A. Tassou, "A review of simple to scientific models for anaerobic digestion," *Renew. Energy*, vol. 71, pp. 701–714, 2014.

[29] J. C. Young and P. L. McCarty, "The anaerobic filter for waste treatment," *J. (Water Pollut. Control Fed.*, pp. R160–R173, 1969.

[30] P. A. Alphenaar, *Anaerobic granular sludge: characterization, and factors affecting its functioning*. Alphenaar, 1994.

[31] L. W. Hulshoff Pol, S. I. De Castro Lopes, G. Lettinga, and P. N. L. Lens, "Anaerobic sludge granulation," *Water Res.*, vol. 38, no. 6, pp. 1376–1389, 2004.

[32] S. McHugh, C. O'reilly, T. Mahony, E. Colleran, and V. O'flaherty, "Anaerobic granular sludge bioreactor technology," *Rev. Environ. Sci. Biotechnol.*, vol. 2, no. 2–4, pp. 225–245, 2003.

[33] F. A. MacLeod, S. R. Guiot, and J. W. Costerton, "Layered structure of bacterial aggregates produced in an upflow anaerobic sludge bed and filter reactor," *Appl.*

*Environ. Microbiol.*, vol. 56, no. 6, pp. 1598–1607, 1990.

[34] Y. Liu, Y. He, S. Yang, and Y. Li, "The settling characteristics and mean settling velocity of granular sludge in upflow anaerobic sludge blanket (UASB)-like reactors," *Biotechnol. Lett.*, vol. 28, no. 20, pp. 1673–1678, 2006.

[35] A. P. H. Association and A. W. W. Association, *Standard methods for the examination of water and wastewater*. American public health association, 1989.

[36] G. Lettinga, A. F. M. Van Velsen, S. W. de Hobma, W. De Zeeuw, and A. Klapwijk, "Use of the upflow sludge blanket (USB) reactor concept for biological wastewater treatment, especially for anaerobic treatment," *Biotechnol. Bioeng.*, vol. 22, no. 4, pp. 699–734, 1980.

[37] G. R. Zoutberg and P. de Been, "The Biobed® EGSB (Expanded Granular Sludge Bed) system covers shortcomings of the upflow anaerobic sludge blanket reactor in the chemical industry," *Water Sci. Technol.*, vol. 35, no. 10, pp. 183–188, 1997.

[38] W. P. Barber and D. C. Stuckey, "The use of the anaerobic baffled reactor (ABR) for wastewater treatment: a review," *Water Res.*, vol. 33, no. 7, pp. 1559–1578, 1999.

[39] I. Angelidaki, B. K. Ahring, H. Deng, and J. E. Schmidt, "Anaerobic digestion of olive oil mill effluents together with swine manure in UASB reactors," *Water Sci. Technol.*, vol. 45, no. 10, pp. 213–218, 2002.

[40] M. Von Sperling, *Wastewater characteristics, treatment and disposal*. IWA publishing, 2017.

[41] J. Yi, B. Dong, J. Jin, and X. Dai, "Effect of increasing total solids contents on anaerobic digestion of food waste under mesophilic conditions: performance and microbial characteristics analysis," *PLoS One*, vol. 9, no. 7, p. e102548, 2014.

[42] E. Metcalf and M. Eddy, "Wastewater engineering: treatment and Resource recovery," *Mic Graw-Hill, USA*, pp. 1530–1533, 2014.

[43] H. B. Møller, S. G. Sommer, and B. K. Ahring, "Methane productivity of manure, straw and solid fractions of manure," *Biomass and Bioenergy*, vol. 26, no. 5, pp. 485–495, 2004.

[44] D. T. Hill, "Simplified monod kinetics of methane fermentation of animal wastes," *Agric. Wastes*, vol. 5, no. 1, pp. 1–16, 1983.

[45] R. Campuzano and S. González-Martínez, "Characteristics of the organic fraction of municipal solid waste and methane production: A review," *Waste Manag.*, vol. 54, pp. 3–12, 2016.

[46] J. D. Browne and J. D. Murphy, "Assessment of the resource associated with biomethane from food waste," *Appl. Energy*, vol. 104, pp. 170–177, 2013.

[47] P. Fongsatitkul, P. Elefsiniotis, and D. G. Wareham, "Effect of mixture ratio, solids concentration and hydraulic retention time on the anaerobic digestion of the organic fraction of municipal solid waste," *Waste Manag. Res.*, vol. 28, no. 9, pp. 811–817, 2010.

[48] M. J. Chin, P. E. Poh, B. T. Tey, E. S. Chan, and K. L. Chin, "Biogas from palm oil mill effluent (POME): Opportunities and challenges from Malaysia's perspective," *Renew. Sustain. Energy Rev.*, vol. 26, pp. 717–726, 2013.

[49] T. Y. Wu, A. W. Mohammad, J. M. Jahim, and N. Anuar, "A holistic approach to managing palm oil mill effluent (POME): Biotechnological advances in the sustainable reuse of POME," *Biotechnol. Adv.*, vol. 27, no. 1, pp. 40–52, 2009.

[50] R. Braun, P. Weiland, and A. Wellinger, "Biogas from energy crop digestion," in *IEA bioenergy task*, 2008, vol. 37, pp. 1–20.

[51] J. Pinnekamp, "Effects of thermal pretreatment of sewage sludge on anaerobic digestion," *Water Sci. Technol.*, vol. 21, no. 4–5, pp. 97–108, 1989.

[52] I. Ferrer, S. Ponsá, F. Vázquez, and X. Font, "Increasing biogas production by thermal (70 C) sludge pre-treatment prior to thermophilic anaerobic digestion,"

*Biochem. Eng. J.*, vol. 42, no. 2, pp. 186–192, 2008.

[53] S. Pilli, S. Yan, R. D. Tyagi, and R. Y. Surampalli, "Thermal pretreatment of sewage sludge to enhance anaerobic digestion: A review," Crit. Rev. Environ. Sci. Technol., vol. 45, no. 6, pp. 669–702, 2015.

[54] L. F. R. Montgomery and G. Bochmann, "Pretreatment of feedstock for enhanced biogas production Pretreatment of feedstock for enhanced biogas production (electronic version)," 2014.

[55] M. T. Myint and N. Nirmalakhandan, "Enhancing anaerobic hydrolysis of cattle manure in leachbed reactors," *Bioresour. Technol.*, vol. 100, no. 4, pp. 1695–1699, 2009.

[56] A. I. Hatakka, "Pretreatment of wheat straw by white-rot fungi for enzymic saccharification of cellulose," *Eur. J. Appl. Microbiol. Biotechnol.*, vol. 18, no. 6, pp. 350–357, 1983.

[57] J. Speda, M. A. Johansson, A. Odnell, and M. Karlsson, "Enhanced biomethane production rate and yield from lignocellulosic ensiled forage ley by in situ anaerobic digestion treatment with endogenous cellulolytic enzymes," *Biotechnol. Biofuels*, vol. 10, no. 1, p. 129, 2017.

[58] J. Mata-Alvarez, J. Dosta, M. S. Romero-Güiza, X. Fonoll, M. Peces, and S. Astals, "A critical review on anaerobic co-digestion achievements between 2010 and 2013," *Renew. Sustain. Energy Rev.*, vol. 36, pp. 412–427, 2014.

[59] M. J. Cuetos, C. Fernández, X. Gómez, and A. Morán, "Anaerobic co-digestion of swine manure with energy crop residues," *Biotechnol. Bioprocess Eng.*, vol. 16, no. 5, p. 1044, 2011.

[60] X. Wu, W. Yao, and J. Zhu, "Biogas and CH4 productivity by co-digesting swine manure with three crop residues as an external carbon source," in *2010 Pittsburgh, Pennsylvania, June 20-June 23, 2010*, 2010, p. 1.

[61] S. Sayed, W. de Zeeuw, and G. Lettinga, "Anaerobic treatment of slaughterhouse waste using a flocculant sludge UASB reactor," *Agric. Wastes*, vol. 11, no. 3, pp. 197–226, 1984.

[62] G. Boari, A. Brunetti, R. Passino, and A. Rozzi, "Anaerobic digestion of olive oil mill wastewaters," *Agric. Wastes*, vol. 10, no. 3, pp. 161–175, 1984.

[63] G. Zeeman, W. T. M. Sanders, K. Y. Wang, and G. Lettinga, "Anaerobic treatment of complex wastewater and waste activated sludge–application of an upflow anaerobic solid removal (UASR) reactor for the removal and pre-hydrolysis of suspended COD," *Water Sci. Technol.*, vol. 35, no. 10, pp. 121–128, 1997.

[64] N. Mahmoud, G. Zeeman, H. Gijzen, and G. Lettinga, "Solids removal in upflow anaerobic reactors, a review," *Bioresour. Technol.*, vol. 90, no. 1, pp. 1–9, 2003.

[65] S. K. Sharma, I. M. Mishra, M. P. Sharma, and J. S. Saini, "Effect of particle size on biogas generation from biomass residues," *Biomass*, vol. 17, no. 4, pp. 251–263, 1988.

[66] M. J. Taherzadeh and K. Karimi, *Pretreatment of lignocellulosic wastes to improve ethanol and biogas production: A review*, vol. 9, no. 9. 2008.

[67] J. G. Usack, W. Wiratni, and L. T. Angenent, "Improved design of anaerobic digesters for household biogas production in Indonesia: one cow, one digester, and one hour of cooking per day," *Sci. World J.*, vol. 2014, 2014.

[68] A. A. Forbis-Stokes, P. F. O'Meara, W. Mugo, G. M. Simiyu, and M. A. Deshusses, "On-site fecal sludge treatment with the anaerobic digestion pasteurization latrine," *Environ. Eng. Sci.*, vol. 33, no. 11, pp. 898–906, 2016.

[69] G. Lettinga and L. W. Hulshoff Pol, "USAB-process design for various types of wastewaters," *Water Sci. Technol.*, vol. 24, no. 8, pp. 87–107, 1991.

# Attachments

## Article 1:

## Settling velocity and size distribution measurement of anaerobic granular sludge using microscopic image analysis.

Tassew, F.A., Bergland, W.H., Dinamarca, C. and Bakke, R., 2019. Settling velocity and size distribution measurement of anaerobic granular sludge using microscopic image analysis. Journal of microbiological methods, 159, pp.81–90. https://doi.org/10.1016/j.mimet.2019.02.013

Journal of Microbiological Methods 159 (2019) 81–90

Contents lists available at ScienceDirect

Journal of Microbiological Methods

journal homepage: www.elsevier.com/locate/jmicmeth

# Settling velocity and size distribution measurement of anaerobic granular sludge using microscopic image analysis

Fasil A. Tassew*, Wenche Hennie Bergland, Carlos Dinamarca, Rune Bakke

*Department of Process, Energy and Environmental Technology, University of South-Eastern Norway, Kjølnes ring 56, NO 3918 Porsgrunn, Norway*

ARTICLE INFO

*Keywords:*
Settling velocity
Anaerobic granule
Size distribution
Biogas reactor
Image analysis
Shape factor

ABSTRACT

Settling velocity and size distribution of anaerobic granular sludge samples were studied using microscopic image analysis and settling column experiments. Five granule samples were considered in this study. Three samples were collected at the Top, Middle and Bottom sections of a lab scale upflow anaerobic sludge bed reactor (UASB). Two other granule samples were obtained from industries. This paper aims to establish a method that uses microscopic image analysis and shape factor as a tool to determine the size distribution and settling velocity of anaerobic granules. Image analysis technique was used to calculate the shape factor and equivalent diameter of granules. The equivalent diameter was then used to calculate the theoretical settling velocities based on Allen's formula and estimate size distributions.

The results showed that there was a good agreement between the theoretical and experimental mean settling velocity values. Both measured and calculated settling velocities increased with increasing Reynolds number (*Re*). However, the agreement between measured and calculated values was found to be weaker at higher *Re* values. Size distribution analyses of the granules have revealed that there was significant difference in the size distribution of granule samples collected at different heights of the lab scale reactor. Overall, granules from the bottom section of the reactor had larger diameter, settling velocity and shape factor than those at the middle and top section granules. Whereas granules collected from the top section exhibited the smallest granular diameter, settling velocity and shape factor.

## 1. Introduction

Settling velocity of anaerobic granular sludge is an important characteristic of a UASB reactor. The resistance of anaerobic granules to washout and remain in the reactor is the main reason for the success of UASB systems. Several factors, ranging from fluid and flow properties to granule size and density influence the settling property of granules. Biogas production process involves a complex set of anaerobic biochemical reactions that result in the breakdown of organic compounds into smaller molecules. This process results in biomass growth (change in the granule size and density) and production of gas, which influences settleability of granules as the process progresses. As a result, it is important to monitor the settling behaviour of granules regularly. Several different methods have been used to measure settling velocity. For example, Ahn and Speece (2003) and Vlyssides et al. (2008) estimated settling velocity of granules by measuring the percentage of washed-out granules when a given up-flow velocity is applied at the bottom of granular sludge bed. Others, such as Ghangrekar et al. (2005), used a glass column to measure settling velocity based on the fraction of granules settled in a given time interval. In this article, the settling velocities of anaerobic granules were directly measured in a settling column using a high-speed camera. Microscopic image analysis was used to quantify granule perimeter, area, shape factor and equivalent diameter to estimate size distribution and theoretical settling velocity. Although there have been works that used image analysis to estimate particulate size (Thaveesri et al., 1995; Tang et al., 2011; Alves et al., 2000; Bellouti et al., 1997), the author of this article has not found studies that applied the granule shape factor method as used in the present article for the study of size distribution and settling velocity of granules from UASB reactors. A correlation of settling velocity of granules and the reactors' flow parameters such as Reynolds number (*Re*) was established.

### 1.1. Settling velocity

Granules settling in a liquid experience three main forces acting upon them: gravity, buoyancy and drag forces. Depending on the type of the flow regime, theoretical calculations of terminal/settling velocity

* Corresponding author.
*E-mail address:* fasil.a.tassew@usn.no (F.A. Tassew).

https://doi.org/10.1016/j.mimet.2019.02.013
Received 31 January 2019; Received in revised form 21 February 2019; Accepted 21 February 2019
Available online 22 February 2019
0167-7012/ © 2019 Elsevier B.V. All rights reserved.

($V_t$) of a granule vary. Early papers about granule settling used Stokes flow ($Re < 1$) for granule settlement calculations (Gupta and Gupta, 2005; Laguna et al., 1999). However, this may not be accurate since it has been shown that the Reynolds number of anaerobic granular sludges in typical UASB reactor conditions falls in the intermediate flow regime category ($Re$ between 1 and 500). Allen's formula has been used to calculate settling velocity of granules in the intermediate flow regime [Liu et al., 2006]. It was derived by inserting the drag coefficient ($C_d$) equation for intermediate regimes into the general terminal velocity equation:

$$V_t = \sqrt{\frac{4g(\rho_g - \rho_f)}{3C_d\rho_f}} \quad (1)$$

$$C_d = 18.5Re^{-0.6} \quad (2)$$

$$Re = \frac{\rho_f D_g V_t}{\mu_f} \quad (3)$$

$$V_t = 0.781\left[\frac{D_g^{1.6}(\rho_g - \rho_f)}{\rho_g^{0.4}\mu_f^{0.6}}\right]^{0.714} \quad (4)$$

Where, D is diameter, ρ is density, μ is viscosity and the subscripts g and f denote granule and fluid respectively. The above equations are formulated assuming that particles are spherical in shape, hence settling velocity calculation for granules have to include a factor for the non-sphericity of the granules. The equation for terminal velocity includes a term for drag coefficient and the drag coefficient equation includes a term for Reynolds number. However, Reynolds number is calculated using terminal velocity value. This is a form of "circular equation" and has to be solved iteratively until the correct values for Re, $V_t$ and $C_d$ are found (Dietrich, 1982).

### 1.2. Granule size distribution

Size and shape of a granule along with density all but determine what the settling behavior of the granule will be. Anaerobic granules are usually assumed to be spherical with a diameter ranging from 0.5–5 mm. Granule size is one of the most important factors in UASB reactors. It has been shown that size of granules affect most aspects of a UASB reactor performance (Wu et al., 2016). The size of granules change during the course of the biogas production process due to microbial growth and decay, granular shear-off, granule-granule collision and granule-wall collisions. As a result, it is important to monitor changes in granule size regularly. Theoretically, increase in the granule size can be estimated from bacterial yield coefficient, specific substrate utilization rate and specific endogenous decay rate. See Yan and Tay (1997).

There are different granule size measurement techniques. The two most often used techniques are the gravimetric method and image analsys methods. In the gravimetric method granular sizes are calculated indirectly from settling experiments (Grotenhuis et al., 1991). Whereas in the image analysis method granule sizes are directly measured from microscopic images using image processing software. Other methods such as Laser particle size analysis (Yan and Tay, 1997) and automated image analysis (Laguna et al., 1999) are also used. In this paper, equivalent diameter of granules were calculated from the perimeter and shape factor of two-dimensional granular images. Once diameters of the granules are known, the size distribution can be expressed in various ways (number, area or volume distributions). A reporting of the mean value alone may be enough for some applications but in this paper, we decided to report the granule size distribution as a number distribution since we believe it carries more information about the size of the granules. In this method, granules are grouped into size ranges and the number of granules in each size range is counted and plotted as a number frequency versus size range plot.

### 1.3. Image analysis

Microscopic image analysis has been used for the determination of size and shape of granule samples. The method is suited for granules that are non-spherical because it enables different definitions of granule sizes to be used to characterize samples (eg. Equivalent diameters) Olson (2011). The accuracy of the measurement depends on several factors such as microscope calibration and the quality of the images taken. The calibration step can be carried out using a standard micrometer ruler (e.g National Institute of Standards and Technology, NIST, traceable stage micrometer). The quality of the image can be affected by granule overlap, presence of bubbles, too much or too little lighting, non-granular solid materials etc.

## 2. Materials and methods

During the course of this study several different methods and equipments have been used. Microscopic image analysis was used to measure equivalent diameter of granules ($D_g$). Equivalent diameter of granules were used for size distribution plots and also to calculate theoretical settling velocity of granules. Experimental measurement of settling velocity was also carried out and compared with the theoretical settling velocity. Factors that affect the measurement methods are also described Fig. 1.

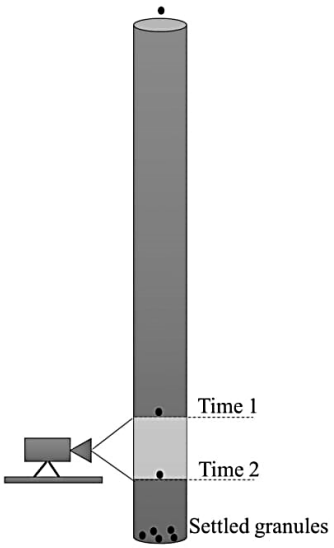


**Fig. 1.** A schematic diagram of settling velocity measurement set-up.

### 2.1. Sample source

The main source of the granular samples is a lab scale vertical UASB reactor that has been treating centrifuged pig manure collected from storage room from a farm near Porsgrunn, Norway. It has a height of 0.85 m, internal dimater of 4.4 cm and a total volume of 1.3 L. The reactor has been operated at an organic loading rate (OLR) of 3.1 Kg/$m^3$d, upflow velocity of 1.75 m/h and hydraulic retention time (HRT) of 5 days at 38C. It is equipped with a heating & recirculation and feed pumps. A biogas flow meter based on volumetric flow measurement was integrated (Dinamarca and Bakke, 2009). Data from temperature sensors and gas flow measurement were collected and monitored using LabVIEW software (LabVIEW 2014 and LabVIEW 2015). Granule samples were taken from three sampling portals in the reactor: Top section, Middle section and bottom section. See Fig. 2. In addition, two

other granule samples from industry were used. The first one is granule sample that has been treating wastewater from paper factory in an internal recirculation anaerobic reactor from Econvert Water & Energy, Netherlands. The other one is from Borregaard treatment plant, Norway. Granules from econvert are also used as a seeding granules for the lab scale reactor and their inclusion in the study will help in the investigation of the effect of reactor conditions on granule characteristics. The granule samples from Borregaard treatment plant are included in the study in part because upon visual inspection they appear to be comparatively flat, as opposed to spherical, than that of granule samples from the UASB reactor. The difference in size and particularly in shape would provide an opportunity to test the validity of the proposed method Table 1.

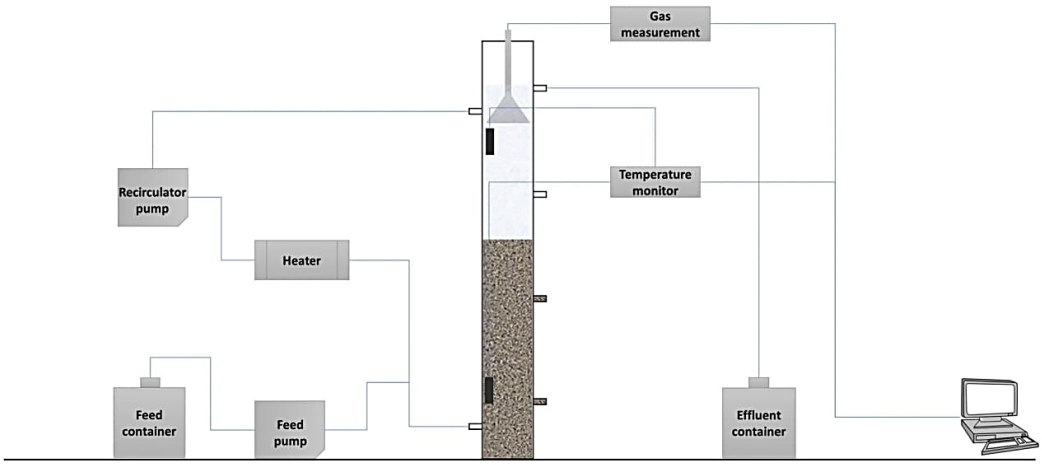


**Fig. 2.** A schematic diagram of lab scale UASB reactor.

**Table 1**
Description of anaerobic granular sludge samples. ($N_{Vt}$ and $N_{sd}$ are number of granules used in settling velocity and size distribution experiments respectively.)

| Sample | Origin | Days in reactor | $N_{Vt}$ | $N_{sd}$ |
|---|---|---|---|---|
| Fresh | Econvert | 0 | 200 | 50 |
| Top | Top sampling portal | 80 | 200 | 50 |
| Middle | Middle sampling portal | 80 | 200 | 50 |
| Bottom | Bottom sampling portal | 80 | 200 | 50 |
| Borregaard | Full scale reactor | 0 | 50 | 50 |

### 2.2. Image analysis

A calibrated Nikon microscope was used to take granular images. The images were taken in such a manner to avoid granule overlap and bubble formation. For granule samples from the lab scale UASB reactor images of up to 200 granule were taken. For Borregaard granule samples 50 images were taken. All images were preprocessed using a matlab code (MATLAB R2015a) to make them ready for size and shape measurement. Image preprocessing was done to separate adjacent granules, remove bubbles, adjust the lightening and eliminate non-granular solid materials. The perimeter, area and shape factor of granules in the preprocessed images were measured using a separate matlab code. The perimeter and area of granules were measured using built-in matlab functions whereas shape factors of the granule were measured according to the following steps: First, the code locates the centroid position of a granule, then all the distances from the centroid location to all the edge points of the granule are measured. The shape factor is then calculated as a standard deviation of all the distances from centroid location to each pixel at the edges of the image of the granule. Ideally, if a granule is spherical, then its two-dimensional image will be circular and all the distances from the centroid to the edges will be equal to its radius giving a standard deviation of zero. However, actual granules exhibit shapes that are different from spherical. As the granule shape becomes more and more irregular, the shape factor value increases. Fig. 3 illustrates the shape factor calculation scheme: The shape factor (SF) of a given granule is calculated by using the standard deviation equation used in matlab. It is given as:

$$SF = \sqrt{\frac{1}{N-1}\sum_{i=1}^{N} |A_i - A_{mean}|^2} \quad (5)$$

$$A_{mean} = \frac{1}{N}\sum_{i=1}^{N} A_i \quad (6)$$

Where: $A_i$ is an individual distance from a centroid of a granule to its edge, $A_{mean}$ is average of all distances from centroid to perimeter edges and N is the number of distances measured.

Calibration of the microscope was carried out for each magnification and zooming level using a standard micrometer ruler. The calibration data was then incorporated in to Matlab code so that granule size results can be converted from pixels to millimetres.

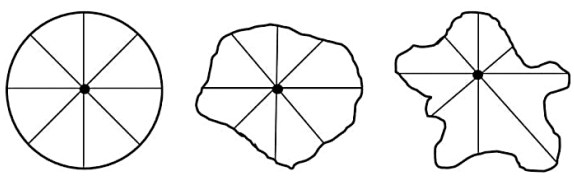

**Fig. 3.** Illustration of shape factor measurement.

### 2.3. Equivalent diameter

There are several methods to calculate equivalent diameter for non-spherical particles such as: Volume equivalent sphere diameter, surface equivalent sphere diameter, projected area diameter etc. One of these methods is based on the circularity of a particle. Circularity (C) of a particle is a measure of similarity of its shape to that of a perfect circle (Olson, 2011). It uses both the area ($S_A$) and perimeter (P) of the particle to estimate its circularity. ISO 9276:2008(en) is a standard from the international organization for standardization that deals with the quantitative representation of particle shape and morphology. In section six of the standard, the circularity of a particle is defined as:

$$C = \sqrt{\frac{4\pi S_A}{P^2}} \tag{7}$$

Podczeck and Newton (1995) suggested an equation for measurement of surface texture/roughness ($S_r$) based on the perimeter and mean of the distances from the centroid to the edge of the perimeter ($A_{mean}$).

$$S_r = \frac{2\pi A_{mean}}{P} \tag{8}$$

In this paper, a modified form of the above equation is used to estimate the equivalent granule diameter ($D_g$). It is based on granule perimeter (P) and its shape factor (SF):

$$D_g = \frac{P}{\pi}\left[\frac{1}{1+\sqrt{\frac{2\pi SF}{P}}}\right] \tag{9}$$

Bouwman et al. (2004) studied different types of shape factors used to analyse the shape of granules. The shape factors studied range from those based on aspect ratio of granular images to those based on Stoke's shape factor. They also studied radial shape factor that estimates the center of gravity of granule images to determine shape factor. Eq. (9) is based on a similar concept and can be considered as a modified form of the radial shape factor. For spherical granules Eq. (9) is equal to $P/\pi$. However, irregular shaped granules have larger perimeters than granules of similar projected area. For example, a circle and a square with 1 $m^2$ area will have a perimeter of ≈3.54 m and 4 m respectively. The term in the bracket in Eq. (9) accounts for the overestimation of diameter of irregularly shaped granules.

### 2.4. Settling velocity

Settling velocity of individual granules were measured using a 1.5 m glass column using a high-speed digital camera followed by image analysis. The settling column was made of a transparent glass and it is 1.5 m in height and 4.5 cm in diameter. The column was set up vertically and filled with tap water at room temperature. Individual granules were released carefully in the middle of the top of the water surface. Then the granules were allowed to settle. At 1.35 m from the top of the glass column, a tape with a known length (0.037 m) was attached in such a way to cover half the circumference of the glass column. Granules will accelerate until they attain a constant settling velocity. As a result, the measurement of settling velocity should be carried out after constant velocity is achieved. The settling column should be long enough to allow the granules to reach their constant settling velocities. Preliminary tests indicated that, granules of 0.5–5 mm diameter and 1050–1090 Kg/$m^3$ density travel around 0.5–1 m before attaining constant velocities. So, a distance of 1.35 m was assumed to be enough length for the granules to reach their settling velocities. Since the granules are black in color a contrasting white tape was used. A high-speed digital camera was placed in front of the tape. The camera recording was set to 50 frames per second (fps) for a precise resolution of time and distance when the granules cross the boundaries of the attached tape. Most of the granules were able to settle vertically without touching the column walls. Granules that touched or collided with the column surface were excluded from the measurement. Similarly, granules that settled without colliding with the wall but crossed the tape boundaries at non-vertical lines were excluded. To avoid hindered settling and influence due to possible particle collisions, individual granules were not allowed to settle in close proximity. Besides the parameters expressed in the previous equations, the settling velocity of granules can also be affected by factors such as shape, surface roughness, wall effect etc. Dietrich (1982) studied the effect of particle shape, roundedness and surface roughness, among others, on settling velocity. It was pointed out that when non-spherical particles settle they tend to orient their largest projected area against the direction of the flow (settling). This leads to a larger drag force and a decrease in the settling velocity of the particle compared to an equivalent particle with spherical shape. Similarly, surface roughness also leads to lower settling velocity by increasing the drag force, however, its effect is not thought to be as significant as particle shape Table 2.

**Table 2**
Theoretical and experimental settling velocity and density of granules.

| Granule | ρ(Kg/$m^3$) | Measured $V_t$ | Calculated $V_t$ |
|---|---|---|---|
| Fresh | 1070 | 63.14 | 66.97 |
| Top | 1075 | 45.02 | 45.93 |
| Middle | 1075 | 58.9 | 56.57 |
| Bottom | 1070 | 68.49 | 63.13 |
| Borregaard | 1015 | 61.95 | 58.54 |

### 2.5. Wall effect

Particles settling in a viscous fluid within a confined wall experience slower settling velocities than those of "free settling" particles (Chhabra et al., 2003). This is due to the wall-effect ($f_w$). Wall effect is usually defined as the ratio of terminal velocities of a particle settling in a confined wall ($V_t$) and a particle settling in a wall of infinite internal diameter ($V_\infty$). A number of papers have been published that deals with the estimation of the wall effect (Ataide et al., 1999; Zhang et al., 2016; Arsenijević et al., 2010). In those papers, β, a ratio of particle diameter (in this case, $D_g$) and diameter of the wall ($D_{pipe}$) was used as a starting point to estimate wall effect. Ataide et al. (1999) studied the wall effect over wide ranges of *Re* and *b* values and proposed Eq. (10) for theoretical estimation of wall effect and found a good fit ($R^2 = 0.96$) between experimental and predicted values. In this paper, wall effect was estimated based on the equation suggested for Re values between 0.38 and 310 and β values between zero and 0.55. This is well within the samples range of *Re* and β values.

$$f_w = \frac{V_t}{V_\infty} = \frac{10}{1 + ARe^B} \tag{10}$$

Where, $\beta = D_g/D_{pipe}$, $A = 8.91e^{2.79\beta}$ and $B = (1.17 \times 10^{-3}) - (0.281\beta)$

The terminal velocity calculated without considering the influence of the wall effect, such as the $V_t$ in Eq. (4) is in fact $V_\infty$. The terminal velocity that takes the wall effect into account is given in Eq. (11).

$$V_t = 0.781 f_w\left[\frac{D_g^{1.6}(\rho_g - \rho_f)}{\rho_g^{0.4}\mu_f^{0.6}}\right]^{0.714} \tag{11}$$

### 2.6. Granule density

Density of the granule samples were measured using a pycnometer. The pycnometer method have been used to determine density of solid particles, powders, granules, and dispersions Pol (1989) and Vlyssides et al. (2008) have used a method adapted from Mahling (1965). In this method, the weights of granules and distilled water at a given temperature are measured and then the granule density is calculated as follows:

$$\rho_g = (\rho_w - \rho_a)\frac{M_2 - M_1}{(M_2 - M_1) + (M_4 - M_3)} + \rho_a \quad (12)$$

Where, $M_1$: Weight of dry pycnometer, $M_2$: Weight of dry pycnometer and granules, $M_3$: Weight of dry Pycnometer, granules and water, $M_4$: Weight of pycnometer and water, $\rho_g$: density of granule, $\rho_w$: density of water and $\rho_a$: density of air.

## 3. Results

### 3.1. Granule size distribution

The size distribution graphs were given as a Perimeter plot, which was obtained directly from image measurement and as an equivalent diameter plot, which was based on Eq. (9). Size distribution measurement for the sample from Borregaard plant involved a different number of granules than the rest of the samples. As a result, it was decided to provide the result in a separate plot. The results are shown in Fig. 4.

The result showed that there is a clear variation in the size distribution along the height of the lab scale UASB reactor. Granules from the top section of the reactor have an average and median perimeter of 2.7 mm and 2.61 mm respectively whereas the average and median equivalent diameters are 0.65 mm and 0.63 mm respectively. For the middle section granules the average and median perimeters were 2.94 mm and 2.84 mm and the average and median equivalent diameters were 0.71 mm and 0.68 mm. This indicates that the overall size of the granules increase towards the bottom of the reactor. This pattern is even more clear when one looks at the result from the the bottom section granules. At average and median diameters of 0.81 mm and 0.75 mm the bottom section is dominated by the biggest granules of the reactor. Laguna et al. (1999) also reported that the biggest granules dominate the bottom section of a reactor they studied. If one considers granules lower than 0.5 mm equivalent diameter, the fresh granules dominate followed by the top section granules. Overall the Fresh and Top section granules show similar size distribution. Size distribution within each sample group also varies. Top section granules are comparatively more uniform in size than that of middle and bottom section granules. The same is true when it comes to shape analysis. Granules from the top section are more spherical (lower shape factor value) than their lower section counterparts. In most of the size frequency groups, the Fresh granules are the smallest compared to the Top, Middle and Bottom section granules. In addition, the median and the average diameters are also the smallest. This is expected because, unlike the Fresh

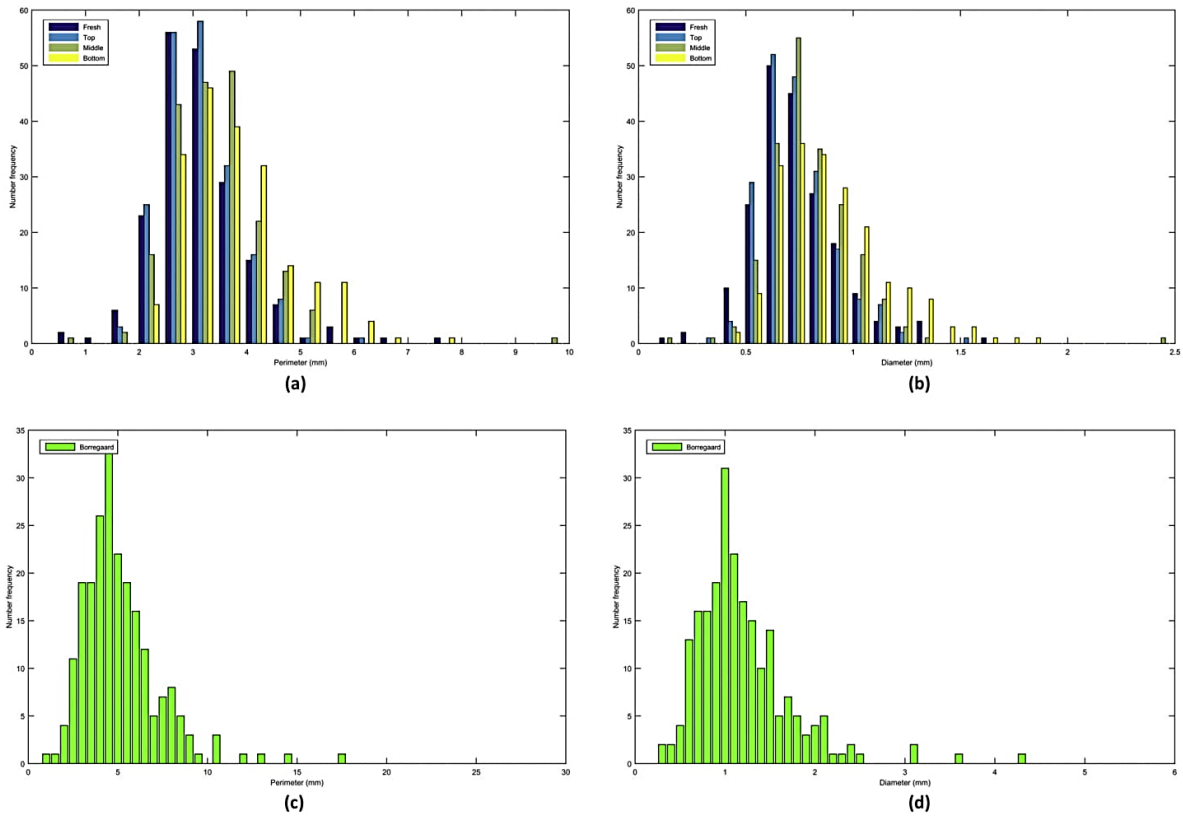


**Fig. 4.** Size distribution of granules based on perimeter and diameter: a& b: granules from lab reactor and c& d: granules from Borregaard reactor.

granules, the Top, Middle and Bottom section granules undergo biomass growth in the reactor over a period of 80 days. As a result, their size increases. Granules from the Borregaard sample are generally bigger than the granules from the UASB reactor. The average and median sizes are 11.01 mm and 10.95 mm for perimeter and 2.65 mm and 2.66 mm for equivalent diameter. There is also a higher size variation of granules in the Borregaard sample than the samples from the UASB reactor. The standard deviation of Borregaard granule diameters is 0.77 mm where as all the other granules samples have a standard deviation below 0.25 mm. The average shape factor of Borregaard granules is 0.19 mm which is much more than the shape factors for the samples from the lab scale reactor (0.05 mm, 0.044 mm, 0.051 mm and 0.057 mm for fresh, top Middle and bottom section samples respectively). This suggests that the Borregaard granules are much less spherical than the other granule samples. This was also confirmed by simple visual inspection Fig. 5Fig. 6 and Fig. 7.

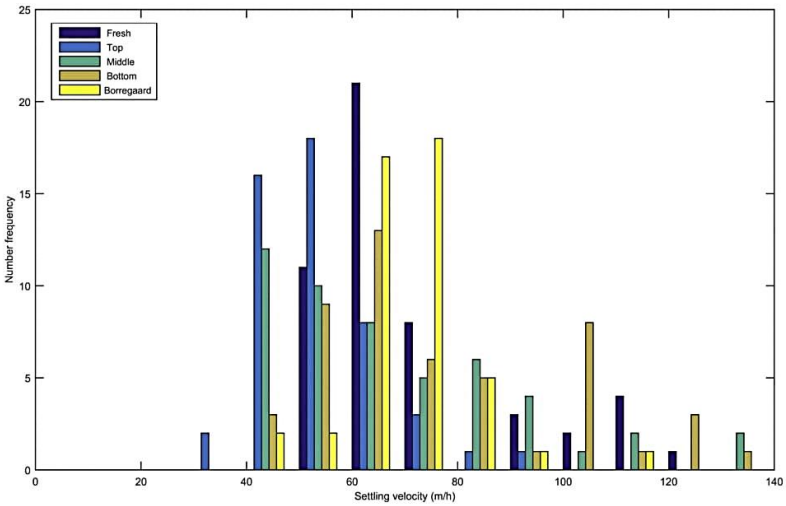


**Fig. 5.** Settling velocity distribution of granules.

### 3.2. Settling velocity

The settling velocity of 50 individual granules from each sample group were measured and compared with theoretical calculations for settling velocity. The results are reported as a mean settling velocity. In addition, the agreement between theoretical and experimental values were compared based on Reynolds number values. The mean settling velocity of the granules is given in Table 2, whereas, comparison of theoretical and experimental settling velocities are given in Fig. 6. Median and Standard deviation values are given in Table 3.

Settling velocity of samples were measured and compared with theoretical values. The results showed good agreement between the theoretical and experimental values. The theoretical and experimental mean settling velocities of each sample is less than relative error of 8.5%. Generally, both the measured and calculated values increase with increasing *Re* for all samples. However, the agreement between the measured and calculated values become weaker at higher *Re* values. Percentage relative error was calculated for each measurement and sorted from the lowest to the highest. Then the average *Re* of those below the median relative error was calculated and compared with those that have relative errors above the median value. For the Fresh sample the average *Re* below and above the median relative errors are 15.01 & 33.85. Those values are 10.63 & 10.65 for the Top section, 13.74 & 17.80 for Middle section, 16.98 & 22.82 for Bottom section and 47.72 & 48.19 for Borregaard samples respectively.

## 4. Discussion

### 4.1. Granule size distribution

The granule size distribution result showed that there is variation in granule size from the top to the bottom section. Generally, granule size increases from top section to the bottom section. The variation in granule size along the reactors height may be simply due to stratification of granules based on their density variation but this was not supported by density measurement and the bottom section granules have similar density with that of the fresh granules and in-fact have marginally lower density than those of the middle and top section granules. Yan and Tay (1997) found that the bottom section of a reactor is also the location where the biggest granules dominate. In addition, they observed that granule formation and growth mainly takes place at the bottom section and theorized that the existence of bigger granules in the bottom section is not only due to stratification but also because of the higher substrate loading around the bottom section compared to the rest of the reactor sections. Laguna et al. (1999) noted that not only do bigger granules tend to be found at the bottom of a reactor but the proportion of bigger granules in each section increases over time. This was observed in the UASB reactor.

Fresh granules (0 days in the reactor) have the smallest granules in most of the size groups in all samples which were in the reactor for 80 days (see Fig. 4).

Fresh granules and granules from the top section of the reactor showed smaller shape factor values than granules from the middle and bottom sections. As a result, Fresh and top section granules can be considered “more spherical”. This may be due to the difference in the growth of microbes across the reactor height. Due to easier substrate

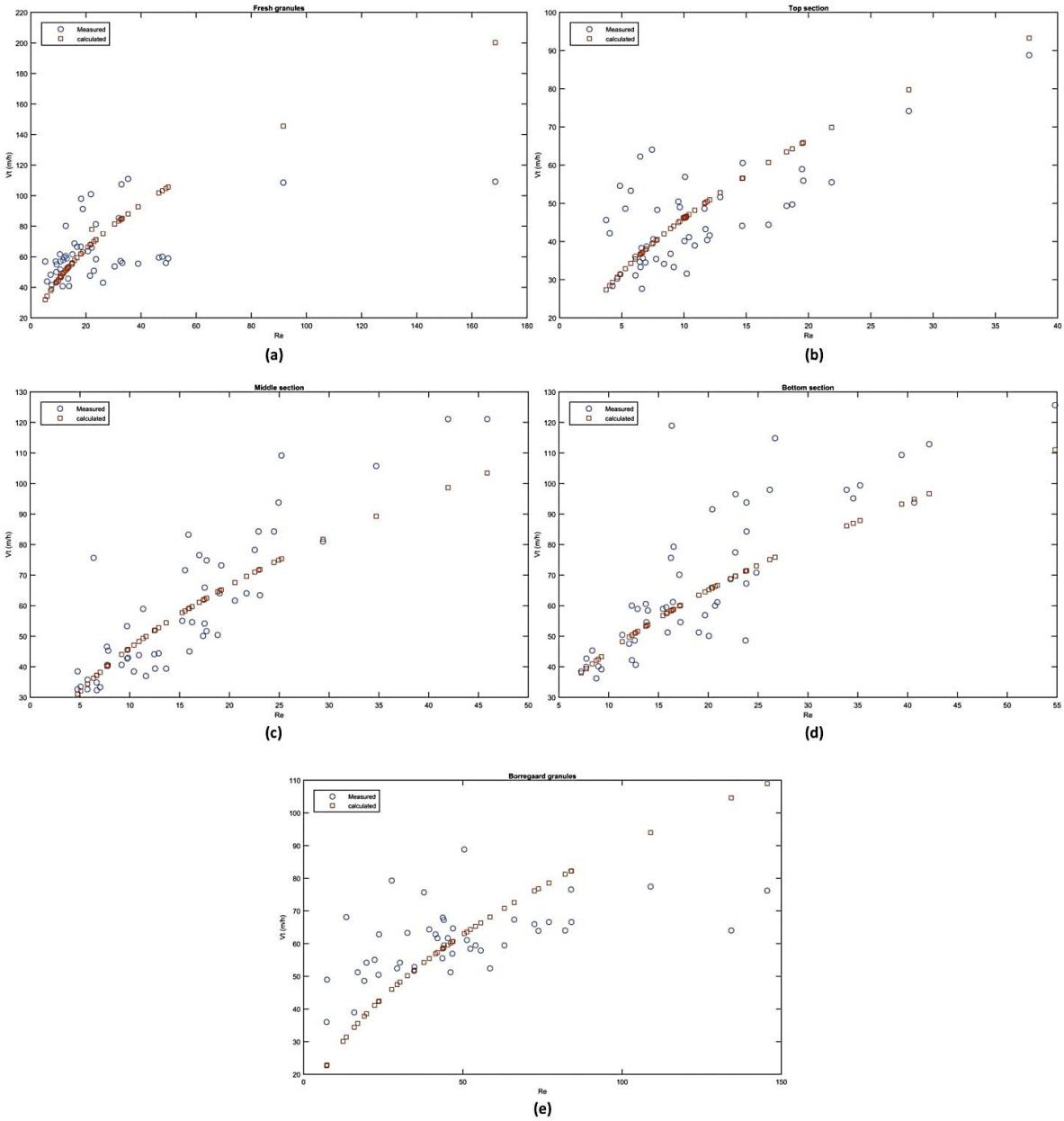


**Fig. 6.** Comparison of theoretical and experimental terminal velocity of granules with respect to *Re*. (a: Fresh b: Top c: Middle d: Bottom e: Borregaard).

access, bottom and middle section granules grow larger than the top section granules. The growth of granules across a granule surface may be uneven and contributes to the higher shape factor. Moy et al. (2002) found evidence of a link between high organic loading rate and formation of irregular shaped granules in their study on effect of loading rate on physical properties of aerobic granules. Higher hydrodynamic activity near the feed inlet at the bottom section may also contribute to granule shear-off. Since the lab scale reactor uses an intermittent feed pattern, the abrupt change in the loading rate may have affected the strength of granules at the bottom. This is corroborated by Alpenaar and granular Sludge (1994) who found evidence that abrupt changes in the loading rate affects the mechanical strength of granules. At the top

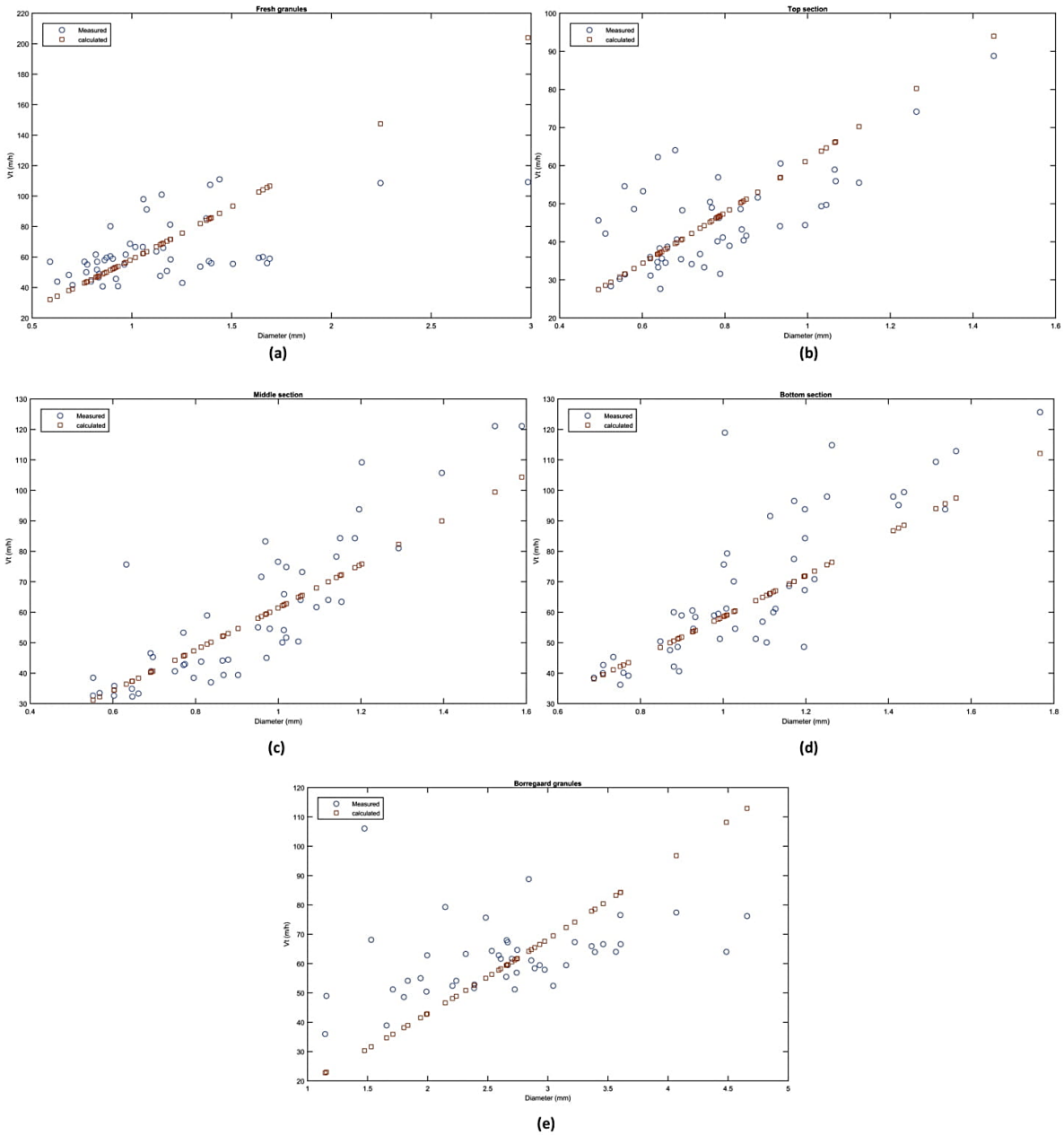


**Fig. 7.** Comparison of theoretical and experimental terminal velocity of granules with respect to granule size. (a:Fresh b: Top c: Middle d: Bottom e: Borregaard).

section granule growth is limited due to poor substrate access and also lower hydrodynamic shear-off.

Borregaard granules showed the highest size variation and shape factor of all the samples. The reason may be related to the mechanical strength of the Borregaard granules. Borregaard granules were broad and flat in shape. Even though no mechanical strength test was done, it was observed that the granules easily break apart during microscopic size measurement and settling velocity measurement. The weak mechanical strength may allow different sized chunks of granules to break-off and this increases the variation in size and shape factor.

**Table 3**
Median and standard deviation of measured and calculated settling velocities in m/h.

| Sample | Test | Median | Standard deviation |
|---|---|---|---|
| Fresh | Measured | 57.58 | 19.04 |
| | Calculated | 58.47 | 29.31 |
| Top | Measured | 43.25 | 12.02 |
| | Calculated | 44.05 | 13.45 |
| Middle | Measured | 52.46 | 23.24 |
| | Calculated | 58.01 | 16.77 |
| Bottom | Measured | 60.27 | 24.04 |
| | Calculated | 60.01 | 16.15 |
| Borregaard | Measured | 61.67 | 11.97 |
| | Calculated | 58.61 | 19.05 |

### 4.2. Settling velocity

The mean settling velocity of granule samples except for the top section granules are in the range of typical anaerobic granule settling velocities. Pol et al. (2004) reported that anaerobic granules usually have settling velocities of approximately 60 m/h. The mean settling velocities of the samples in this study are close to that value. However, at 45.02 m/h, top section granules have significantly lower mean settling velocity than that of the reported value. Granules from the top section are also smaller in size than the rest of the granules in the reactor. Based on Eq. (11), it is expected that top section granules will also be the ones with the lowest settling velocity. Other studies such as, Ahn and Speece (2003) also found low settling velocities for granules in the upper section of a reactor.

Granules at the top section also have a limited access to substrates since they are located the furthest from the feed inlet. This may have restricted microbial growth while facilitating decay & granular shear-off. However, granular shear-off is likely to happen more at the bottom section where bigger granules populate, then the sheared-off and presumably smaller granules float upwards and accumulate at the top section. In a study of granular strength, Pereboom (1997) found out that methanogenic granules with bigger sizes are more likely to face abrasion and shear-off than smaller ones. This contributes to keeping the granules at the top to be relatively smaller than granules from other section and by continuation also contributes to the low settling velocity (granules may contain organisms that can apply tropism, such as in clostridia, but it is assumed not to be expressed in such granules given the strong mixing and shear forces in all efficient sludge bed reactors). The agreement between calculated and measured settling velocities showed dependence on the *Re* value. At lower Re values there was a better agreement than at higher Re value. Granules with small size also have small *Re* and as a result their measured and calculated settling velocities have better agreement than bigger granules. The best agreement between measured and calculated settling velocities is found in the top section granules, which are the smallest in size, while the worst agreement is in the Borregaard granules. Borregaard granules showed the highest relative error even at lower *Re* values. In addition to the contribution due to their relatively bigger size, the high relative error can also be explained by the effect of the shape of the granules on the measured settling velocity. Dietrich (1982) pointed out that granules that deviate from the ideal spherical shape will have surface curvatures, usually next to the maximum projected area, that are more curved than if the granules were spherical. This increases the drag coefficient and leads to lower settling velocity than that of a spherical granule of the same size. Borregaard granules were, in general, broad and flat and their shape factor measurement was the highest of all the samples. In addition, being broad and flat makes them susceptible to shear-off and rotation during settling which may also influence the accuracy of the measured settling velocity.

## 5. Conclusion

In this article size distribution and settling velocity of granules from a lab scale reactor and industry were studied and the following conclusions were made:

- The shape factor and equivalent diameter used in this article are demonstrated to be a good way to quantify size distribution and settling velocity of granules from lab scale reactors and industries.
- Size and shape of UASB granules vary across a reactor height. Both size and shape factor increases from top section to bottom section of a reactor.
- Settling velocity of UASB granules depend not only on their size and density but also on the shape factor of the granules.

## Acknowledgement

This work is part of a PhD project supported by Interreg Biogas2020 in collaboration with University of South-Eastern Norway. The authors would like to thank M.*Sc*. Samee Maharjan for helping with image analysis.

## References

Ahn, Y.-H., Speece, R.E., 2003. Settleability assessment protocol for anaerobic granular sludge and its application. Water SA 29 (4), 419–426.
Alpenaar, A., granular Sludge, A., 1994. Characterization and Factors Affecting Its Functioning. PhD thesis, PhD Thesis. Wageningen University, The Netherlands.
Alves, M., Cavaleiro, A.J., Ferreira, E.C., Amaral, A.L., Mota, M., da Motta, M., Vivier, H., Pons, M.-N., 2000. Characterisation by image analysis of anaerobic sludge under shock conditions. Water Sci. Technol. 41 (12), 207–214.
Arsenijević, Z.L., Grbavčić, Ž., Garić-Grulović, R., Bošković-Vragolović, N., 2010. Wall effects on the velocities of a single sphere settling in a stagnant and counter-current fluid and rising in a co-current fluid. Powder Technol. 203 (2), 237–242.
Ataide, C., Pereira, F., Barrozo, M., 1999. Wall effects on the terminal velocity of spherical particles in newtonian and non-newtonian fluids. Braz. J. Chem. Eng. 16 (4), 387–394. http://www.scielo.br/scielo.php?script=sci_arttext&pid=S0104-66321999000400007.
Bellouti, M., Alves, M., Novais, J., Mota, M., 1997. Flocs vs granules: differentiation by fractal dimension. Water Res. 31 (5), 1227–1231.
Bouwman, A.M., Bosma, J.C., Vonk, P., Wesselingh, J.H.A., Frijlink, H.W., 2004. Which shape factor (s) best describe granules? Powder Technol. 146 (1), 66–72.
Chhabra, R., Agarwal, S., Chaudhary, K., 2003. A note on wall effect on the terminal falling velocity of a sphere in quiescent newtonian media in cylindrical tubes. Powder Technol. 129 (1), 53–58.
Dietrich, W.E., 1982. Settling velocity of natural particles. Water Resour. Res. 18 (6), 1615–1626.
Dinamarca, C., Bakke, R., 2009. Apparent hydrogen consumption in acid reactors: observations and implications. Water Sci. Technol. 59 (7), 1441–1447.
Ghangrekar, M., Asolekar, S., Joshi, S., 2005. Characteristics of sludge developed under different loading conditions during uasb reactor start-up and granulation. Water Res. 39 (6), 1123–1133.
Grotenhuis, J., Kissel, J.C., Plugge, C., Stams, A., Zehnder, A., 1991. Role of substrate concentration in particle size distribution of methanogenic granular sludge in uasb reactors. Water Res. 25 (1), 21–27.
Gupta, S.K., Gupta, S., 2005. Morphological study of the granules in uasb and hybrid reactors. Clean Techn. Environ. Policy 7 (3), 203–212.
Laguna, A., Ouattara, A., Gonzalez, R., Baron, O., Fama, G., El Mamouni, R., Guiot, S., Monroy, O., Macarie, H., 1999. A simple and low cost technique for determining the granulometry of upflow anaerobic sludge blanket reactor sludge. Water Sci. Technol. 40 (8), 1–8.
Liu, Y.-h., He, Y.-l., Yang, S.-c., Li, Y.-z., 2006. The settling characteristics and mean settling velocity of granular sludge in upflow anaerobic sludge blanket (uasb)-like reactors. Biotechnol. Lett. 28 (20), 1673–1678.
Mahling, A., 1965. Die dichte. In: Analytik der Lebensmittel, pages 14–40. Springer. https://link.springer.com/chapter/10.1007%2F978-3-662-31684-9_2.
Moy, B.-P., Tay, J.-H., Toh, S.-K., Liu, Y., Tay, S.-L., 2002. High organic loading influences the physical characteristics of aerobic sludge granules. Lett. Appl. Microbiol. 34 (6), 407–412.
Olson, E., 2011. Particle shape factors and their use in image analysis-part 1: theory. J. GXP Compliance 15 (3), 85.
Pereboom, J., 1997. Strength characterisation of microbial granules. Water Sci. Technol. 36 (6–7), 141–148.
Podczeck, F., Newton, J., 1995. The evaluation of a three-dimensional shape factor for the quantitative assessment of the sphericity and surface roughness of pellets. Int. J. Pharm. 124 (2), 253–259.
Pol, L.H., 1989. The Phenomenon of Granulation of Anaerobic Sludge. PhD thesis. Hulshoff Pol.

Pol, L.H., de Castro Lopes, S., Lettinga, G., Lens, P., 2004. Anaerobic sludge granulation. Water Res. 38 (6), 1376–1389.
Tang, C.-J., Zheng, P., Wang, C.-H., Mahmood, Q., Zhang, J.-Q., Chen, X.-G., Zhang, L., Chen, J.-W., 2011. Performance of high-loaded anammox uasb reactors containing granular sludge. Water Res. 45 (1), 135–144.
Thaveesri, J., Daffonchio, D., Liessens, B., Verstraete, W., 1995. Different types of sludge granules in uasb reactors treating acidified wastewaters. Antonie Van Leeuwenhoek 68 (4), 329–337.
Vlyssides, A., Barampouti, E., Mai, S., 2008. Simple Estimation of Granule Size Distribution and Sludge Bed Porosity in a uasb Reactor. a a. 2(1). pp. 4.
Wu, J., Afridi, Z.U.R., Cao, Z.P., Zhang, Z.L., Poncin, S., Li, H.Z., Zuo, J.E., Wang, K.J., 2016. Size effect of anaerobic granular sludge on biogas production: a micro scale study. Bioresour. Technol. 202, 165–171.
Yan, Y.-G., Tay, J.-H., 1997. Characterisation of the granulation process during uasb start-up. Water Res. 31 (7), 1573–1580.
Zhang, G.-D., Li, M.-Z., Xue, J.-Q., Wang, L., Tian, J.-L., 2016. Wall-retardation effects on particles settling through non-newtonian fluids in parallel plates. Chem. Pap. 70 (10), 1389–1398.

## Article 2:

# Granular sludge bed processes in anaerobic digestion of particle-rich substrates.

Tassew FA, Bergland WH, Dinamarca C, Kommedal R, Bakke R. Granular sludge bed processes in anaerobic digestion of particle-rich substrates. Energies. 2019; 12(15):2940. https://doi.org/10.3390/en12152940

energies

MDPI

*Review*

# Granular Sludge Bed Processes in Anaerobic Digestion of Particle-Rich Substrates

**Fasil Ayelegn Tassew [1,*], Wenche Hennie Bergland [1], Carlos Dinamarca [1], Roald Kommedal [2] and Rune Bakke [1]**

[1] Department of Process, Energy and Environmental Technology, University of South-Eastern Norway, Kjølnes ring 56, 3918 Porsgrunn, Norway
[2] Institute of Chemistry, Biosciences and Environmental Engineering Stavanger, University of Stavanger, 4021 Stavanger, Norway
* Correspondence: fasil.a.tassew@usn.no

Received: 8 July 2019; Accepted: 28 July 2019; Published: 31 July 2019


**Abstract:** Granular sludge bed (GSB) anaerobic digestion (AD) is a well-established method for efficient wastewater treatment, limited, however, by the wastewater particle content. This review is carried out to investigate how and to what extent feed particles influence GSB to evaluate the applicability of GSB to various types of slurries that are abundantly available. Sludge bed microorganisms evidently have mechanisms to retain feed particles for digestion. Disintegration and hydrolysis of such particulates are often the rate-limiting steps in AD. GSB running on particle-rich substrates and factors that affect these processes are stdied especially. Disintegration and hydrolysis models are therefore reviewed. How particles may influence other key processes within GSB is also discussed. Based on this, limitations and strategies for effective digestion of particle-rich substrates in high-rate AD reactors are evaluated.

**Keywords:** high-rate anaerobic digestion; granular sludge; disintegration; hydrolysis; suspended solids; particulates

## 1. Introduction

Anaerobic digestion (AD) has been used to treat organic wastes for renewable energy production for decades. Due to the ongoing shift towards renewable energy, biomethane produced by AD is getting increased attention as an energy carrier [1] and as a potential chemical platform for synthesis of added value products such as polysaccharides, single-cell protein, and polyhydroxyalkanoates [2]. Biomethane can be produced from a wide variety of organic feedstocks such as agricultural and domestic wastes [3]. However, the low energy density of some of the largest feed sources, such as sludge and manure, limits production rates and process efficiency in continuous flow stirred tank reactors (CSTR) currently used for sludge and manure AD [4]. Such processes without efficient biomass retention are voluminous and therefore expensive to build and operate [5]. High-rate AD, such as up-flow anaerobic sludge bed (UASB) reactors, are used to obtain more sustainable energy recovery as it provides high COD (Chemical Oxygen Demand) removal even at high OLR (Organic Loading Rate) and short HRT (Hydraulic Retention Time). Its design is simple and compact, requiring relatively low construction cost. It has, however, some limitations regarding feed composition that require discussion, especially: The particle content of some of the most abundant substrates, such as sludge and manure slurries, is well above the levels considered appropriate as UASB reactor influent [6]. Large quantities of slurries that can and should be used for biogas production exist (e.g., the Norwegian government aims to utilize 30% of manure slurries for AD by 2020 while <1% was used according to a 2011 report [5]), and this study can contribute to expanding the applicability of high-rate sludge bed AD. We address

some of the main challenges associated with high-rate anaerobic digestion of particle-rich substrates with special emphasis on manure as a substrate, due to its abundance. Most high-rate AD processes in operation depend on granular sludge to retain sufficient active biomass. Granules are formed by the aggregation of microorganisms that develop into dense masses with sedimentation velocity high enough to avoid washout even under high hydraulic load [7]. It is observed that UASB reactors treating particle-rich manure slurries also accumulates suspended solids from the feed, forming an additional suspended fraction together with the granules [8,9]. The influence of such solids on AD is not understood well, leading some experts to claim that granular sludge bed (GSB) processes may not be appropriate for particle-rich substrates. [10]. It appears, however, that a significant fraction of feed particles can be digested and enhance methane production [11]. This review was undertaken to investigate to what extent and how sludge bed high-rate AD can be used to treat particle-rich substrates. We aim to find more evidence for particle digestion in granular sludge beds, identify process limitations, and find appropriate kinetic models in order to establish design criteria for such processes. There is little directly relevant literature on the topic, limiting this review to mainly indirectly relevant literature. The review covers particle-rich substrates characteristics; particle disintegration and hydrolysis, including models for such; physical characteristics of granular sludge; sludge bed reactor designs and observations of particle effects.

## 2. Anaerobic Sludge Bed Processes

Various anaerobic processes have been used for the treatment of wastewater for decades. These processes include septic and Imhoff tanks, which are some of the earliest methods used to treat wastewater. They are simple systems where low to moderate COD and suspended solids removal can be achieved. Anaerobic lagoons are also used for larger volumes of wastewater or manure. In this system, the wastewater is held for a prolonged time. The lagoon must have sufficient depth to ensure anaerobic condition. It is a low maintenance process but it is inefficient and has a negative environmental impact due to gas release and odor. With the increasing understanding of the underlying anaerobic processes, newer, more controlled reactors were developed. In continuous flow stirred tank reactors complete mixing of reactor contents is assumed, and both design and operation are simple. Horizontal plug flow and anaerobic sequential batch reactors have also been used over the years. These reactors are generally low-rate systems with maintenance requirements but require long HRT and large reactor volumes. The need for fast, efficient, and more environmentally friendly alternatives for anaerobic wastewater treatment led to the development of sludge bed processes. High loading rate, short HRT, and efficient conversion of organic compounds to biogas were possible due to increased bioreactor densities of active biomass by decoupling sludge retention time (SRT) from HRT. Starting from the 1970s, a number of high-rate reactors have been developed. Some of the most common high-rate reactors and their advantages and disadvantages are summarized in Table 1. Lettinga [12] specified four essential requirements that enabled the proliferation of anaerobic sludge bed processes. The first is the formation of balanced and immobilized microorganisms. In many anaerobic reactors, immobilization is achieved in the form of microbial aggregates or granules. The second requirement is high settleability of microbial aggregates in order to ensure that the microbial biomass remains in the reactor even if high flow velocity is applied (SRT > HRT). Sludge bed reactors are often equipped with gas–solid or gas–liquid–solid separators that aid retaining granular sludge. Third, a high degree of contact between sludge and substrate must be achieved (convective mass transfer). The last requirement is the presence of a high rate of mass transfer in and out of the microbial aggregates (mainly diffusive mass transfer).

**Table 1.** Applications, advantages, and disadvantages of commonly used high-rate reactors.

| Name | Common Applications | Advantages | Disadvantages |
| --- | --- | --- | --- |
| Anaerobic contact process (ACP) | Wastewater containing suspended solids | Good contact between biomass and substrate<br>Efficiency | Poor sludge settling<br>Complex system |
| Anaerobic filter (AF) | Low or high strength wastewater | Requires small area<br>Stable sludge<br>Long service time | Difficulty to maintain contact between sludge and wastewater<br>Affected by accumulation of non-degradable matter<br>Difficult clean-up process |
| Up-flow anaerobic sludge blanket (UASB) | High strength industrial wastewater | Simple design<br>Relatively low cost<br>Low excess sludge production<br>High removal efficiency | Recovery time may be long after stress conditions<br>May require expert maintenance<br>Internal mixing may not be optimal (dead zones) |
| Anaerobic fluidized bed (AFBR) | Industrial wastewater (dilute, low in suspended solids) | High biomass retention<br>High surface area due to attached growth of microbes on carrier media | Difficult scale-up<br>Expensive |
| Expanded granular sludge bed (EGSB) | Low strength wastewater (low suspended solids) | Improved mixing (no dead zones)<br>High removal efficiency for soluble constituents | Suspended solids removal is low |
| Internal circulation (IC) | Low or high strength wastewater | High organic loading<br>High contact between sludge and wastewater<br>Larger granular sludge | Sludge washout may be a problem<br>Low granular sludge strength |
| Anaerobic baffled reactor (ABR) | Low or high strength wastewater | No mechanical mixing<br>Biomass do not need good settling properties<br>Tolerates shock loads | Influent distribution is not even through reactor<br>Variable sludge retention |

*Up-Flow Anaerobic Sludge Blanket (UASB)*

UASB is a high-rate AD reactor usually used for the treatment of industrial wastewater, invented by Lettinga et al. [13] in the 1970s. After a slow start, there has been a rapid growth in its application over the last decades. There has also been an increase in design variations where the two most common are: EGSB (Expanded Granular Sludge Blanket) which is a reactor that is essentially a UASB with higher up-flow rate and recirculation of effluent; IC (Internal Recirculation) reactor where two UASB-type reactors are stacked and used in series and enables efficient mixing without external recycle pumping. These encompass one or more up-flow anaerobic sludge blankets, so this review does not distinguish between such concepts and considers all as UASB, in accordance with the view of Prof. Lettinga (personal communication). UASB reactors differ from conventional AD by the facts that they can handle much higher organic loading rates [13,14] (up to 15–40 gCOD $L^{-3}$ $d^{-1}$) and short hydraulic retention time (0.3–7 days). The reason for the high efficiency of UASB and other high-rate reactors is that the sludge retention time (SRT) is decoupled from the hydraulic retention time (HRT) so that SRT > HRT while SRT = HRT in conventional CSTR reactors. Typical UASB SRT values are in excess of 30 d and biomass concentration can reach up to 100 kg/$m^3$ at the bottom of the sludge bed [10]. This is achieved when the microorganisms are aggregated in granules that have higher densities than the wastewater/substrate they are treating, such that the granular sludge is retained in the reactor even if high feed flow rates are used. The anaerobic microorganisms naturally aggregate into dense granules of 0.1–8 mm diameter under UASB conditions [15]. Size and density of the granules are important characteristics because they influence the settling of granules and mass transfer between the granules and the surrounding liquid. The inlet is at the bottom and the outlet is at the top of UASB, as illustrated in Figure 1.

An up-flow velocity of 0.7–1.0 m/h is recommended by Tilley et al. (2014) [16] so that granules remain in the reactor, however, up-flow velocities of 1–3 m/h are also typically used with mean settling velocities ranging from 20 to 100 m/h [7]. Fragments of granules and particles introduced in the feed may, however, be susceptible to wash-out from the reactor due to lower settling velocities. UASB reactors are equipped with gas–liquid–solid separators that are located at the top (Figure 1) to primarily separate liquid and biogas for collection. Such arrangements are also intended to help retain particles carried out of the sludge bed by gas bubbles that can be knocked off when passing through the separator. The separator narrows so that the particles can settle back down. UASB is suitable to treat high strength industrial wastewater such as from pulp and paper processing, tanneries, distilleries, chemical, and pharmaceuticals industries while substrates with high-suspended solids, high lipid, and protein content are considered less appropriate [17]. For example, wastewater from slaughterhouses is considered unsuitable for treatment in UASB because it contains high concentrations of lipids and suspended solids [17]. Accumulation of lipids and suspended solids in the sludge bed supposedly leads to biomass wash-out and process failure. Difficulties experienced with the treatment of high particulate substrates, such as manure, that contains straws and other long fibers are mainly mechanical as it often leads to pipe blockage and channeling. During storage, however, such fibers tend to float if the substrate is left undisturbed for a day or more [18,19] and a supernatant can be withdrawn and used as UASB substrate. Even at suspended solids concentrations above what is considered appropriate for UASB, high conversion rates and yields, and substantial conversion of the particulates at low HRT is achieved [11]. The question remains: How can this be, given the slow disintegration and hydrolysis of particulates and the low settling velocity of such particles?

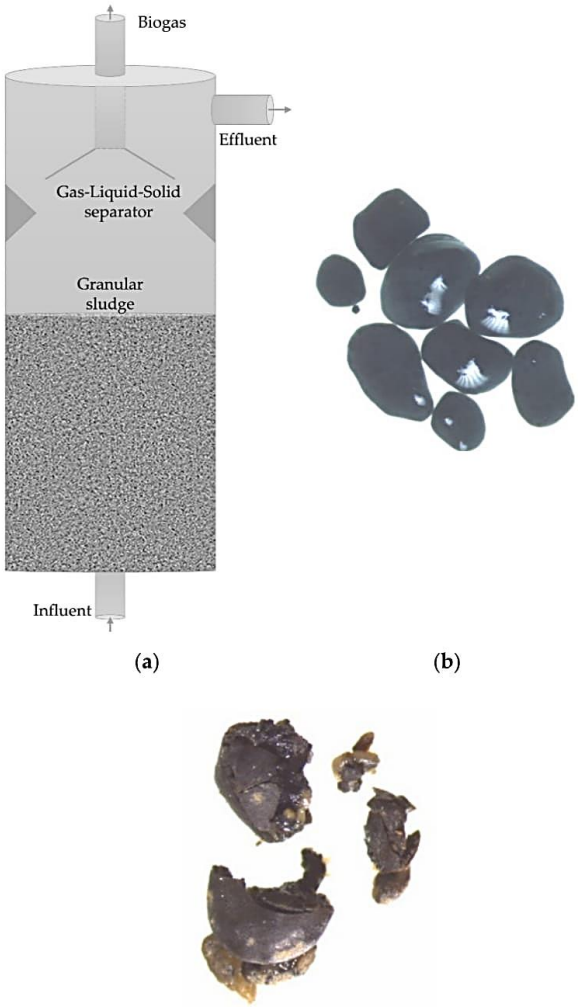


**Figure 1.** Up-flow anaerobic sludge bed (UASB) reactor components (**a**) and examples of granular sludge (**b**,**c**).

## 3. Particle-Rich Substrates

Several sources of substrates are used for the production of biogas by anaerobic digestion. The most common sources include industrial waste, food waste, agricultural waste, and manure. Each substrate has their own physical and chemical characteristics that make them suitable or unsuitable for a given AD reactor. For example, UASB reactor is considered ideal for the treatment of industrial and municipal wastewater with low total solids (TS) and particulate content while CSTR reactors are instead used for pumpable particle-rich substrates, such as manure slurries, AD processes can be classified into three categories based on the total solids (TS) content of the substrates used. These are: Wet (0–10% TS), semi-dry (10–20% TS), and dry (above 20% TS) [20]. Increase in TS content up to

around 30% can increase the biogas production [21], while above this level biogas production may be curbed by mass transfer limitation: The substrate is simply too thick to allow efficient mixing and mass transfer of metabolites, resulting in low methane yield [22]. Batstone and Jensen evaluated appropriate reactors depending on solid content as summarized in Figure 2. Later cases are also added to this figure, such as Bergland et al. [11] who demonstrated in lab-scale that particle-rich substrates (pig manure slurry supernatant) can be efficiently treated in high-rate AD. There are potential benefits of using particle-rich substrates (degradable organics) since it implies relatively high digestible substrate content per total liquid volume and therefore high substrate energy density. This can imply increased biogas production efficiency, reduced cost of feed transport, compact reactors, and low operational energy demand [20]. Massé et al. [23] carried out high rate digestion of dairy manure with TS of 35% using dry anaerobic digestion (PDAD) at 20 °C in sequential batch reactor and 21 d cycle length. They achieved an average methane yield of 152 ± 8 L $CH_4$/kgVS and VS removal of 42 ± 4% (UASB is certainly not suitable for such high TS). Such sludge bed high-rate reactors are often used for substrates with low suspended solids content, usually <1% TS but there are studies that show sludge bed treatment of relatively high-solids containing substrates: Fujihira et al. [24] used a modified 'anaerobic baffled reactor' (ABR) system at HRT of 7.3 d and OLR of 4.8 gCOD $L^{-3}$ $d^{-1}$ to treat a substrate that contains high levels of suspended solids (7 ± 12 gTSS/L) and showed that a COD removal of 95% was achievable. Andalib et al. [25] showed, using corn stillage (by-product from bioethanol production) substrate with 47 gTSS/L, that 78% TSS removal was achievable by using anaerobic fluidized bed reactor (AFBR) at HRT of 3.5 d (with a methane yield of 0.345 L $CH_4$/g COD consumed). Successful treatment of substrates with TS content above 10% at short HRT has also been reported in more conventional UASB-type reactors: Fang et al. [26] reported 90% COD removal capability for both UASB and EGSB in treating palm oil mill Effluent (POME) with substrate TS well over 10% at HRT of 5 d. A study carried out by Borja et al. [27] even showed that UASB reactors are capable of treating POME at HRT of <1 d with suspended solids concentrations reaching 5.4 g/L and OLR reaching up to 17.3 gCOD $L^{-3}$ $d^{-1}$ at HRT of 0.9 d.

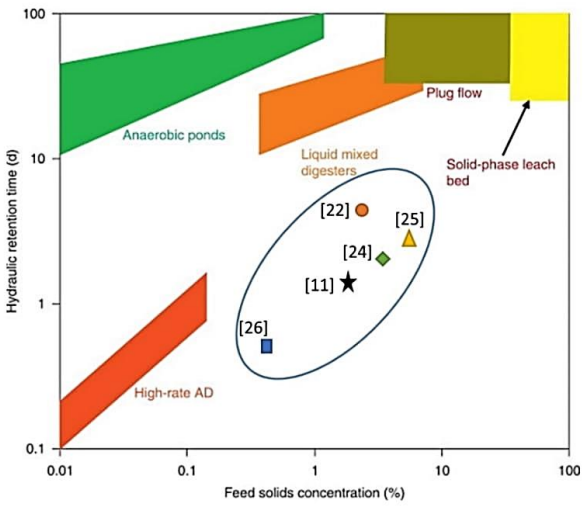


**Figure 2.** Hydraulic retention time for various anaerobic digestion (AD) reactors depending on feed solids content (Adapted from Batstone and Jensen [28]) where data from [11,23,25–27] are added.

### *3.1. Manure*

Physical and chemical properties of manure influence how it can be used as a substrate for anaerobic digesters. Manure collected from storage facilities usually contains a large amount of water

that has been used for cleaning and flushing raw manure from barns, especially for pig and cow manure. In addition, bedding materials, unused animal feed, and other materials can enter the water-manure mix. Animal age, sex, health, weight, type (ruminant or non-ruminant), whether pregnant or not also affects the chemical composition of manure [29]. Manure has high contents of Carbon (C), Nitrogen (N), and Phosphorus (P). The C:N ratio is an important characteristic of manure in AD because it is linked to ammonia inhibition both when too low [30] and too high [31]. Manure with high solids content is dominated by high C content and hence usually has a high C:N ratio whereas liquid manure contains a lower C:N ratio [32]. A comparison of typical total solids content (dry matter) of raw manure with liquid manure is provided in Table 2.

**Table 2.** Comparison of typical dry matter content of different types of manure with and without dilution.

| Manure Type | Dry Matter (%) | |
|---|---|---|
| | Raw Manure (As Excreted) | Liquid Manure |
| Pig | 9–11 [29,32] | 2–5 [33] |
| Cattle | 8–12 [29,32] | 3–8 [33] |
| Poultry | 25–35 [31,34] | <15 [34] |
| Horse | 14–20 [29,35] | <15 [35] |
| Sheep | 25 [29] | - |

Livestock farming usually incorporates manure storage pits, in which its physical and chemical properties are altered. During storage, denser contents settle at the bottom, a liquid fraction with less large particles (manure supernatant) establish above and lighter material, such as straw, float at the top. Hence characteristics, including density and organic content, differ with time and height from which the manure is taken in storage pits. Anaerobic conditions during manure storage can lead to emission of a significant amount of biogas and further alter the chemical composition of manure [36,37], largely dependent on storage temperature [19]. Feng et al. [37] estimated methane loss of 1–46% for pig manure and 1–2% for cattle manure. Manure also undergoes hydrolysis, fermentation, and acidogenesis while stored, potentially leading to improved digestibility [19].

### 3.2. *Swine Manure Characteristics*

Swine manure is abundant and AD of swine sludge is extensively studied. Typically about 4–5 kg manure per day per animal is produced (corresponding to organic content of 0.4–0.5 kgCOD/d with C:N ratio of 7–8) [38]. Reported values for total and volatile solids per animal are usually 0.5–0.8 and 0.4–0.5 kg $d^{-1}$, respectively [29]. Swine manure has a high content of solid particulates that are difficult to digest [24,39]. Straw or saw-dust (as bedding material), other fibers, and lignocellulosic particulates pose a challenge in achieving the full biogas potential. Møller et al. [40] showed through batch experiments that the average methane potential from swine manure (pig and sow) is only about 60% of the manure COD value (calculated based on the volume of methane per mass of volatile solids). The relatively high content of protein and lipids further challenge high-rate AD due to potential ammonia inhibition and foam formation. Møller et al. [40] estimated the protein and lipid content of swine manure and found average values of 240 and 143 g/kgVS, respectively [40]. Ammonia comes from deamination of urine and amino acids and is split between free ammonia ($NH_3$) and ammonium ion ($NH_4^+$) depending on pH and temperature, both of which can play an inhibitory role in the Methanogenesis step [30,41]. In addition, the degradation of amino acids can lead to the formation of hydrogen sulphide ($H_2S$) which exacerbates inhibition [41,42]. One of the strategies used to alleviate ammonia inhibition as well as increase biogas generation is co-digestion of swine manure with other substrates that are low on N-based compounds [43,44]. Common substrates for co-digestion with swine manure are crop residue, food waste, and municipal organic waste. Reports on the topic have focused on co-digestion of manure in UASB or UASB-type reactors [45–47]. Bergland et al. [11] and Nordgård et al. [48] have, however, shown the feasibility of single substrate swine manure supernatant

digestion in high-rate reactors, explained by UASB population adaptation to much higher ammonia concentrations than those causing inhibition in conventional manure AD.

## 4. Disintegration of Solid Particulates

Total solids are comprised of soluble and particulate contents (Figure 3). The particulate fraction requires disintegration as well as hydrolysis steps before it can be taken up by microorganisms. Disintegration is defined as the (slow) release from a complex composite material of macromolecules that will be further hydrolyzed. Disintegration or hydrolysis is assumed to be the rate-limiting step in AD when particle-rich substrates are applied [49]. Inactive or dead biomass is considered as part of the particulate fraction available for digestion. The disintegration of particulates results in degradable and non-degradable fractions. The non-degradable fractions are soluble and non-soluble inert particulates, whereas the degradable fractions consist of biopolymers, in ADM1 (Anaerobic Digestion Model No. 1) limited to polysaccharides, proteins, and lipids [49–51]. Disintegration is mostly described by first-order kinetics, sometimes assumed to be part of the hydrolysis step. Disintegration in AD reactors depends on various factors such as particle size, morphology, strength, temperature, and chemical composition. Substrates with high solids content are often pretreated before AD to speed up disintegration and hydrolysis. There are thermal, chemical, mechanical, and biological pretreatment methods (and combinations of such), including milling, alkaline treatment, thermal treatment, ultrasound agitation, and composting [52]. An objective of the pretreatment is to increase the surface area of the solid particulates available for enzymatic activity [53].

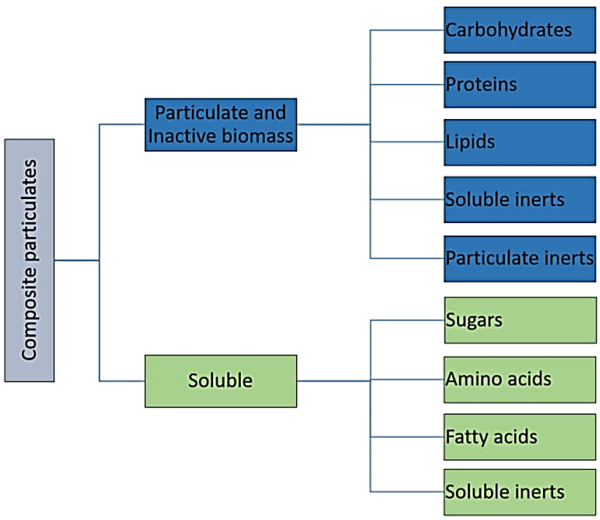


**Figure 3.** Composite particulate fractions according to the Anaerobic Digestion Model No. 1 (ADM1) model. Particulate contents and dead biomass undergo disintegration and hydrolysis to become soluble.

### 4.1. *Factors Affecting the Degradation of Particles*

Due to the typical short HRT of UASB, feed particles must somehow be retained longer than HRT to be degraded but mechanisms for such are not described in the literature so indirect evidence is considered. UASB reactors treating particle-rich manure slurries accumulate suspended solids from the feed, forming an additional suspended fraction together with the granules [8,9] and a significant fraction of feed particles can be digested and contribute significantly to methane production at low HRT [11]. The density of such feed particles can be low so that they remain suspended during storage and in feed containers [11], implying that their sedimentation characteristics are such that they should

have reactor retention time similar to HRT unless somehow 'captured' by the sludge bed. Such capture mechanisms can be by adsorption to granular sludge and/or granular sludge (or fragments of such) colonizing the feed particles. Fletcher (1994) [54] claims that "molecular biology has demonstrated that bacteria are able to "sense" surface environments, altering their pattern of gene expression" and have a diversity of attachment mechanisms. Several studies have demonstrated the importance of extracellular polymeric substance (EPS) in granular sludge (such as summarized by van Lier et al. (2017) [15]) with similar composition and roles as in biofilms so it seems likely that the bacteria on the surface of granules can use the mechanisms described by Fletcher (1994) [54] to actively attach particles for the purpose of retaining and digesting.

Mahmoud et al. [8] identified three categories of factors that affect solid removal in up-flow reactors. These are: (1) Reactor operational conditions (such as temperature OLR, HRT, and up-flow velocity), (2) influent characteristics, and (3) sludge bed characteristics. They noted that temperature increase leads to an increase in solids removal. They proposed that an increase in temperature decreases viscosity, leading to reduced hydraulic shear force acting on the particles. Alternatively or additionally, increased temperature will enhance solubility rates (especially of fats and lipids in organic particles) and increase depolymerization. Other studies have also reported an increase in the removal of solids with temperature [55–57]. Increase in HRT also increases the removal of solids, however, HRT is linked with OLR for a given substrate and these are intertwined parameters with organic compound concentrations, and up-flow velocity, so it is not clear that HRT has a direct effect on particle degradation. The results presented by Bergland et al. [11] did not seem to suggest this since a similar particle contribution to the biogas production was observed for HRT from 40 to 2 h. Sludge blankets that entrap suspended solids can enhance digestion, as described above, but may also lead to a decrease in settleablity of the granular sludge. This may interfere with process performance unless it is countered by disintegration and hydrolysis. It is therefore important to understand what the fate of the accumulated suspended solids can be. Accumulated particulates interact with the surrounding liquid phase and microorganisms in the sludge bed. Large particles undergo separation into smaller ones due to a combination of structural weakening due to hydration, hydrodynamic shear force or mixing, enzymatic dissolution, etc. By and large, disintegration depends on particle retention time—hence, the reactor SRT is the controlling process parameter. Continuous and prolonged entrapment of suspended solids that are voluminous and not degraded sufficiently fast can decrease sludge bed particle settleability, and eventually to sudden washout of the sludge bed. Lettinga et al. [6] observed such phenomenon both in lab-scale and in full-scale reactors. Suspended solids may also accumulate at the reactor top, creating an inverted solid profile, leading to inadequate contact between particulates and microbial biomass especially in digesters with gas-mixers [58,59]. This is explained by the formation of foam and produced biogas lifting up low-density particles by floatation.

### 4.2. *Hydrolysis of Particulates*

Hydrolysis is defined as a chemical process of decomposition involving the splitting of a molecular covalent bond and the addition of the hydrogen cation and the hydroxide anion of water [60]. Hydrolysis is the second step in anaerobic digestion of organic substances where macromolecules are degraded into smaller molecules by bacterially excreted extracellular enzymes [61]. Strictly speaking, this mechanism is one of several depolymerization reactions possible, but in the terminology of wastewater and sludge treatment, hydrolysis is used for the net sum of these. Stoichiometrically, hydrolysis products are monomers, oligomers, or polymers of reduced molecular weight of random combinations dictated by the reaction mechanism of enzymes involved, the substrate composition and molecular weight, and the often diffusion limited bioaggregate environment of the reaction. Based on a combination of empirical evidence, and model complexity reduction arguments, hydrolysis products are simplified to the respective mono- and oligomers of the polymers in a single reaction stoichiometry [49]. Along with disintegration, it is often the slowest and hence the rate-limiting step of the entire anaerobic digestion process [62,63]. The rate limitation is mechanistically linked to the diffusion-controlled physical contact

between substrate particles and the hydrolytic enzymes. The majority of extracellular enzymes, but not all, are bound to, or retained by the bacteria, and therefore hydrolysis rates are directly proportional to the density of active bacteria. This has also been compared by direct observations of particulate cellulose-degrading consortia (Wang et al. (2011) [64]). For particulate substrates, this means that the rate-controlling factor is dictated by the contact area to the active bacteria, or by the adsorption kinetics of soluble enzymes to the same surface [65]. This resembles the general reaction kinetic model of surface catalyzed reactions, a process which for biocatalyzed reactions usually is described by Contois kinetics [66–69]. In contrast to the direct growth Contois model, hydrolysis in the activated sludge models and the ADM1 is a separate process leading to substrates for the bacterial growth process. While Contois kinetics is implemented in ASM, pseudo-first-order kinetics with respect to particulate substrates is used in ADM1 [65,69], which is a high biomass to substrate particle extreme. Specific rates can be determined using batch reactor tests: Biomethane potential (BMP) and hydrolysis rate constant ($K_h$) can be obtained by performing data fitting from batch reactor data, assuming hydrolysis to be the rate-limiting step. Batstone et al. [49] provide the simplest and most common hydrolysis rate expressions for biopolymers as follows:

$$\frac{dX}{dt} = K_h X, \tag{1a}$$

$$\frac{dX_{ch}}{dt} = K_{h,ch} X_{ch}, \tag{1b}$$

$$\frac{dX_{pr}}{dt} = K_{h,pr} X_{pr}, \tag{1c}$$

$$\frac{dX_{li}}{dt} = K_{h,li} X_{li}, \tag{1d}$$

where $K_h$ is the pseudo-first-order hydrolysis rate constant in $d^{-1}$, X is particulate component in kg COD $m^{-3}$, and subscripts ch, pr, and li denote carbohydrate (polysaccharides), proteins, and lipids, respectively. This first-order kinetics is a special case of Vavilin's two-phase model (Vavilin's (1996) [65]) and the Contois model at high active biomass values, which, however, may not be the case during the initial batch test stage.

### *4.3. Role of Microorganisms in the Hydrolysis of Particulates*

Anaerobic hydrolytic microorganisms carry out the process of breakdown of biopolymers into their respective monomers. There is a diverse group of hydrolytic microorganisms. Azman et al. [70] reported that the most abundant hydrolytic bacteria in biogas plants belong to the phylum Firmicutes and Bacteroidetes. Bacteria that belong to Phylum Fibrobacter, Spirochaetes, Thermotogae, and Chlorobi were also found, but less abundantly. Apart from some thermophilic hydrolytic bacteria such as Caldicellulosiruptor, most produce a multi-enzyme complex called Cellulosome. Cellulosome is an extracellular enzyme complex that is crucial in the adherence of bacterial cells onto surfaces, breakdown of macromolecules, and eventual absorption of soluble components into the cells. Lamed et al. [71] first described Cellulosome where they reported selective adherence of Clostridium thermocellum to cellulose particulates. All phyla containing anaerobic chemoheterotrophs may, however, be among hydrolytic bacteria to be found in anaerobic digesters. This can be investigated using a gene search for classical hydrolases to check whether these enzymes are widespread or not (not found in this survey) but in general (and for a diverse set of substrates) anything but a diverse hydrolytic bacteria community would be surprising. Microorganisms secrete a wide array of enzymes such as cellulase, protease, and lipase that facilitate hydrolysis. The mechanism of enzymatic action has been studied by several authors but gaps remain in the understanding of how enzyme-mediated hydrolysis occurs. According to Batstone et al. [49], the mechanism of release of enzymes can be carried out in three ways. The first is by directly releasing enzyme into the bulk liquid, the second way is bacteria attach to particles first and then release enzyme, and lastly, bacteria possess an enzyme that acts as a channel to the cell

interior. Regardless of the mechanism of enzymatic release, transport, and diffusion of the enzyme to particles followed by reaction and enzyme deactivation occur. The description of hydrolysis in ADM1 is limited and a more general review on enzymes and enhancement of the biogas process is given by Parawira (2012) [72]. In addition to the description of cellulases for polysaccharides above, Ravndal and Kommedal (2017) [73] present a mechanistic description of starch degradation (from particulate to soluble polymers and final mineralization). Review by Jaeger et al. (1994) [74], Kanmani et al. (2015) [75], and Cammarota and Freire (2006) [76] for microbial lipases and esterases present further knowledge regarding mechanisms of enzymatic action. Temperature, pH, particulate size, and available surface area all influence hydrolysis. Various types of bacteria produce a wide range of enzymes each with its own optimal operational temperature; as a result, reports of optimum temperatures of hydrolytic microorganisms vary, but normally fall between 30 °C and 60 °C. Various studies have shown that the size of substrate particles and the rate of hydrolysis are inversely related [77–79]. It has also been observed that the amounts of particulates affect the microbial community [20]. Dai et al. [20] studied the effects of food waste TS on the microbial community composition at mesophilic conditions and observed changes in microbes involved in hydrolysis as well as methanogenesis.

### *4.4. Disintegration and Hydrolysis Models*

Both disintegration and hydrolysis steps are extracellular processes. This is in contrast with the rest of anaerobic digestion processes of acidogenesis, acetogenesis and methanogenesis that are intracellular. Enzyme mediated breakdown of complex molecules into smaller ones occur during hydrolysis. Disintegration consists of mostly physical processes that result in the breakdown of solid composite particulates into smaller and easier-to-hydrolyze components. Understanding the kinetics of these processes is crucial in understanding the overall AD process. As rate-limiting steps, disintegration, and hydrolysis kinetics play a role in determining various AD parameters such as residence time and reactor size. Various attempts have been made to model disintegration and hydrolysis kinetics. A brief overview of some of the most applied models is provided below. First-order kinetics is the most common kinetics used to describe both disintegration and hydrolysis kinetics. Disintegration kinetics is provided in Equation (2) whereas Equations (1a)–(1d) show hydrolysis kinetics.

$$\frac{dX_C}{dt} = -K_{dis}X_c \tag{2}$$

where $X_c$ is complex particulates in kgCOD $m^{-3}$ and $K_{dis}$ is disintegration rate constant in $d^{-1}$. First-order kinetics has been extensively used due to its simplicity but there are some drawbacks. First-order kinetics considers disintegration as a purely chemical process while it is partly a biological process that incorporates several other processes such as lysis and physical breakdown [80]. First-order kinetics does not account for the contribution of microorganisms in the disintegration process [80]. Therefore, models that use first-order kinetics such as ADM1 have limited precision when complex substrates such as manure are used. Both disintegration and hydrolysis are modeled by first-order kinetics in ADM1. Some modify the first-order kinetics by introducing a term to account for biological effects, such as Valentini et al. [81], who introduced the concentration of biomass into the hydrolysis kinetics equation as follows:

$$\frac{dX_C}{dt} = -K_hX_cX_{biom} \tag{3}$$

where $K_h$ is hydrolysis rate constant. Varieties of this model, where the term $X_{biom}$ in Equation (3) is replaced by $X_{biom}^A$('A-order biomass kinetics') by such as $X_{biom}^{1/2}$ has been proposed [82]. The value of A is between 0 and 1 and it depends on the particle's shape. Values of 0, 1/2 and 2/3 are proposed for flat, cylinder, and spherical shaped particles, respectively [78].

A two-phase model proposed the surface area of solid particulates covered by microorganisms to formulate kinetics of hydrolysis [51,65]. In the first phase, microbes colonize and cover all available surface of the particulates. In the second phase, the attached microbes release enzymes that progressively

degrade the particulates at a constant depth per unit time. The two-phase model was developed based on the assumptions that:

- Particles are spherical;
- Hydrolysis rate is limited by the particle–bacteria contact area;
- Particle size > depth of bacterial layer;
- Number of particles per volume remains constant during hydrolysis;
- Size of particles decrease due to hydrolysis.

Based on these assumptions, Vavilin et al. [65] formulated a rate expression for particle degradation (Equation (4)) and an expression for a rate constant that is dependent on particle size and bacterial layer depth (Equation (5)).

$$X_h = K_h X_f^{1/3} X^{2/3} \tag{4}$$

$$K_h = 6K_{m,h}\frac{\rho_B}{\rho_X}\frac{\partial}{d_X} \tag{5}$$

where $X_h$ is the rate of particle degradation in kgCOD $m^{-3}$ $d^{-1}$, $K_h$ is hydrolysis rate constant in $d^{-1}$, $X_f$ is the concentration of influent biodegradable organic matter in kgCOD $m^{-3}$, X is the concentration of biodegradable suspended solids in kgCOD $m^{-3}$, $K_{m,h}$ is maximum specific hydrolysis rate in $d^{-1}$, $\rho_B$ is the density of the microbial layer in kgCOD $m^{-3}$, $\rho_X$ is the density of particulate in kgCOD $m^{-3}$, $d_X$ is the current diameter of the hydrolyzed particle in m, and $\partial$ is the depth of the bacterial layer in m. The two-phase model shows a good fit for various types of substrates including swine manure [65]. A modified version of the Monod equation is sometimes used to model hydrolysis. It was first formulated for dissolved substrates. Because of that, there are critics who argue against using it for particle-rich substrates. However, Lin [83] showed, using anaerobic digestion of landfill leachate, that it can be applicable for substrates with suspended solids. The basic equation is given as follows:

$$\frac{dX_C}{dt} = -K_h\frac{X_c X_{biom}}{K_s + X_c} \tag{6}$$

where $K_s$ is half-saturation concentration, $X_C$ is complex particulates, $K_h$ is hydrolysis rate constant, $X_{biom}$ is active biomass.

Terashima and Lin [84] suggested a hydrolytic flux model based on the quantity of solid matter hydrolyzed per unit surface area per unit time. It is similar to the surface kinetic model suggested by Sanders et al. [85] (Equation (8)).

$$\frac{dX_C}{dt} = -K_h S_{surf} X_{biom} \rho_{solid} \tag{7}$$

$$\frac{dX_C}{dt} = -K_h S_{surf} \tag{8}$$

where $S_{surf}$ is the surface area of solid particulates and $\rho_{solid}$ is the density of solid particulates.

Various authors report that Contois kinetics provides a better fit for AD of complex substrates compared to first-order kinetics [86–88]. Contois kinetics (Equation (9)) takes effects of active biomass ($X_{biom}$) and its ratio to the slowly degradable substances (Xc) in the substrate into account.

$$\frac{dX_C}{dt} = -K_{m,dis}\frac{\frac{X_c}{X_{biom}}}{K_{s,dis} + \frac{X_c}{X_{biom}}}X_{biom} \tag{9}$$

where $K_{m,dis}$ is maximum disintegration rate in $d^{-1}$, $K_{s,dis}$ is a dimensionless half-saturation coefficient.

Dimock et al. [89] studied the influence of the size of protein particles on hydrolysis. They observed that hydrolysis results not only in the release of readily digested substrates but also in the break-up of

large particles into smaller ones. The break-up increases the available surface area for hydrolysis. This shows that disintegration and hydrolysis cannot easily be distinguished (also justifying the way the two steps are presented together in this chapter). They suggested a surface-based particle break-up model (PBM) for disintegration and hydrolysis that takes into account the increase in the surface area due to the disintegration of large particles.

$$\frac{dX_C}{dt} = -K'_h f_{av} X_c = \rho_{PBM} \tag{10}$$

$$\frac{df_{av}}{dt} = c_{av} \rho_{PBM} \tag{11}$$

where $K'_h$ is modified hydrolysis constant in m/d, $f_{av}$ is surface to volume ratio variable in $m^{-1}$, $c_{av}$ is a constant that correlates particle breakup and hydrolysis rates in $m^2$/kg. Studies on the influence of particle size of carbohydrates on the rate of hydrolysis and disintegration were also carried out by Kommedal et al. [90] who studied the effect of molecular weight of Dextrans (a form of polymeric carbohydrate) on microbial hydrolysis. They found that polymers of 6–500 kDa molecular weight range showed an inverse correlation to a half-order degradation rate expression (i.e., rate~M.Wt$^{-0.2}$).

$$\frac{dS_b}{dt} = -\frac{r_a A_f}{V} \tag{12}$$

$$r_A = K_{1/2,A} \sqrt{S_b - K_s \ln\left[\frac{K_s + S_b}{K_s}\right]} \tag{13}$$

where $S_b$ is the polymer bulk-phase concentration in gTOC $m^{-3}$ (TOC = total organic carbon), V is the bulk-phase reactor volume in $m^3$, $r_A$ is areal removal rate in gTOC $m^{-2}$ $h^{-1}$, $K_{1/2,\,A}$ is areal specific removal rate coefficient in $g^{1/2}$ $m^{-1/2}$ $d^{-1}$, $K_s$ is Monod half-saturation coefficient in g/$m^3$, and $A_f$ is the biofilm area in $m^2$. Particulate starch has also been used as a model substrate to investigate the degradation of suspended solids and colloids in aerobic granular sludge by de Kreuk et al. [91]. They studied the effect of particulate starch on granule morphology and overall conversion processes in aerobic granular sludge (sequencing batch reactor). They observed that the starch particles undergo fast adsorption onto granules followed by slow hydrolysis. Oxygen Uptake Rate (OUR) data indicated that particulate starch hydrolysis follows first-order kinetics (Equation (2)) as opposed to the zero-order kinetics observed when soluble starch was used. Soluble starch removal was similar both in aerobic and anaerobic conditions indicating that hydrolysis was independent of the presence of oxygen. Their results indicate that disintegration and not hydrolysis is the rate-limiting step in starch particle degradation. Presence of suspended solids in the influent also affected the morphology of aerobic granules, favoring the growth of filamentous structures on granule surfaces [92], suggesting active mechanisms to retain, and degrade feed particles in granular sludge processes (as also argued in Section 4.1). This mechanism of filamentous structures extending out of granules may also contribute to sludge loss, such as reported for slaughterhouse wastewater treatment [16], by a similar mechanism as sludge bulking in activated sludge processes [10].

## 5. Treatment Strategies for Particle-Rich Substrates

In earlier sections, we discussed problems associated with high-rate digestion of substrates with high suspended solids content. The main problem is usually the slow rate of particle degradation and as a result, excessive solids accumulation. This section reviews treatment strategies for particle-rich substrates, mainly focusing on enhancing the rate at which solid particulates are disintegrated and hydrolyzed. One of the most common strategies when dealing with particle-rich substrates is pretreatment. It has become an essential aspect of high-rate AD reactors with particle-rich substrates. Several methods of pretreatment discussed in earlier sections are based on reducing the size of the particulates in the substrate. Particle-rich substrates such as manure slurries produce a relatively high

amount of biogas after pretreatment; however, economically sustainable pretreatment methods are limited. Many of the pretreatment methods assessed for the purpose of this article seem to add a significant amount to the overall cost (both capital and operational costs). Disintegration and hydrolysis within the AD reactors to limit cost are therefore the main topic here. Optimizing process parameters that affect disintegration and hydrolysis can have desired effects. Temperature, HRT, loading rate, and other process parameters have to be tuned but the main issue appears to be sludge retention. If the degradable feed particles can be retained much longer than the HRT, they can be degraded even if their degradation rates are low.

Several studies have shown promising results with regard to increased hydrolysis as well as increased biogas production due to the addition of enzymes [87]. Enhancing the degradation of lignocellulosic substances using enzymes that degrade lignin, cellulose, and other polysaccharides has been the focus of enzymatic treatment studies. Lignocellulosic materials constitute a significant percentage of solid particulates in manure slurries, food waste, and other substrates. Use of enzyme, combined with alkali, not only increases the yield but also the rate of production of biogas from such materials [88]. Microorganisms that are not usually associated with anaerobic digestion, such as fungi, may be used to break down lignocellulosic substances. Myint et al. [92] reported an increase in the hydrolysis of cattle manure using brown-rot fungi, which degrades cellulose and hemicellulosic substances. There are also reports of white-rot and soft-rot fungi being effective in degrading cellulose and lignin-based substrates [93]. There are indications that oxygen consuming facultative microorganisms can also be helpful in increasing hydrolysis through 'micro-aeration' or nitrate addition [54,61,94,95]. Research to enhance hydrolysis by a selection of microorganisms that can carry out fast and efficient hydrolysis is also carried out [96]. Anaerobic co-digestion of two or more complementary substrates is a strategy to alleviate problems associated with one substrate by adding another substrate that can improve the growth conditions for the entire AD microbial community. Co-digestion of particle-rich substrates such as manure slurries and industrial wastewater with low suspended solids content has been carried out extensively in the past few years, however, with moderate success [97]. Substrates with high solid content are associated with operational difficulties such as pumping problems like clogging, channeling, and mixing problems, indicating that operation and design of the reactor can affect not only hydrolysis but also the overall digestion process. Pumps used for high solid substrates must be able to operate under adverse conditions. Chopper pumps that are equipped with a cutting system could be a good fit for particle-rich substrates due to their contribution to particle size reduction and avoidance of clogging. The reactor design and configuration must be made in consideration with optimum solid hydrolysis.

Van Lier [98] stated that one way to treat suspended solids in high-rate reactors is to use separate reactor units such as clarifiers coupled to sludge digesters to enhance the digestion. In such an arrangement, the particle disintegration and hydrolysis steps are separately enhanced and hydrolyzed matter recycled to the main digester. An example of such a system is the UASB-digester system presented by Mahmoud et al. [99], where suspended solids are separated and transported to a separate digester with long retention time and high temperature for disintegration and hydrolysis before recycled to the main UASB reactor. Various other hybrid reactor systems have been proposed to enhance suspended solids removal such as up-flow anaerobic sludge bed fixed film (UASFF), hybrid anaerobic solid–liquid-UASB (HASL-UASB), and anaerobic filter-UASB [100], finding that such reactors are capable of treating substrates with a significant content of particulates and achieve high suspended solids removal. For example, Ahmad et al. [101] and Ohimain and Izah [102] show that UASB-type reactors could treat palm oil mill effluent with 50–60 g/L suspended solids content. Design features, such as reactors with recirculation that promote longer particle retention time, better contact, and solids removal should be considered when particle-rich substrates are used. Such strategies may, however, involve extra costs, while [11,23,25–27] show that conventional UASB-type reactors could treat high suspended solids content.

## 6. Concluding Remarks

This review paper assesses the state of high-rate digestion of particle-rich substrates. Successful high-rate AD of particle-rich substrates with TS content as high as 35% is possible as demonstrated by various authors. In conventional high-rate reactors such as UASB, the TS limit seemed to be lower with examples found at around 10% TS, above which mass transfer limitation becomes a problem. In many cases, some forms of reactor modification are applied and there may be HRT or OLR restrictions due to the high solid content of the substrates. We further conclude that:

- High-rate anaerobic digestion of particle-rich substrates has the potential to increase biogas production significantly due to the abundance of such substrates. However, economically sustainable methods of pretreatment are limited and several methods have been tried to improve the hydrolysis of solid particulates with varying degree of success (e.g., use of hydrolytic enzymes);
- Slow disintegration and hydrolysis of particulates is the main bottleneck in fully achieving the biogas potential of particle-rich substrates in high-rate sludge bed processes;
- Disintegration and hydrolysis of particulates within high-rate AD appear more promising;
- High-rate AD is traditionally assumed to only handle low particulate levels such as in industrial waste while newer studies show that high-rate reactors, especially hybrid types, may handle high levels of particulates;
- The degree of particle degradation within AD depends mainly on retention time so the challenge is to obtain long SRT in reactors with low HRT (SRT > HRT);
- Feed particles have typically much lower density than granular sludge and may therefore not be retained by the same reactor configurations as the granules. They may float when associated with biogas bubbles;
- Devices to retain floating sludge may, therefore, be required to obtain efficient disintegration and hydrolysis of particulates;
- There is evidence that the bacteria in the outer layer of granules can use extracellular polymeric structures to attach particles for the purpose of retaining and digesting feed particles;
- Disintegration and hydrolysis are treated as a single step in some models when they are both assumed to have first-order kinetics and this works well for non-complex substrates. Most particle-rich substrates are however quite complex and a wide range of models are proposed to handle such but more research is needed to find the best modeling approach. The relevance is emphasized by the fact that these are often the rate-limiting steps of the entire AD process on particle-rich substrates. However, modified first-order kinetics that classifies solid particles into fast and slow disintegrating fractions may be a good approach for particle-rich substrates since it retains the simplicity of first-order kinetics and improves on its accuracy.

**Author Contributions:** Conceptualization, All authors; methodology, F.A.T.; validation, F.A.T.; formal analysis, All authors; investigation, F.A.T.; resources, F.A.T.; data curation, F.A.T.; writing—original draft preparation, F.A.T.; writing—review and editing, All authors; visualization, F.A.T.; supervision, R.B. and W.H.B.; project administration, F.A.T. and R.B.; funding acquisition, R.B.

**Funding:** This research was part of a PhD project funded by Interreg BioGas2020 and partly funded by the Research Council of Norway ("Energyx project 269444 Bærekraftig biogass").

**Conflicts of Interest:** The authors declare no conflict of interest.

## References

1. Bagi, Z.; Ács, N.; Böjti, T.; Kakuk, B.; Rákhely, G.; Strang, O.; Szuhaj, M.; Wirth, R.; Kovács, K.L. Biomethane: The Energy Storage, Platform Chemical and Greenhouse Gas Mitigation Target. *Anaerobe* **2017**, *46*, 13–22. [CrossRef] [PubMed]
2. Cantera, S.; Muñoz, R.; Lebrero, R.; López, J.C.; Rodríguez, Y.; García-Encina, P.A. Technologies for the Bioconversion of Methane into More Valuable Products. *Curr. Opin. Biotechnol.* **2018**, *50*, 128–135. [CrossRef] [PubMed]

3. Batstone, D.J.; Virdis, B. The Role of Anaerobic Digestion in the Emerging Energy Economy. *Curr. Opin. Biotechnol.* **2014**, *27*, 142–149. [CrossRef] [PubMed]
4. Boe, K.; Angelidaki, I. Serial CSTR Digester Configuration for Improving Biogas Production from Manure. *Water Res.* **2009**, *43*, 166–172. [CrossRef] [PubMed]
5. Berglann, H.; Krokann, K. *Biogassproduksjon På Basis Av Husdyrgjødsel—Rammebetingelser, Økonomi Og Virkemidler*; Norsk Institutt for Landbruksøkonomisk Forskning (NILF): Oslo, Norway, 2011.
6. Lettinga, G.; Hulshoff Pol, L.W. USAB-Process Design for Various Types of Wastewaters. *Water Sci. Technol.* **1991**, *24*, 87–107. [CrossRef]
7. Liu, Y.H.; He, Y.L.; Yang, S.C.; Li, Y.Z. The Settling Characteristics and Mean Settling Velocity of Granular Sludge in Upflow Anaerobic Sludge Blanket (UASB)-like Reactors. *Biotechnol. Lett.* **2006**, *28*, 1673–1678. [CrossRef] [PubMed]
8. Mahmoud, N.; Zeeman, G.; Gijzen, H.; Lettinga, G. Solids Removal in Upflow Anaerobic Reactors, a Review. *Bioresour. Technol.* **2003**, *90*, 1–9. [CrossRef]
9. Montoya AC, V.; Mazareli RD, S.; Da Silva, D.C.; De Oliveira, R.A.; Leite, V.D. Dairy Manure Wastewater in Serial UASB Reactors for Energy Recovery and Potential Effluent Reuse. *Braz. J. Chem. Eng.* **2017**, *34*, 971–983. [CrossRef]
10. Tchobanoglous, G.; Burton, F.L.; Stensel, H.D. *Wastewater Engineering Treatment and Reuse*; McGraw-Hill Higher Education: Boston, MA, USA, 2003.
11. Bergland, W.H.; Dinamarca, C.; Toradzadegan, M.; Nordgård, A.S.R.; Bakke, I.; Bakke, R. High Rate Manure Supernatant Digestion. *Water Res.* **2015**, *76*, 1–9. [CrossRef]
12. Lettinga, G. Sustainable Integrated Biological Wastewater Treatment. *Water Sci. Technol.* **1996**, *33*, 85–98. [CrossRef]
13. Lettinga GA, F.M.; Van Velsen AF, M.; Hobma, S.D.; De Zeeuw, W.; Klapwijk, A. Use of the Upflow Sludge Blanket (USB)Reactor Concept for Biological Wastewater Treatment, Especially for Anaerobic Treatment. *Biotechnol. Bioeng.* **1980**, *22*, 699–734. [CrossRef]
14. Rajeshwari, K.V.; Balakrishnan, M.; Kansal, A.; Lata, K.; Kishore, V.V.N. State-of-the-Art of Anaerobic Digestion Technology for Industrial Wastewater Treatment. *Renew. Sustain. Energy Rev.* **2000**, *4*, 135–156. [CrossRef]
15. Van Lier, J.B.; Van Der Zee, F.P.; Frijters, C.T.M.J.; Ersahin, M.E. Celebrating 40 Years Anaerobic Sludge Bed Reactors for Industrial Wastewater Treatment. *Rev. Environ. Sci. Biotechnol.* **2015**, *14*, 681–702. [CrossRef]
16. Tilley, E.; Lüthi, C.; Morel, A.; Zurbrügg, C.; Schertenleib, R. *Compendium of Sanitation Systems and Technologies*, 2nd ed.; Swiss Federal Institute of Aquatic Science and Technology (Eawag): Dübendorf, Switzerland, 2014; pp. 121–122.
17. Zeeman, G.; Sanders, W.T.M.; Wang, K.Y.; Lettinga, G. Anaerobic Treatment of Complex Wastewater and Waste Activated Sludge–application of an Upflow Anaerobic Solid Removal (UASR) Reactor for the Removal and Pre-Hydrolysis of Suspended COD. *Water Sci. Technol.* **1997**, *35*, 121–128. [CrossRef]
18. Bergland, W.; Dinamarca, C.; Bakke, R. Efficient Biogas Production from the Liquid Fraction of Diary Manure. *Renew. Energy Power Qual. J.* **2014**, *12*. [CrossRef]
19. Bergland, W.; Dinamarca, C.; Bakke, R. Effects of Psychrophilic Storage on Manures as Substrate for Anaerobic Digestion. *BioMed Res. Int.* **2014**, *2014*, 712197. [CrossRef] [PubMed]
20. Yi, J.; Dong, B.; Jin, J.; Dai, X. Effect of Increasing Total Solids Contents on Anaerobic Digestion of Food Waste under Mesophilic Conditions: Performance and Microbial Characteristics Analysis. *PLoS ONE* **2014**, *9*, e102548. [CrossRef] [PubMed]
21. Fagbohungbe, M.O.; Dodd, I.C.; Herbert, B.M.J.; Li, H.; Ricketts, L.; Semple, K.T. High Solid Anaerobic Digestion: Operational Challenges and Possibilities. *Environ. Technol. Innov.* **2015**, *4*, 268–284. [CrossRef]
22. Abbassi-Guendouz, A.; Brockmann, D.; Trably, E.; Dumas, C.; Delgenès, J.-P.; Steyer, J.-P.; Escudié, R. Total Solids Content Drives High Solid Anaerobic Digestion via Mass Transfer Limitation. *Bioresour. Technol.* **2012**, *111*, 55–61. [CrossRef]
23. Massé, D.I.; Droste, R.L. Comprehensive Model of Anaerobic Digestion of Swine Manure Slurry in a Sequencing Batch Reactor. *Water Res.* **2000**, *34*, 3087–3106. [CrossRef]
24. Fujihira, T.; Seo, S.; Yamaguchi, T.; Hatamoto, M.; Tanikawa, D. High-Rate Anaerobic Treatment System for Solid/Lipid-Rich Wastewater Using Anaerobic Baffled Reactor with Scum Recovery. *Bioresour. Technol.* **2018**, *263*, 145–152. [CrossRef] [PubMed]

25. Andalib, M.; Hafez, H.; Elbeshbishy, E.; Nakhla, G.; Zhu, J. Treatment of Thin Stillage in a High-Rate Anaerobic Fluidized Bed Bioreactor (AFBR). *Bioresour. Technol.* **2012**, *121*, 411–418. [CrossRef] [PubMed]
26. Fang, C.; Sompong, O.; Boe, K.; Angelidaki, I. Comparison of UASB and EGSB Reactors Performance, for Treatment of Raw and Deoiled Palm Oil Mill Effluent (POME). *J. Hazard. Mater.* **2011**, *189*, 229–234. [CrossRef] [PubMed]
27. Borja, R.; Banks, C.J.; Sánchez, E. Anaerobic Treatment of Palm Oil Mill Effluent in a Two-Stage up-Flow Anaerobic Sludge Blanket (UASB) System. *J. Biotechnol.* **1996**, *45*, 125–135. [CrossRef]
28. Jensen, P.; Batstone, D. *Energy and Nutrient Analysis on Individual Waste Streams*; Meat and Livestock Australia Limited: North Sydney, Australia, 2012.
29. Lorimor, J.; Powers, W.; Sutton, A. *Manure Characteristics: Manure Management Systems Series: MWPS 18, Section 1*; MidWest Plan Service: Ames, IA, USA, 2004.
30. Wang, X.; Lu, X.; Li, F.; Yang, G. Effects of Temperature and Carbon-Nitrogen (C/N)Ratio on the Performance of Anaerobic Co-Digestion of Dairy Manure, Chicken Manure and Rice Straw: Focusing on Ammonia Inhibition. *PLoS ONE* **2014**, *9*, e97265. [CrossRef]
31. Hills, D.J. Effects of Carbon: Nitrogen Ratio on Anaerobic Digestion of Dairy Manure. *Agric. Wastes* **1979**, *1*, 267–278. [CrossRef]
32. Manitoba Agriculture. Food and Rural Development. Properties of Manure. Available online: https://www.gov.mb.ca/agriculture/environment/nutrient-management/pubs/properties-of-manure.pdf (accessed on 15 January 2019).
33. Hartmann, H.; Ahring, B.K. The Future of Biogas Production. In Proceedings of the Risø International Energy Conference, Risø, Denmark, 23 May 2005; pp. 23–25.
34. Moore, P.A.; Daniel, T.C.; Sharpley, A.N.; Wood, C.W. Poultry Manure Management: Environmentally Sound Options. *J. Soil Water Conserv.* **1995**, *50*, 321–327.
35. Hadin, Å.; Eriksson, O. Horse Manure as Feedstock for Anaerobic Digestion. *Waste Manag.* **2016**, *56*, 506–518. [CrossRef]
36. Kebreab, E.; Clark, K.; Wagner-Riddle, C.; France, J. Methane and Nitrous Oxide Emissions from Canadian Animal Agriculture: A Review. *Can. J. Anim. Sci.* **2006**, *86*, 135–157. [CrossRef]
37. Feng, L.; Ward, A.J.; Moset, V.; Møller, H.B. Methane Emission during On-Site Pre-Storage of Animal Manure Prior to Anaerobic Digestion at Biogas Plant: Effect of Storage Temperature and Addition of Food Waste. *J. Environ. Manag.* **2018**, *225*, 272–279. [CrossRef]
38. Hamilton, D.W.; Luce, W.G.; Heald, A.D. *Production and Characteristics of Swine Manure*; Oklahoma Cooperative Extension Service: Stillwater, MN, USA, 1997.
39. Jurado, E.; Antonopoulou, G.; Lyberatos, G.; Gavala, H.N.; Skiadas, I.V. Continuous Anaerobic Digestion of Swine Manure: ADM1-Based Modelling and Effect of Addition of Swine Manure Fibers Pretreated with Aqueous Ammonia Soaking. *Appl. Energy* **2016**, *172*, 190–198. [CrossRef]
40. Møller, H.B.; Sommer, S.G.; Ahring, B.K. Methane Productivity of Manure, Straw and Solid Fractions of Manure. *Biomass Bioenergy* **2004**, *26*, 485–495. [CrossRef]
41. Yenigün, O.; Demirel, B. Ammonia Inhibition in Anaerobic Digestion: A Review. *Process Biochem.* **2013**, *48*, 901–911. [CrossRef]
42. Kovács, E.; Wirth, R.; Maróti, G.; Bagi, Z.; Rákhely, G.; Kovács, K.L. Biogas Production from Protein-Rich Biomass: Fed-Batch Anaerobic Fermentation of Casein and of Pig Blood and Associated Changes in Microbial Community Composition. *PLoS ONE* **2013**, *8*, e77265. [CrossRef] [PubMed]
43. Molnar, L.; Bartha, I. High Solids Anaerobic Fermentation for Biogas and Compost Production. *Biomass* **1988**, *16*, 173–182. [CrossRef]
44. Kaparaju, P.; Rintala, J. Anaerobic Co-Digestion of Potato Tuber and Its Industrial by-Products with Pig Manure. *Resour. Conserv. Recycl.* **2005**, *43*, 175–188. [CrossRef]
45. Nuchdang, S.; Phalakornkule, C. Anaerobic Digestion of Glycerol and Co-Digestion of Glycerol and Pig Manure. *J. Environ. Manag.* **2012**, *101*, 164–172. [CrossRef]
46. Aangelidaki, I.; Ahrin, B.K.; Deng, H.; Schmidt, J.E. Anaerobic Digestion of Olive Oil Mill Effluents Together with Swine Manure in UASB Reactors. *Water Sci. Technol.* **2002**, *45*, 213–218. [CrossRef]
47. Lo, K.V.; Liao, P.H.; Gao, Y.C. Anaerobic Treatment of Swine Wastewater Using Hybrid UASB Reactors. *Bioresour. Technol.* **1994**, *47*, 153–157. [CrossRef]

48. Nordgård, A.S.R.; Bergland, W.H.; Vadstein, O.; Mironov, V.; Bakke, R.; Østgaard, K.; Bakke, I. Anaerobic Digestion of Pig Manure Supernatant at High Ammonia Concentrations Characterized by High Abundances of Methanosaeta and Non-Euryarchaeotal Archaea. *Sci. Rep.* **2017**, *7*, 15077. [CrossRef]
49. Batstone, D.J.; Keller, J.; Angelidaki, I.; Kalyuzhnyi, S.V.; Pavlostathis, S.G.; Rozzi, A.; Sanders, W.T.; Siegrist, H.; Vavilin, V.A. The IWA Anaerobic Digestion Model No 1 (ADM1). *Water Sci. Technol.* **2002**, *45*, 65–73. [CrossRef] [PubMed]
50. Polizzi, C.; Alatriste-Mondragón, F.; Munz, G. Modeling the Disintegration Process in Anaerobic Digestion of Tannery Sludge and Fleshing. *Front. Environ. Sci.* **2017**, *5*, 37. [CrossRef]
51. Vavilin, V.A.; Fernandez, B.; Palatsi, J.; Flotats, X. Hydrolysis Kinetics in Anaerobic Degradation of Particulate Organic Material: An Overview. *Waste Manag.* **2008**, *28*, 939–951. [CrossRef] [PubMed]
52. Ariunbaatar, J.; Panico, A.; Esposito, G.; Pirozzi, F.; Lens, P.N.L. Pretreatment Methods to Enhance Anaerobic Digestion of Organic Solid Waste. *Appl. Energy* **2014**, *123*, 143–156. [CrossRef]
53. Zheng, Y.; Zhao, J.; Xu, F.; Li, Y. Pretreatment of Lignocellulosic Biomass for Enhanced Biogas Production. *Prog. Energy Combust. Sci.* **2014**, *42*, 35–53. [CrossRef]
54. Fletcher, M. Bacterial biofilms and biofouling. *Curr.Opin. Biotechnol.* **1994**, *5*, 302–306. [CrossRef]
55. Lew, B.; Belavski, M.; Admon, S.; Tarre, S.; Green, M. Temperature Effect on UASB Reactor Operation for Domestic Wastewater Treatment in Temperate Climate Regions. *Water Sci. Technol.* **2003**, *48*, 25–30. [CrossRef] [PubMed]
56. Uemura, S.; Harada, H. Treatment of Sewage by a UASB Reactor under Moderate to Low Temperature Conditions. *Bioresour. Technol.* **2000**, *72*, 275–282. [CrossRef]
57. Lew, B.; Tarre, S.; Belavski, M.; Green, M. UASB Reactor for Domestic Wastewater Treatment at Low Temperatures: A Comparison between a Classical UASB and Hybrid UASB-Filter Reactor. *Water Sci. Technol.* **2004**, *49*, 295–301. [CrossRef]
58. Ganidi, N.; Tyrrel, S.; Cartmell, E. Anaerobic Digestion Foaming Causes—A Review. *Bioresour. Technol.* **2009**, *100*, 5546–5554. [CrossRef]
59. Pagilla, K.R.; Craney, K.C.; Kido, W.H. Causes and Effects of Foaming in Anaerobic Sludge Digesters. *Water Sci. Technol.* **1997**, *36*, 463–470. [CrossRef]
60. Dictionary by Merriam-Webster: America's Most-Trusted Online Dictionary. Available online: https://www.merriam-webster.com/ (accessed on 15 February 2019).
61. Morgenroth, E.; Kommedal, R.; Harremoës, P. Processes and modeling of hydrolysis of particulate organic matter in aerobic wastewater treatment-a review. *Water Sci. Technol.* **2002**, *45*, 25–40. [CrossRef] [PubMed]
62. Noike, T.; Endo, G.; Chang, J.; Yaguchi, J.; Matsumoto, J. Characteristics of Carbohydrate Degradation and the Rate-limiting Step in Anaerobic Digestion. *Biotechnol. Bioeng.* **1985**, *27*, 1482–1489. [CrossRef] [PubMed]
63. Ma, J.; Frear, C.; Wang, Z.W.; Yu, L.; Zhao, Q.; Li, X.; Chen, S. A Simple Methodology for Rate-Limiting Step Determination for Anaerobic Digestion of Complex Substrates and Effect of Microbial Community Ratio. *Bioresour. Technol.* **2013**, *134*, 391–395. [CrossRef] [PubMed]
64. Wang, Z.W.; Lee, S.H.; Elkins, J.G.; Morrell-Falvey, J.L. Spatial and temporal dynamics of cellulose degradation and biofilm formation by Caldicellulosiruptor obsidiansis and Clostridium thermocellum. *AMB Express* **2011**, *1*, 1–10. [CrossRef]
65. Vavilin, V.A.; Rytov, S.V.; Lokshina, L.Y. A Description of Hydrolysis Kinetics in Anaerobic Degradation of Particulate Organic Matter. *Bioresour. Technol.* **1996**, *56*, 229–237. [CrossRef]
66. Contois, D.E. Kinetics of bacterial growth: Relationship between population density and specific growth rate of continuous cultures. *J. Gen. Microbiol.* **1959**, *21*, 40–50. [CrossRef]
67. Henze, M.; Gujer, W.; Mino, T.; Van Loosdrecht, M. *Activated Sludge Models ASM1, ASM2, ASM2d and ASM3*; IWA Publishing: London, UK, 2000.
68. Wang, Z.W.; Li, Y. A theoretical derivation of the Contois equation for kinetic modeling of the microbial degradation of insoluble substrates. *Biochem. Eng. J.* **2014**, *82*, 134–138. [CrossRef]
69. Koch, K.; Drewes, J.E. Alternative Approach to Estimate the Hydrolysis Rate Constant of Particulate Material from Batch Data. *Appl. Energy* **2014**, *120*, 11–15. [CrossRef]
70. Azman, S.; Khadem, A.F.; Van Lier, J.B.; Zeeman, G.; Plugge, C.M. Presence and Role of Anaerobic Hydrolytic Microbes in Conversion of Lignocellulosic Biomass for Biogas Production. *Crit. Rev. Environ. Sci. Technol.* **2015**, *45*, 2523–2564. [CrossRef]

71. Bayer, E.A.; Kenig, R.; Lamed, R. Adherence of Clostridium Thermocellum to Cellulose. *J. Bacteriol.* **1983**, *156*, 818–827. [CrossRef] [PubMed]
72. Parawira, W. Enzyme research and application in biotechnological intensification of biogas production. *Crit. Rev. Biotechnol.* **2012**, *32*, 172–186. [CrossRef] [PubMed]
73. Ravndal, K.T.; Kommedal, R. Starch degradation and intermediate dynamics in flocculated and dispersed microcosms. *Water Sci. Technol.* **2017**, *76*, 2928–2940. [CrossRef] [PubMed]
74. Jaeger, K.E.; Ransac, S.; Dijkstra, B.W.; Colson, C.; Van Heuvel, M.; Misset, O. Bacterial lipases. *FEMS Microbial. Rev.* **1994**, *15*, 29–63. [CrossRef] [PubMed]
75. Kanmani, P.; Aravind, J.; Kumaresan, K. An insight into microbial lipases and their environmental facet. *Int. J. Environ. Sci. Technol.* **2015**, *12*, 1147–1162. [CrossRef]
76. Cammarota, M.C.; Freire, D.M.G. A review on hydrolytic enzymes in the treatment of wastewater with high oil and grease content. *Bioresour. Technol.* **2006**, *97*, 2195–2210. [CrossRef] [PubMed]
77. Dasari, R.K.; Berson, R.E. The Effect of Particle Size on Hydrolysis Reaction Rates and Rheological Properties in Cellulosic Slurries. In *Applied Biochemistry and Biotecnology*; Springer: Berlin/Heidelberg, Germany, 2007; pp. 289–299.
78. Yeh, A.-I.; Huang, Y.-C.; Chen, S.H. Effect of Particle Size on the Rate of Enzymatic Hydrolysis of Cellulose. *Carbohydr. Polym.* **2010**, *79*, 192–199. [CrossRef]
79. Ramirez, I.; Mottet, A.; Carrère, H.; Déléris, S.; Vedrenne, F.; Steyer, J.-P. Modified ADM1 Disintegration/Hydrolysis Structures for Modeling Batch Thermophilic Anaerobic Digestion of Thermally Pretreated Waste Activated Sludge. *Water Res.* **2009**, *43*, 3479–3492. [CrossRef]
80. Rozzi, A.; Merlini, S.; Passino, R. Development of a Four Population Model of the Anaerobic Degradation of Carbohydrates. *Environ. Technol.* **1985**, *6*, 610–619. [CrossRef]
81. Valentini, A.; Garuti, G.; Rozzi, A.; Tilche, A. Anaerobic Degradation Kinetics of Particulate Organic Matter: A New Approach. *Water Sci. Technol.* **1997**, *36*, 239–246. [CrossRef]
82. Aldin, S. *The Effect of Particle Size on Hydrolysis and Modeling of Anaerobic Digestion*; Electronic Thesis and Dissertation Repository: Western Ontario, ON, Canada, 2010; p. 60.
83. Lin, C.Y. Anaerobic Digestion of Landfill Leachate. *Water SA* **1991**, *17*, 301–306.
84. Terashima, Y.; Lin, S. On the Modeling of Microbiological Hydrolysis of Organic Solids. *Water Sci. Technol.* **2000**, *42*, 11–19. [CrossRef]
85. Sanders, W.T.M.; Geerink, M.; Zeeman, G.; Lettinga, G. Anaerobic hydrolysis kinetics of particulate substrates. *Water Sci. Technol.* **2000**, *41*, 17–24. [CrossRef] [PubMed]
86. Hashimoto, A.G.; Chen, Y.R.; Varel, V.H. Theoretical Aspects of Methane Production: State-of-the-Art. In *Livestock Waste, a Renewable Resource*; American Society of Agricultural Engineers: St. Joseph, Michigan, USA, 1981; pp. 86–91.
87. Speda, J.; Johansson, M.A.; Odnell, A.; Karlsson, M. Enhanced Biomethane Production Rate and Yield from Lignocellulosic Ensiled Forage Ley by in Situ Anaerobic Digestion Treatment with Endogenous Cellulolytic Enzymes. *Biotechnol. Biofuels* **2017**, *10*, 129. [CrossRef] [PubMed]
88. Liu, X.; Zicari, S.M.; Liu, G.; Li, Y.; Zhang, R. Pretreatment of Wheat Straw with Potassium Hydroxide for Increasing Enzymatic and Microbial Degradability. *Bioresour. Technol.* **2015**, *185*, 150–157. [CrossRef] [PubMed]
89. Dimock, R.; Morgenroth, E. The Influence of Particle Size on Microbial Hydrolysis of Protein Particles in Activated Sludge. *Water Res.* **2006**, *40*, 2064–2074. [CrossRef] [PubMed]
90. Kommedal, R.; Milferstedt, K.; Bakke, R.; Morgenroth, E. Effects of Initial Molecular Weight on Removal Rate of Dextran in Biofilms. *Water Res.* **2006**, *40*, 1795–1804. [CrossRef]
91. De Kreuk, M.K.; Kishida, N.; Tsuneda, S.; Van Loosdrecht, M.C.M. Behavior of Polymeric Substrates in an Aerobic Granular Sludge System. *Water Res.* **2010**, *44*, 5929–5938. [CrossRef]
92. Myint, M.T.; Nirmalakhandan, N. Enhancing Anaerobic Hydrolysis of Cattle Manure in Leachbed Reactors. *Bioresour. Technol.* **2009**, *100*, 1695–1699. [CrossRef]
93. Hatakka, A.I. Pretreatment of Wheat Straw by White-Rot Fungi for Enzymic Saccharification of Cellulose. *Eur. J. Appl. Microbiol. Biotechnol.* **1983**, *18*, 350–357. [CrossRef]
94. Montalvo, S.; Vielma, S.; Borja, R.; Huiliñir, C.; Guerrero, L. Increase in Biogas Production in Anaerobic Sludge Digestion by Combining Aerobic Hydrolysis and Addition of Metallic Wastes. *Renew. Energy* **2018**, *123*, 541–548. [CrossRef]

95. American Public Health Association. *Standard Methods for the Examination of Water and Wastewater*, 20th ed.; American Public Health Association: Washington, DC, USA, 1999; p. 1325, ISBN 978-08-7553-235-6.
96. de Lourdes Moreno, M.; Pérez, D.; García, M.T.; Mellado, E. Halophilic Bacteria as a Source of Novel Hydrolytic Enzymes. *Life* **2013**, *3*, 38–51. [CrossRef] [PubMed]
97. Mata-Alvarez, J.; Dosta, J.; Romero-Güiza, M.S.; Fonoll, X.; Peces, M.; Astals, S. A Critical Review on Anaerobic Co-Digestion Achievements between 2010 and 2013. *Renew. Sustain. Energy Rev.* **2014**, *36*, 412–427. [CrossRef]
98. Van Lier, J.B. High-Rate Anaerobic Wastewater Treatment: Diversifying from End-of-the-Pipe Treatment to Resource-Oriented Conversion Techniques. *Water Sci. Technol.* **2008**, *57*, 1137–1148. [CrossRef] [PubMed]
99. Mahmoud, N.; Zeeman, G.; Gijzen, H.; Lettinga, G. Anaerobic Sewage Treatment in a One-Stage UASB Reactor and a Combined UASB-Digester System. *Water Res.* **2004**, *38*, 2348–2358. [CrossRef] [PubMed]
100. Tauseef, S.M.; Abbasi, T.; Abbasi, S.A. Energy Recovery from Wastewaters with High-Rate Anaerobic Digesters. *Renew. Sustain. Energy Rev.* **2013**, *19*, 704–741. [CrossRef]
101. Ahmad, A.; Ghufran, R.; Abd Wahid, Z. Effect of COD Loading Rate on an Upflow Anaerobic Sludge Blanket Reactor during Anaerobic Digestion of Palm Oil Mill Effluent with Butyrate. *J. Environ. Eng. Landsc. Manag.* **2012**, *20*, 256–264. [CrossRef]
102. Ohimain, E.I.; Izah, S.C. A Review of Biogas Production from Palm Oil Mill Effluents Using Different Configurations of Bioreactors. *Renew. Sustain. Energy Rev.* **2017**, *70*, 242–253. [CrossRef]


© 2019 by the authors. Licensee MDPI, Basel, Switzerland. This article is an open access article distributed under the terms and conditions of the Creative Commons Attribution (CC BY) license (http://creativecommons.org/licenses/by/4.0/).

## Article 3:

# Effect of particulate disintegration on biomethane potential of particle-rich substrates in batch anaerobic reactor.

Tassew FA, Bergland WH, Dinamarca C, Bakke R. Effect of Particulate Disintegration on Biomethane Potential of Particle-rich Substrates in Batch Anaerobic Reactor. Applied Sciences. 2019; 9(14):2880. https://doi.org/10.3390/app9142880

applied sciences

MDPI

*Article*

# Effect of Particulate Disintegration on Biomethane Potential of Particle-Rich Substrates in Batch Anaerobic Reactor

**Fasil Ayelegn Tassew *, Wenche Hennie Bergland, Carlos Dinamarca and Rune Bakke**

Department of Process, Energy and Environmental Technology, University of South-Eastern Norway, Kjølnes Ring 56, NO 3918 Porsgrunn, Norway

* Correspondence: fasil.a.tassew@usn.no

Received: 24 June 2019; Accepted: 15 July 2019; Published: 18 July 2019

**Featured application: The findings in this article contribute to understanding solid particle disintegration and hydrolysis kinetics and how the presence of solid particulates in the form of lignocellulosic substances affect biomethane production rate and yield. It has a potential application in anaerobic digestion of particle-rich feeds in high-rate reactors.**

**Abstract:** An investigation of particle disintegration was carried out using batch anaerobic reactors and a particle-rich substrate from pig manure supernatant. Two types of samples were applied, one high in suspended particles (raw feed) and another low in suspended particle content (centrifuged feed). Both feeds were digested with and without cellulase enzyme addition to obtain a better understanding of particle degradation mechanisms. An automatic methane potential test system (AMPTS) was used to carry out batch reactions at 35 °C. The raw feed with high-suspended solids had higher biomethane potential than the centrifuged feed but the conversion rate and methane yield was lower. The addition of cellulase increased biomethane production rates in both high- and low-particle content samples enhancing yield by 54% and 40%, respectively and converting 69% and 87% of feed chemical oxygen demand (COD), respectively. This implies that the feed particles have high contents of cellulose. This is also the case for the smaller particles remaining after centrifugation. Comparisons of anaerobic digestion model no. 1 (ADM1) simulations with experimental data reveal that classifying substrate particles into a fast and a slow degrading fraction with separate disintegration kinetics fit the experimental data better than lumping all particles into one parameter.

**Keywords:** anaerobic digestion; particle-rich substrate; suspended solids disintegration; disintegration kinetics; cellulase

## 1. Introduction

Biomethane potential (BMP) test is an anaerobic digestion carried out, normally, in batch reactors for a prolonged time in order to estimate the ultimate biomethane or biogas potential of a specific substrate. There is no defined volume for batch reactors but volumes 0.5–1 L are often used. The substrate and inoculum used during anaerobic digestion are characterized in terms of total and soluble chemical oxygen demand (COD), total and volatile solids (TS and VS) as well as various other parameters (Table 1). The theoretical biomethane potential is calculated using various chemical equation relationships and compared with the estimate from the BMP tests in terms of yield, such as L $CH_4$/g VS or g $CH_4$ COD/g feed COD. BMP tests are widely used due to their low cost, simplicity and repeatability. Even though BMP tests take a relatively long time, usually longer than 30 days [1],

they are crucial in assessing design parameters for full-scale anaerobic reactors. Full-scale reactors, especially those that are high-rate, often face difficulty in achieving the full biomethane potential of particle-rich substrates due to slow degradation of solid particles. Significant parts of the organic substances contained in the substrate remain undigested, limiting the efficiency of the reactors. It is important to unlock the biomethane potential of such substrates. Particle-rich substrates such as the organic fraction of municipal solid waste (OFMSW) and manure are abundantly available resources that are prime candidates for anaerobic digestion and biomethane production. If the problem of slow solid disintegration were solved, the efficiency of high-rate digestion of particle-rich substrates such as manure would be greatly improved. Estimating the BMP of particle-rich substrates is one of the steps towards achieving that goal. In this article, we aim to clarify the effect of solid particle content on disintegration and hydrolysis of substrates by comparing batch test results from high-particle and low-particle substrates. The tests were carried out with and without the addition of enzyme to obtain a better understanding of the limiting factors in disintegration of particulates. Finally, we aim to establish a simple but adequate kinetic model that uses classification of complex particulates into fast and slow degrading fractions to accurately represent the disintegration of particle-rich substrates.

**Table 1.** Feed sample characteristics.

| Property | Raw Feed (RF) | Centrifuged Feed (RF) |
|---|---|---|
| TS (g/L) | 21.5 | 12.2 |
| VS (g/L) | 13.8 | 5.9 |
| TSS (g/L) | 14.2 | 2.5 |
| VSS (g/L) | 12.0 | 2.3 |
| TDS (g/L) | 7.3 | 9.7 |
| VDS (g/L) | 1.7 | 3.6 |
| $COD_{total}$ (g/L) | 33.2 | 19.7 |
| $COD_{soluble}$ (g/L) | 16.6 | 11.4 |
| $NH_4^+$ (g/L) | 1.8 | 1.3 |
| pH | 7.0 | 7.0 |

TS: Total Solids; VS: Volatile Solids; TSS: Total Suspended Solids; VSS: Volatile Suspended Solids; TDS: Total Dissolved Solids; VDS: Volatile Dissolved Solids; COD: Chemical Oxygen Demand.

### *1.1. Lignocellulosic Substances*

Presence of lignocellulosic substances in substrates is one of the main reasons for the low conversion efficiency of particle-rich substrates. Lignocellulosic substances consist of three biopolymers called cellulose, hemicellulose and lignin that are present in the cell walls of plant matter. The relative composition of the polymers differs from plant to plant. Hardwoods and softwoods contain a relatively high amount of cellulose whereas straws and grass contain higher hemicellulose content [2]. Glucose molecules are linked through beta-(1,4) glycosidic bonds to form a disaccharide that is polymerized into cellulose (Figure 1). Cellulose is homogenous because it is formed from a single monosaccharide. Hemicellulose, on the other hand, is formed from several monosaccharides including xylose and glucose. This results in a heterogeneous polymer that is more amorphous and has a more hydrolysable structure than that of cellulose. Lignin is made up of phenol-based monomers that are cross-linked to form a large and complex chemical structure that is chemically and biologically resistant to degradation.

Particle-rich substrates such as manure slurry contain a significant amount of lignocellulosic substances [3]. The source of such lignocellulosic substances is plant matter that is fed to the animals and used as bedding material for the animals. Readily biodegradable material in the animal feed is absorbed in the intestine and the leftover manure is composed of a substantial amount of lignocellulosic matter that is difficult to biodegrade. Up to 40–50% of the total solids in manure are lignocellulosic substances [3]. Lignocellulosic substances are difficult to biodegrade because their composite structure limits the accessibility of substrates by hydrolyzing enzymes [4]. A total of 20–300 monomers of cellulose are bound together by hydrogen and Van der Waals forces to make packed

cellulosic microfibrils. The microfibrils are mostly in crystalline form and their outer layer is covered with hemicellulose chains. Lignin polymer binds the cellulosic microfibrils and hemicelluloses together and acts like a "glue" to form a rigid macromolecular structure that is inaccessible for enzymatic attack. Due to this reinforced concrete-like structure, disintegration and hydrolysis are difficult. By some estimates, up to 80% of lignocellulosic substances remain undegraded in biogas reactors [5]. The composition of the lignocellulosic content of manure differs from animal to animal as well as the age of the animal. For swine manure, typical cellulose, hemicellulose and lignin contents are 30–50%, 20–30% and 10–20%, respectively (Figure 2). Despite favorable qualities such as abundance, easy availability and being renewable, lignocellulosic substances have not been efficiently used for biogas production due to their strong resistance to biodegradation. Various physical, chemical and biological methods were tried to unlock the biogas potential of lignocellulosic substances with various degrees of success. One of these methods involves the addition of enzymes to facilitate the breakdown of lignocellulose components into their monosaccharides. Bacteria naturally secrete enzymes such as cellulase and hemicellulase that facilitate hydrolysis of lignocellulosic substances. Both cellulase and hemicellulase are groups of several enzymes that can carry out cellulolysis and hemicellulolysis. Other microorganisms such as fungi are also known to produce enzymes that hydrolyze lignocellulose substances. Identifying and isolating enzymes for lignocellulose hydrolysis is a growing field of research due to the advantages associated with enzymatic hydrolysis of lignocellulose such as increased biogas yield and low energy demand [6,7]. Several authors reported an increased biogas yield due to the addition of hydrolytic enzymes [8–10]. The increase in biogas yield due to the addition of enzymes depends on the type and concentration of enzymes added, temperature, pH and other parameters. There are commercially available cocktails of hydrolytic enzymes that are extracted from various microorganisms including fungi.

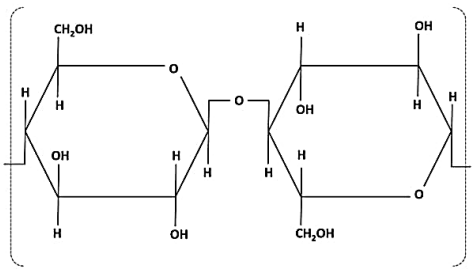


**Figure 1.** Building block of cellulose polymer.

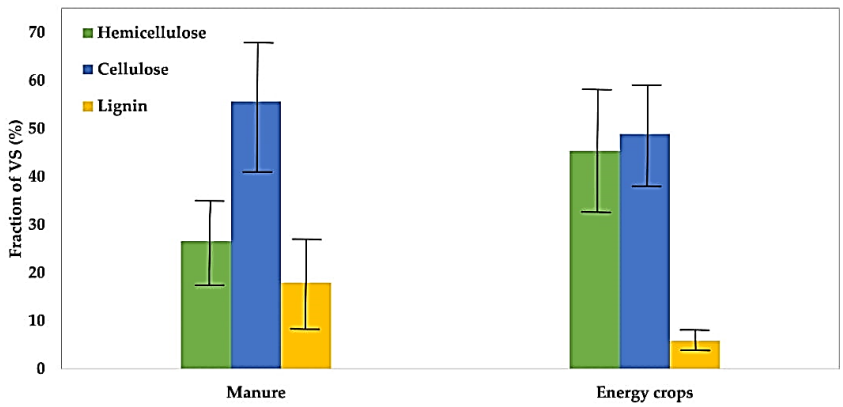


**Figure 2.** Composition of hemicellulose, cellulose and lignin contents as a percentage of volatile solids (VS) in manure and energy crops (data from Triolo et al. [11]).

*1.2. Hydrolysis Kinetics*

Hydrolysis is often assumed to be a first-order reaction [12,13] and its rate can be determined using batch reactor tests. Biomethane potential (BMP) and hydrolysis rate constant ($K_h$) are obtained by performing data fitting from batch reactor data. First-order kinetics is the simplest and most common hydrolysis rate expression.

$$\frac{dX}{dt} = K_h X \quad (1)$$

$$\frac{dX_{ch}}{dt} = K_{h,ch} X_{ch} \quad (1.1)$$

$$\frac{dX_{pr}}{dt} = K_{h,pr} X_{pr} \quad (1.2)$$

$$\frac{dX_{li}}{dt} = K_{h,li} X_{li} \quad (1.3)$$

where dX/dt is hydrolysis rate in kg $CODm^{-3}d^{-1}$, $K_h$ is hydrolysis rate constant in $d^{-1}$, X is the particulate component in kg $CODm^{-3}$ and subscripts ch, pr, and li denote carbohydrate, protein and lipid, respectively. Angelidaki et al. [14] proposed a protocol for the determination of $K_h$ from batch tests using an integrated form of the generalized hydrolysis rate expression (Equation (1)).

$$\ln\frac{X_\infty - X}{X_\infty} = -K_h t \quad (2)$$

$$X = X_\infty(1 - e^{-K_h t}) \quad (3)$$

where, $X_\infty$ is the value of ultimate methane production and X is the amount of methane produced at a given time, t. After batch test data are collected, a graph is plotted where $K_h$ is determined as a slope of $\ln\frac{X_\infty - X}{X_\infty}$ and t. The last day of the batch test should be when the difference between biogas productions at day n and day n + 1 is less than or equal to 1% of the cumulative biogas production. This is in accordance with the German Guideline VDI 4630 for BMP estimation [15]. The value of $K_h$ is important because it is a unique characteristic of a substrate and it can be used to assess the suitability of a given substrate for anaerobic digestion. It tells us how much time it takes to reach a certain percentage of the ultimate methane production [16]. There are also other methods to determine $K_h$ experimentally such as the one suggested by Eastman and Ferguson [17].

## 2. Materials and Methods

Two swine manure slurry samples, with high- and low-suspended particle content, were applied. Both samples were digested with and without cellulase enzyme addition. Automatic methane potential test system (AMPTS) was used to carry out batch reactions at 35 °C. The digestion, without cellulase enzyme addition, was simulated in anaerobic digestion model no. 1 (ADM1) using two disintegration constants to describe fast and slow digestible particles.

*2.1. Sample Preparation*

Swine manure slurry was collected at a swine production farm in Porsgrunn, Norway. Samples were collected at various depths in intermediate indoor storage and mixed. In order to avoid the thick solid mass found at the bottom of the storage, sampling was made only in the top half of the storage. The samples still contained a substantial amount of suspended solids. This mixed sample was labelled "Raw feed" (RF). One additional sample called "Centrifuged feed" (CF) was prepared by centrifuging the raw feed sample and discarding most of the solids, thereby reducing the total and suspended solid contents. A high-speed centrifuge was used to carry out centrifugation (Beckman J-25, with JA-10 rotor). All samples were characterized immediately after preparation and kept in a refrigerator at 4 °C until they were transferred to the reactor bottles. Two separate sample groups

were also prepared by adding 1.2 g cellulase in 75 mL of both RF and CF samples to form RF-cellulase (RF-CEL) and CF-cellulase (CF-CEL), respectively (Table 2). Two types of blanks were prepared, one that contained only distilled water and inoculum (BLANK) and another one that contained distilled water, inoculum and 1.2 g cellulase (BLANK-CEL). Preliminary tests, as well as reviews of works by other authors, indicated that low enzyme concentration might lead to an insignificant increase in biogas yield. As a result, we decided to use a relatively high concentration of enzyme so that the enzymatic effects are sufficiently noticeable (used 1.2 g enzyme/1.03 g VS for RF and 1.2 g Enzyme/0.44 g VS for CF).

**Table 2.** Sample preparation for batch test initial conditions.

| Sample Name | Sample Description | Feed (mL) | Granule (mL) | Total (mL) | Headspace (mL) |
|---|---|---|---|---|---|
| RF1 | Raw feed parallel 1 | 75 (sample) | 200 | 275 | 200 |
| RF2 | Raw feed parallel 2 | 75 (sample) | 200 | 275 | 200 |
| RF3 | Raw feed parallel 3 | 75 (sample) | 200 | 275 | 200 |
| RF-CEL1 | Raw feed and cellulase parallel 1 | 1.2 g cellulase + 75 (sample) | 200 | 275 | 200 |
| RF-CEL2 | Raw feed and cellulase parallel 2 | 1.2 g cellulase + 75 (sample) | 200 | 275 | 200 |
| RF-CEL3 | Raw feed and cellulase parallel 3 | 1.2 g cellulase + 75 (sample) | 200 | 275 | 200 |
| CF1 | Centrifuged feed parallel 1 | 75 (sample) | 200 | 275 | 200 |
| CF2 | Centrifuged feed parallel 2 | 75 (sample) | 200 | 275 | 200 |
| CF3 | Centrifuged feed parallel 3 | 75 (sample) | 200 | 275 | 200 |
| CF-CEL1 | Centrifuged feed and cellulase parallel 1 | 1.2 g cellulase + 75 (sample) | 200 | 275 | 200 |
| CF-CEL2 | Centrifuged feed and cellulase parallel 2 | 1.2 g cellulase + 75 (sample) | 200 | 275 | 200 |
| CF-CEL3 | Centrifuged feed and cellulase parallel 3 | 1.2 g cellulase + 75 (sample) | 200 | 275 | 200 |
| BLANK1 | Blank parallel 1 | 75 (distilled water) | 200 | 275 | 200 |
| BLANK2 | Blank parallel 2 | 75 (distilled water) | 200 | 275 | 200 |
| BLANK-CEL | Blank and cellulase parallel 1 | 1.2 g cellulase + 75 (distilled water) | 200 | 275 | 200 |

RF: Raw Feed; CF: Centrifuged Feed; CEL: Cellulase; BLANK: Distilled water and inoculum.

**Table 3.** Volatile fatty acid (VFA) concentration in feed samples.

| VFA | Concentration (g/L) |
|---|---|
| Acetic acid | 3.9 |
| Propionic acid | 0.2 |
| Isobutyric acid | 0.0 |
| Butyric acid | 0.6 |
| Isovaleric acid | 0.2 |
| Valeric acid | 0.1 |
| Isocaproic acid | 0.0 |
| Caproic acid | 0.0 |
| Heptanoic acid | 0.0 |
| Total | 4.9 |

### 2.2. *Sample Analysis*

Total solids (TS), volatile solids (VS), total suspended solids (TSS) and volatile suspended solids (VSS) of samples were measured according to the American public health association standard method 2540 (APHA 1999) [18]. Total and soluble COD of feed samples were also measured according to the APHA standard (method 5220 D). Sample pH was measured using a Beckman 300 pH meter equipped with Sentix-82 pH electrode. Ammonium–nitrogen content ($NH_4^+$-N) was measured according to APHA 4500-$NH_3$. Both COD and $NH_4^+$-N concentrations were measured using commercially available test kits and Spectroquant Pharo 300 spectrophotometer (Darmstadt, Germany). Total and individual VFA (volatile fatty acid) content of samples were measured using an Agilent gas chromatography flame ionization detector (GC-FID). Sample characterization results are provided in Table 1 and VFA concentrations are provided in Table 3. Total and volatile solids contents of granular sludge were also measured as a mass percentage (% *w*/*w*) according to AMPTS II manual (Bioprocess control 2016) [19].

*2.3. Reactor and Experimental Procedure*

Automatic methane potential test system (AMPTS II) from Bioprocess control, Sweden was used to carry out batch anaerobic digestion experiments [19]. The instrument includes a water bath, a $CO_2$ removal set-up using NaOH, adjustable motor stirrers and an apparatus for the measurement of methane flow (Figure 3). In addition, the instrument provides software to control/monitor reactor settings and plot gas measurement. The batch test was carried out in three parallels for RF, RF-CEL, CF and CF-CEL samples. The maximum number of batch reactors in the AMPTS II set up was 15 allowing two parallels for BLANK and only one parallel for BLANK-CEL. The experiment was carried out at 35 °C. Reactor contents were stirred every hour to allow proper mixing and to facilitate gas removal from the reactors.

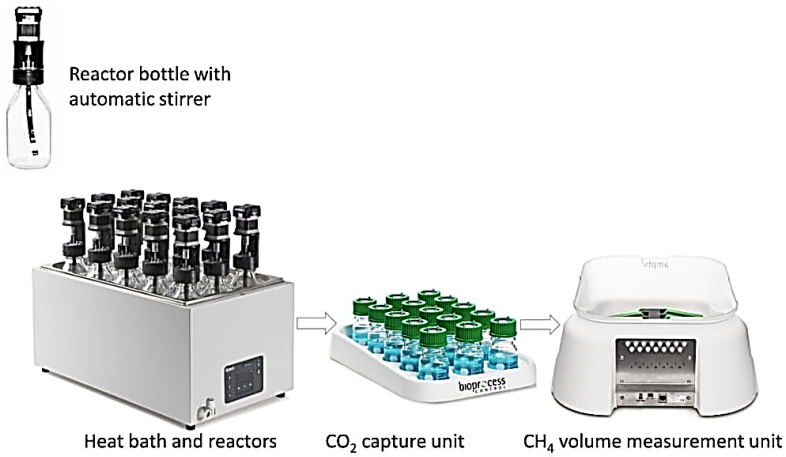


**Figure 3.** Automatic methane potential test system (AMPTS) II batch reactor experimental setup (pictures from Bioprocess control's homepage).

*2.4. Granular Sludge Degassing*

A mixture of granules from various sources was used as inoculum for the batch experiments (mainly granules that have been used to treat wastewater from pulp and paper industry mixed with granules obtained from econvert Water & Energy, Heerenveen, the Netherlands). The granules were degassed before samples were added [14]. Degassing was performed by placing granule containers in a water bath at the reaction temperature (35 °C) for 10 days. The total solid and volatile solid contents of the granule were measured after degassing.

*2.5. $CO_2$ Removal*

The $CO_2$ removal set-up requires solution preparation and the following solutions were prepared [19]. A solution of 1.2 L NaOH (3 M) was prepared by mixing 144 g of NaOH in 1.2 L distilled water. pH indicator thymolphthalein solution (0.4%) was prepared by mixing 40 mg of thymolphthalein in 9 mL of ethanol (99.5%) and 1 mL distilled water. A total of 6 mL of the thymolphthalein solution was added into 1.2 L NaOH solution. The resulting mixture was transferred to $CO_2$ removal bottles, one for each batch test and each with an 80 mL mixture. The thymolphthalein-NaOH mixture has a bright blue color and when enough $CO_2$ is absorbed, the blue color fades and becomes colorless. Thymolphthalein is bright blue in basic solutions but it turns colorless in acidic or neutral solutions. At this point, a new mixture has to be used. According to the $CO_2$ removal manual, this method absorbs more than 98% of $CO_2$ produced during the biogas production process. The removal is based on the following reaction [20]:

$$CO_{2\,(g)} \rightarrow CO_{2\,(aq)} \quad (4)$$

$$CO_{2\,(aq)} + OH^-_{(aq)} \rightarrow HCO_3^-{}_{(aq)} \quad (5)$$

$$HCO_3^-{}_{(aq)} + OH^-_{(aq)} \rightarrow CO_3^{2-}{}_{(aq)} + H_2O_{(l)} \quad (6)$$

*2.6. Theoretical Methane Yield*

Theoretical methane yield was calculated based on the total COD of RF and CF samples. Theoretical calculation was performed as follows [21].

a. Determine COD equivalent of methane:

One mole of methane requires two moles of oxygen, meaning the chemical oxygen demand of methane is:

$$CH_4 + 2O_2 \rightarrow CO_2 + 2H_2O \quad (7)$$

$$\text{COD/mole } CH_4 = 2 \times 32 \text{ g } O_2\text{/mole} = 64 \text{ g } O_2\text{/mole}$$

b. Determine the theoretical volume of methane based on g COD

The volume of a mole of methane gas at standard conditions of 0 °C and one atm (atmospheric pressure) is 22.4 L. The theoretical volume of methane that can be obtained from a gram of COD is calculated as:

$$22.4 \text{ L } CH_4\text{/64 g COD} = 0.35 \text{ L } CH_4\text{/g COD}$$

To calculate the theoretical methane yield at 35 °C, we used the ideal gas law:

$$\frac{P_1V_1}{T_1} = \frac{P_2V_2}{T_2} = \text{Constant} \quad (8)$$

$$\text{Yield at } 35\,^{\circ}\text{C} = \frac{(1 \text{ atm})(0.35 \text{ L } CH_4\text{/g COD})(308.15 \text{ K})}{(1 \text{ atm})(298.15 \text{ K})} = 0.36 \text{ L } CH_4\text{/g COD}$$

c. Calculate theoretical methane yield of sample

Theoretical methane yields of all samples were calculated from total COD, sample volume and the value for yield at 35 °C.

$$CH_4 \text{ yield of sample (L)} = (COD_{total})(V_{sample})(0.36 \text{ L } CH_4\text{/g COD}) \quad (9)$$

d. Compare theoretical and experimental methane yield

Experimental methane yield was corrected by subtracting the average volume of methane produced by blank parallels ($V_{B1}$, $V_{B2}$, $V_{B3}$) from that of samples ($V_{P1}$, $V_{P2}$, $V_{P3}$).

$$\text{Experimental } CH_4 \text{ yield (L)} = \frac{\sum(V_{P1} + V_{P2} + V_{P3})}{N_{sample}} - \frac{\sum(V_{B1} + V_{B2} + V_{B3})}{N_{blank}} \quad (10)$$

*2.7. Anaerobic Digestion Model No. 1 (ADM1) Simulation*

Aquasim software was used to implement the ADM1 model to simulate the batch reactors (Table 4). Two modes of disintegration kinetics were used. In the first mode, first-order disintegration kinetics was used, and all complex particulates were assumed to be equally degradable (single disintegration constant, $K_{dis}$ used). In the second mode, the complex particulates were classified into fast degrading and slow degrading fractions, where two separate disintegration constants, $K_{dis1}$ for fast degrading and $K_{dis2}$ for slow degrading fractions, were used (Figure 4).

**Table 4.** Selected simulation parameters and values used to implement ADM1 in Aquasim.

| Parameter | RF | RF | CF | CF |
|---|---|---|---|---|
| | $K_{dis}$ | $K_{dis1}$ and $K_{dis2}$ | $K_{dis}$ | $K_{dis1}$ and $K_{dis2}$ |
| Disintegration constant ($d^{-1}$) | 0.17 | 0.17, 0.075 | 0.17 | 0.17, 0.075 |
| Amino acid degrading organisms (kg COD/$m^3$) | 1.70 | 1.70 | 1.70 | 1.70 |
| Acetate degrading organisms (kg COD/$m^3$) | 2.23 | 2.23 | 2.23 | 2.23 |
| Butyrate/valerate degrading organisms (kg COD/$m^3$) | 0.69 | 0.69 | 0.69 | 0.69 |
| Fatty acid degrading organisms (kg COD/$m^3$) | 1.85 | 1.85 | 1.85 | 1.85 |
| Hydrogen degrading organisms (kg COD/$m^3$) | 1.05 | 1.05 | 1.05 | 1.05 |
| Propionate degrading organisms (kg COD/$m^3$) | 0.29 | 0.29 | 0.29 | 0.29 |
| Sugar degrading organisms (kg COD/$m^3$) | 1.68 | 1.68 | 1.68 | 1.68 |
| Soluble amino acids (kg COD/$m^3$) | 0.2 | 0.2 | 0.2 | 0.2 |
| Soluble fatty acids (kg COD/$m^3$) | 0.25 | 0.25 | 0.25 | 0.25 |
| Soluble acetates (kg COD/$m^3$) | 0.66 | 0.66 | 0.66 | 0.66 |
| Soluble butyrates (kg COD/$m^3$) | 0.15 | 0.15 | 0.15 | 0.15 |
| Soluble propionates (kg COD/$m^3$) | 0.05 | 0.05 | 0.05 | 0.05 |
| Soluble valerates (kg COD/$m^3$) | 0.08 | 0.08 | 0.08 | 0.08 |

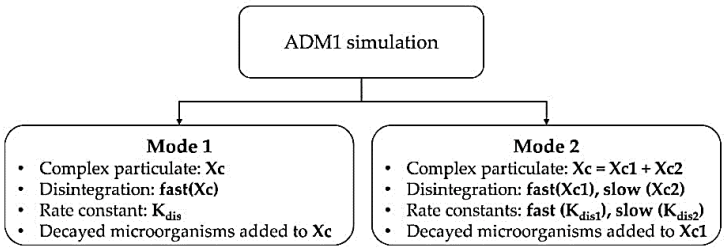


**Figure 4.** ADM1 simulation scheme for mode 1 and mode 2 simulations.

Classification of particulates into fast degrading and slow degrading was carried out as follows:

a. Calculate particulate COD (Xc)

$$\text{Particulate COD} = \text{COD}_{\text{total}} - \text{COD}_{\text{soluble}} \quad (11)$$

$$\text{COD}_{\text{total}} = \text{Total g COD in reactor}/V_{\text{reactor}} = \text{Sample COD}_{\text{total}} \times V_{\text{sample}}/V_{\text{reactor}} \quad (12)$$

For simplification of the simulation, soluble COD was assumed to equal to COD of volatile fatty acids ($\text{COD}_{\text{VFA}}$) and some minor constituents as seen in Table 4, according to Equation (13).

$$\text{COD}_{\text{soluble}} = \text{COD}_{\text{VFA}} + (\text{COD}_{\text{soluble amino acids}} + \text{COD}_{\text{soluble fatty acids}} + \text{COD}_{\text{soluble inerts}} + \text{COD}_{\text{soluble sugars}}) \quad (13)$$

b. Classify particulate COD into fast (Xc1) and slow (Xc2) degrading fractions:

Classification of Xc into Xc1 and Xc2 was carried out separately for RF and CF. The ratio of total dissolved solids to total solids was used as a basis to estimate the fast degrading fraction (Xc1) from which Xc2 was estimated (Xc2 = 1 − Xc1). Since RF contains a relatively large fraction of solid particulates, it was estimated that 85% of the COD comes from slowly degrading fragments and the rest from fast degrading fragments. In the case of CF, most of the solid particulates are removed due to centrifugation making COD from solid particles constitute a small part of the total COD. We estimated that 15% of COD comes from slow degrading and 85% comes from fast degrading particulates.

For RF:

Particulate COD (Xc) = (33.24 g COD/L sample × 0.075 L sample / 0.275 L) − (1.35 g/L) = 7.72 g COD/L

$$Xc1 = 0.85 \times 7.72 \text{ g COD/L} = 6.56 \text{ g COD/L}$$

$$Xc2 = 0.15 \times 7.72 \text{ g COD/L} = 1.16 \text{ g COD/L}$$

For CF:

Particulate COD (Xc) = (19.74 g COD/L sample × 0.075 L sample / 0.275 L) − (1.35 g/L) = 4.03 g COD/L

$$Xc1 = 0.15 \times 4.03 \text{ g COD/L} = 0.605 \text{ g COD/L}$$

$$Xc2 = 0.85 \times 4.03 \text{ g COD/L} = 3.43 \text{ g COD/L}$$

Based on suggestions from preliminary experimental data and literature survey [22], we used $K_{dis}$ value of 0.17 $d^{-1}$ for swine manure samples. For fast degrading fraction, $K_{dis1}$ stays at 0.17 $d^{-1}$ and for $K_{dis2}$ we used 0.075 $d^{-1}$ (~45% of $K_{dis1}$, estimated from biogas production data for straws, fibers and other solids). We used hydrolysis constants (10 $d^{-1}$) as suggested by Batstone et al. [23].

In the ADM1 model, decayed microorganisms are added into complex particulates (Xc). In the first mode of simulation, there is no change; all decayed microorganisms are added back to Xc, however, in the second mode, the decayed microorganisms are recycled back to the fast degrading (Xc1) fraction only.

## 3. Result and Discussion

The raw feed with high-suspended solids had higher biomethane potential per liter of substrate than the centrifuged feed but the conversion rate and methane yield (g $COD_{CH4}$/g $COD_{total}$) was lower. Addition of cellulase increased biomethane production rates and yields in both high- and low-particle content samples.

### *3.1. Yields*

Measured average methane production for the four cases investigated and two blank cases are presented in Figure 5. Blank adjusted total methane productions after 40 d were 403 ± 73 mL for RF, 621 ± 54 mL for RF-CEL, 331 ± 61 mL for CF and 462 ± 57 mL for CF-CEL. The highest volumes of methane were produced by cellulase containing samples RF-CEL and CF-CEL. Cellulase enhanced the COD conversions from 45% to 69% and 62% to 87% for RF and CF samples, respectively (Table 5). As expected, centrifuged samples resulted in lower ultimate methane production but higher specific methane yield than their non-centrifuged counterparts. From RF to RF-CEL specific yield increased from 390 to 600 L $CH_4$/kg VS and from CF to CF-CEL it increased from 742 to 1037 L $CH_4$/kg VS (Table 6).

**Table 5.** Comparison of theoretical (assuming complete feed COD conversion) and experimental methane productions.

| Sample | Experimental (mL) | Theoretical (mL) | Efficiency (%) |
|---|---|---|---|
| RF | 403 ± 73 | 898 | 45 |
| RF-CEL | 621 ± 54 | 898 | 69 |
| CF | 331 ± 61 | 533 | 62 |
| CF-CEL | 462 ± 57 | 533 | 87 |

**Table 6.** Specific methane yield of samples.

| Specific Methane Yield | RF | RF-CEL | CF | CF-CEL |
|---|---|---|---|---|
| L $CH_4$/g TS | 0.25 | 0.38 | 0.36 | 0.51 |
| L $CH_4$/g VS | 0.4 | 0.6 | 0.7 | 1.0 |
| L $CH_4$/g $COD_{total}$ | 0.16 | 0.25 | 0.22 | 0.31 |
| L $CH_4$/g $COD_{soluble}$ | 0.32 | 0.5 | 0.39 | 0.54 |
| g $COD_{CH4}$/g $COD_{total}$ | 0.44 | 0.69 | 0.61 | 0.86 |

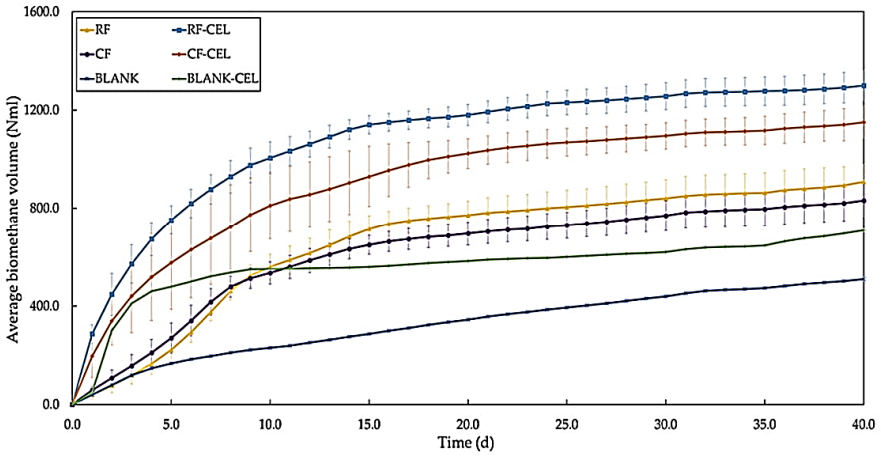


**Figure 5.** Average biomethane production for raw feed (RF) and centrifuged feed (CF), with and without cellulase, and two blank cases.

### *3.2. Production Rates*

Biomethane production rates peaked faster with much higher maximum production rates in samples with cellulase addition (RF-CEL and CF-CEL) than those without addition (Figure 6). Cellulase-added samples showed maximum biomethane production rate in the first 30 h of the experiment while the cases without enzyme addition had much lower maximum production and it was distributed over a longer time span, peaking after ~150 h. A brief peak during startup in all cases is assumed irrelevant (methane release from methane saturated inoculum due to temperature increase). RF-CEL reached a maximum of 34 mL/h at 17 h and CF-CEL reached 19 mL/h at 19 h followed by a decrease to ~3 mL/h at 250 h. The BLANK-CEL sample with cellulase but without added substrates reached a methane production rate of 48 mL/h at 28 h, showing that the cellulase itself has a significant BMP and can be degraded quickly. Fortunately, the cellulase was degraded after the main degradation peaks for the feeds, implying that it can carry out the intended enzymatic attack on the feed particulates before it is itself degraded and converted to methane. Cellulase can, therefore, be added to anaerobic digesters to enhance biomethane production from cellulose containing feeds but it is not analyzed here whether this is a sustainable solution.

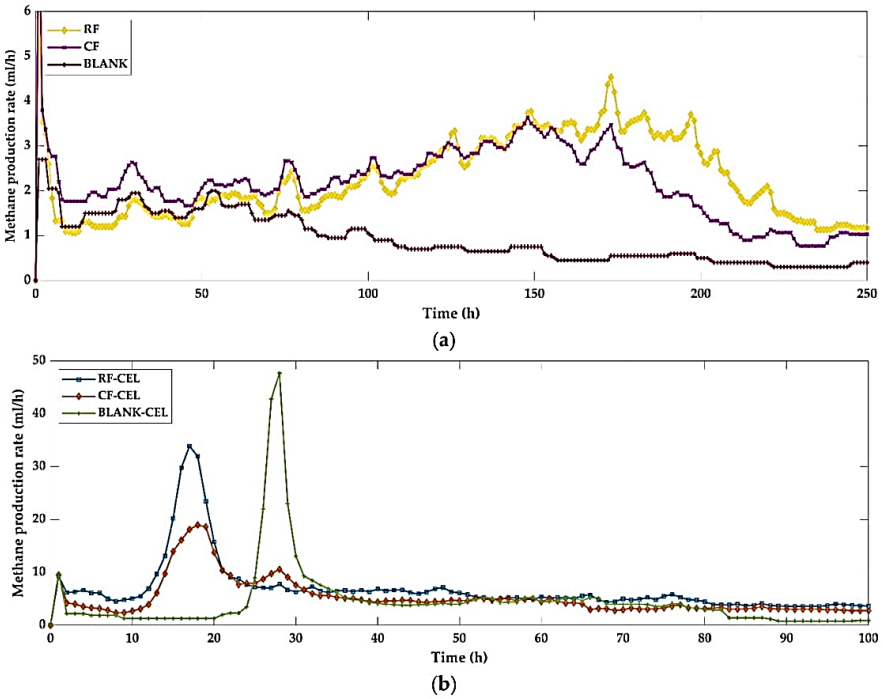


**Figure 6.** Measured average biomethane production rate: without cellulase (**a**) for the first 250 h and with cellulase (**b**) for the first 100 h.

### *3.3. Effect of Cellulase Addition and Centrifugation*

Enzyme additions were expected to have a stronger effect on samples that contain more particles, as observed. However, methane yield increase from CF to CF-CEL was quite high (40%) considering that centrifugation removed more than 80% of feed VSS (Table 1). The observation that addition of cellulase enzyme had a positive and comparable impact on methane yield both in raw and centrifuged samples (specific methane yield increased by 54% and 40% for RF and CF, respectively (Table 5)) suggests that there are similar fractions of cellulose in large and small particles in such animal manure slurries. The small particles evidently needed to undergo a similar disintegration process as those removed by centrifugation, with maximum rates at approximately the same time both with (Figure 6b) and without (Figure 6a) enzyme addition. Hydrolysis rate constants, $K_h$, determined from the slope of the plot $\ln\frac{X_\infty - X}{X_\infty}$ against t show how these observations can be included in process modeling. Only the first few days of the plot, where the curve was at its steepest was used to determine $K_h$ in accordance with suggestions by Angelidaki et al. [14]. Enzyme addition led to much higher $K_h$ values while centrifugation caused marginally larger $K_h$ (Table 7).

**Table 7.** Hydrolysis rate constant values estimated using Equation (2).

| Sample | $K_h$ ($d^{-1}$) |
|---|---|
| RF | 0.088 |
| RF-CEL | 0.154 |
| CF | 0.094 |
| CF-CEL | 0.120 |
| BLANK | 0.062 |
| BLANK-CEL | 0.148 |

*3.4. Simulation Results*

Using a single disintegration constant assumes all particulates disintegrate equally. $K_{dis}$ values in this mode of simulation are usually estimated based on the fast degrading fractions and this leads to an overestimation of methane production. In mode 1 simulation of the RF sample, methane production peaked very early in the digestion process (4–5 d) and continued to decline for the rest of the digestion, which differs significantly from the pattern of methane production observed in the experimental results. This phenomenon is visible in Figure 7a. Classifying particulates into fast degrading and slow degrading fractions seemed to rectify the overestimation of methane production (mode 2). Accounting for slow degrading particulates led to similar patterns in the timing of peak methane production. When the two modes of simulations are compared, it is apparent that the contribution of slow degrading particulates to the methane production became more and more significant at the later stages of digestion. Application of both modes of simulations on CF samples did not lead to significantly different results. Unlike RF, CF samples contain relatively small quantities of solid particulates, which are the main causes of reduced disintegration rate. Even if $K_{dis}$, $K_{dis1}$ and $K_{dis2}$ values for CF and RF are the same, the relative proportion of fast and slow degrading fractions are different. RF contains far more slow disintegrating particulates than CF. As a result, it is expected that simulations of CF in mode 1 (where all particulates are assumed to be degraded at $K_{dis}$ of 0.17 $d^{-1}$) and mode 2 (where 85% of particulates are assumed to be degraded at $K_{dis1}$ of 0.17 $d^{-1}$) lead to similar patterns of methane production. Both modes of simulations suggested peak methane productions slightly earlier than observed. Comparing both modes of simulations for CF samples (Figure 7b) it is noticeable that mode 1 simulation seemed a better fit for CF samples than mode 2, suggesting that classification of particulates into fast and slow degrading fractions may be better suited for particle-rich substrates than particle "free" substrates.

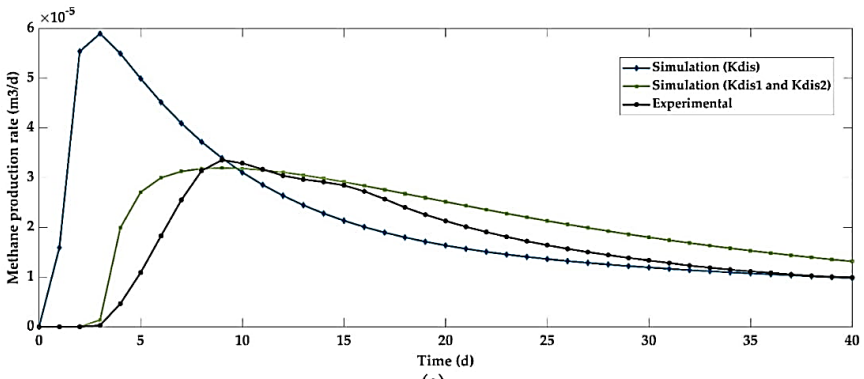


(a)

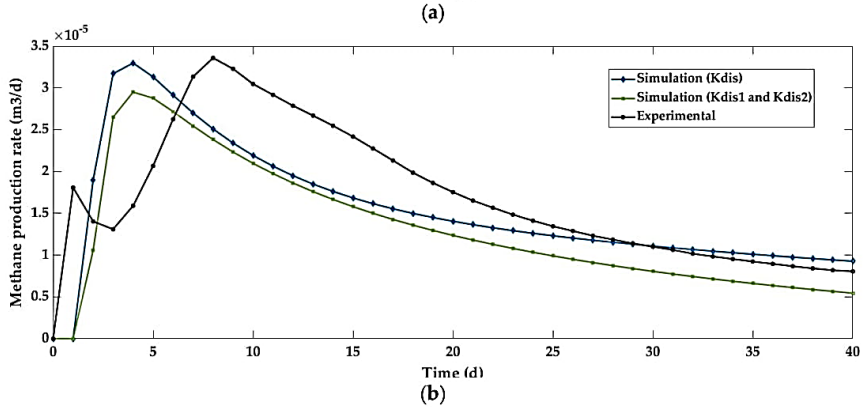


(b)

**Figure 7.** Methane production rate of simulation and experimental results: RF (**a**) and CF (**b**).

The patterns of degradation of particulates were compared using data from mode 1 and mode 2 simulation results (Figure 8). In both RF and CF mode 1 simulations, Xc followed a "logarithmic" decline throughout the course of the digestion process. In RF mode 2 simulation, slow degrading particulates decline in a similar fashion as the one observed by Xc in mode 1 simulations, however fast degrading particulates increased first (until 8–10 days) followed by a gradual decline. The increase in the fast degrading particulates is partly attributed to decaying microorganisms being added into Xc1. Particle size and presence of recalcitrant substances contribute heavily to the slow degradation of solid particulates. After disintegration, the rest of the anaerobic digestion process continues the same way whether the disintegrated particulate originated from slow or fast disintegrating fractions. As a result of this, the slowly disintegrated particulates are continuously being added into a rapidly disintegrated fraction that contributes to the increase in Xc1 at the beginning of the digestion. Mode 2 simulation of the CF sample did not show increasing Xc1 mainly due to the absence of enough slowly disintegrating particulates continuously added to it. In addition, the contribution from microbial decay was minimal.

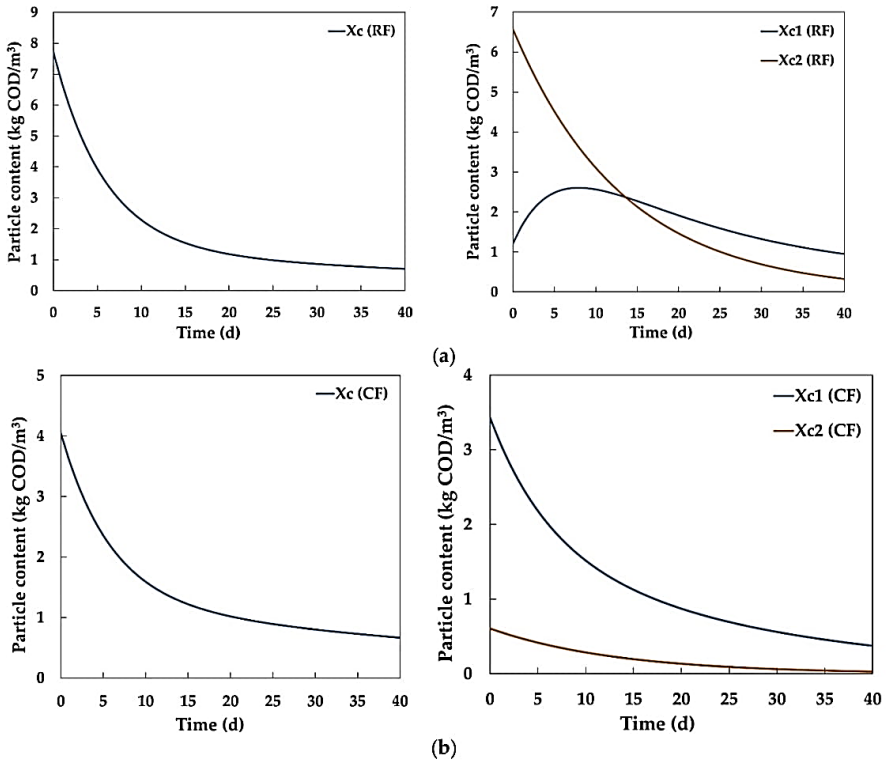


**Figure 8.** Comparison of particulate degradation in samples: RF (**a**) and CF (**b**).

Sensitivity analysis was carried out on $K_{dis1}$ and $K_{dis2}$ parameters in mode 2 simulation. Sensitivity analysis, which combines identifiability and uncertainty analysis, is used to check if $K_{dis}$ parameters can be uniquely determined from available data [24]. The sensitivity function of methane production with respect to $K_{dis1}$ and $K_{dis2}$ are shown in Figures 9 and 10. In both RF and CF, the methane production was much more sensitive to $K_{dis1}$ than $K_{dis2}$. Sensitivity to $K_{dis2}$ was more apparent in RF than CF. The sensitivity of various other variables to $K_{dis1}$ and $K_{dis2}$ is also given in the

form of sensitivity functions (SensAR) in Appendix A. The absolute-relative sensitivity function (Equation (A1)), was used to measure the absolute change in y (methane production) for 100% change in p ($K_{dis1}/K_{dis2}$).

Comparison of rates for RF and CF samples showed that the rate of biomethane production is faster in particles with lower solid particles, but it also showed that solid particulates breakdown slowly resulting in a steady biomethane production over a long period. In continuous reactors, solid accumulation may occur when substrates are added continuously without efficient solid disintegration and removal. Ideally, there should be a balance between rates of solid substrate addition and solid disintegration for a stable digestion process. In granular sludge bed reactors, solid particulates are often trapped in the sludge bed for long periods, meaning solid retention times much longer than the hydraulic retention time can be achieved, but appreciable disintegration of trapped solid may be hindered due to various reasons among which are large particle size, inefficient mixing, and mass transfer limitation. A carefully adjusted balance between influent solids and solid disintegration kinetics has to be established and considered during reactor design in order to use the granular sludge bed for particle-rich substrates. Reactor conditions such as volume temperature, HRT (Hydraulic Retention Time) and SRT (Solids Retention Time) have to consider possible solid accumulations. In addition, a combination periodic removal of excess solids, pretreatment of solid substrates before and during reaction and continuous monitoring of reactor conditions have to be maintained.

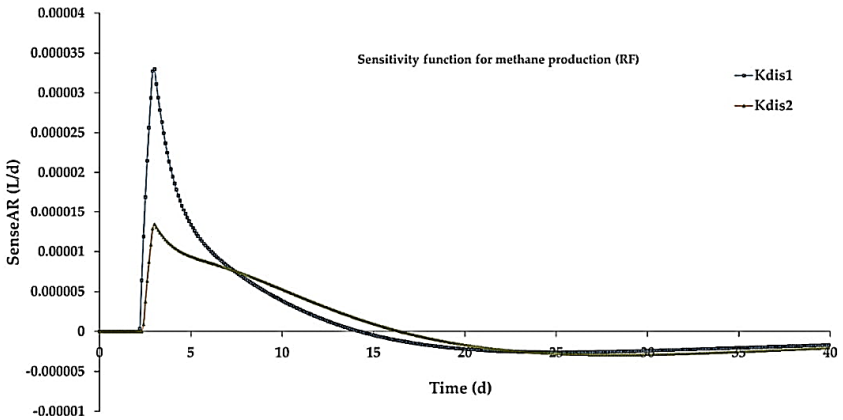


**Figure 9.** Sensitivity function of methane production with respect to $K_{dis1}$ and $K_{dis2}$ (RF).

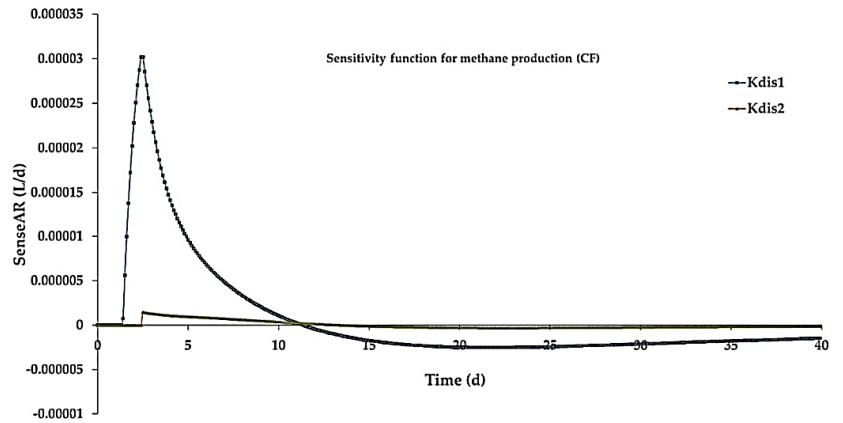

**Figure 10.** Sensitivity function of methane production with respect to $K_{dis1}$ and $K_{dis2}$ (CF).

## 4. Conclusions

After conducting batch reactor tests and analyzing results from substrates with high- and low-suspended particle contents, we have made the following conclusions:

- High biomethane production was observed in samples with higher particle content however, specific biomethane yield was low compared to samples with low particle contents.
- Centrifugation of samples decreased the volume of methane produced but increased the rate of methane production regardless of the addition of cellulase.
- Cellulase addition improved overall and specific methane productions both in raw and centrifuged samples but the improvement was higher in samples that contained higher suspended solids.
- Simulation results revealed that classifying complex particulates into fast and slow disintegrating fractions led to a more accurate modeling of particle-rich substrates.

*Suggestions for Future Work*

This article is based on experimental results from batch anaerobic reactors. As a result, its applicability may be limited. In order to increase the validity of the findings in this work, the authors recommend future investigations on how the classification of complex particulates into fast and slow degrading fractions could be implemented in continuous anaerobic reactors. The effect of temperature on the disintegration of particulates would also be an interesting investigation to carry out.

**Author Contributions:** Conceptualization, F.A.T., W.H.B., C.D. and R.B.; methodology, F.A.T.; software, F.A.T.; validation, F.A.T.; formal analysis, All authors; investigation, All authors; resources, F.A.T.; data curation, F.A.T.; writing—original draft preparation, F.A.T.; writing—review and editing, All authors; visualization, F.A.T.; supervision, R.B. and W.H.B.; project administration, R.B.; funding acquisition, R.B.

**Funding:** This research was part of a PhD project funded by the European Regional Development Fund; Interreg BioGas2020.

**Acknowledgments:** The authors would like to thank Dag Øvrebø for his help during sample collection.

**Conflicts of Interest:** The authors declare no conflicts of interest.

## Appendix A

The absolute-relative sensitivity function is used in Aquasim software to measure the absolute change in y for 100% change in P. In this case, y is methane production and P is parameter $K_{dis1}$ or $K_{dis2}$.

$$\text{Absolute} - \text{Relative sensitivity function} = \mathrm{P}\frac{\partial y}{\partial \mathrm{P}} \quad \text{(A1)}$$

In the tables below, the sensitivity function (SensAR) is expressed in: root mean square (r(av(SensAR²))) and mean absolute (av(|SensAR|)) and for error contributions as: (av(|ErrCont|)). S_CH4, S_CO2 and S_H2 are concentrations of $CH_4$, $CO_2$ and $H_2$, respectively.

**Table A1.** Variables ranked based on sensitivity to $K_{dis1}$ and $K_{dis2}$ in the headspace (RF).

| Variable | r(av(SensAR²)) | | av(\|SensAR\|) | | av(\|ErrCont\|) | |
|---|---|---|---|---|---|---|
| | $K_{dis1}$ | $K_{dis2}$ | $K_{dis1}$ | $K_{dis2}$ | $K_{dis1}$ | $K_{dis2}$ |
| S_CH4 | 0.03 | 0.02 | 0.01 | 0 | 0.05 | 0.03 |
| S_CO2 | 0 | 0 | 0 | 0 | 0 | 0 |
| S_H2 | 0 | 0 | 0 | 0 | 0 | 0 |

**Table A2.** Variables ranked based on sensitivity to $K_{dis1}$ and $K_{dis2}$ in the bulk reactor (RF).

| Variable | r(av(SensAR²)) | | av(\|SensAR\|) | | av(\|ErrCont\|) | |
|---|---|---|---|---|---|---|
| | $K_{dis1}$ | $K_{dis2}$ | $K_{dis1}$ | $K_{dis2}$ | $K_{dis1}$ | $K_{dis2}$ |
| S_CH4 | 0.001 | 0.001 | 0 | 0 | 0.002 | 0.001 |
| S_CO2 | 0 | 0 | 0 | 0 | 0.002 | 0.002 |
| S_H2 | 0 | 0 | 0 | 0 | 0 | 0 |
| Other parameters | | | | | | |
| Xc1 | 0.32 | 0.10 | 0.12 | 0.02 | 0.73 | 0.32 |
| Xc2 | 0 | 0.25 | 0 | 0.06 | 0 | 0.83 |

**Table A3.** Variables ranked based on sensitivity to $K_{dis1}$ and $K_{dis2}$ in the headspace (CF).

| Variable | r(av(SensAR²)) | | av(\|SensAR\|) | | av(\|ErrCont\|) | |
|---|---|---|---|---|---|---|
| | $K_{dis1}$ | $K_{dis2}$ | $K_{dis1}$ | $K_{dis2}$ | $K_{dis1}$ | $K_{dis2}$ |
| S_CH4 | 0.09 | 0 | 0.04 | 0 | 0.24 | 0.04 |
| S_CO2 | 0 | 0 | 0 | 0 | 0.01 | 0 |
| S_H2 | 0 | 0 | 0 | 0 | 0 | 0 |

**Table A4.** Variables ranked based on sensitivity to $K_{dis1}$ and $K_{dis2}$ in the bulk reactor (CF).

| Variable | r(av(SensAR²)) | | av(\|SensAR\|) | | av(\|ErrCont\|) | |
|---|---|---|---|---|---|---|
| | $K_{dis1}$ | $K_{dis2}$ | $K_{dis1}$ | $K_{dis2}$ | $K_{dis1}$ | $K_{dis2}$ |
| S_CH4 | 0.003 | 0 | 0.001 | 0 | 0.008 | 0.001 |
| S_CO2 | 0.001 | 0 | 0.001 | 0 | 0.003 | 0.001 |
| S_H2 | 0 | 0 | 0 | 0 | 0 | 0 |
| Other parameters | | | | | | |
| Xc1 | 0.63 | 0.03 | 0.53 | 0.02 | 3.09 | 0.28 |
| Xc2 | 0 | 0.07 | 0.00 | 0.06 | 0 | 0.75 |

## References


1. Esposito, G. Bio-Methane Potential Tests To Measure The Biogas Production From The Digestion and Co-Digestion of Complex Organic Substrates. *Open Environ. Eng. J.* **2012**, *5*, 1–8.
2. Bajpai, P. *Pretreatment of Lignocellulosic Biomass for Biofuel Production*; Springer Science and Business Media LLC: Berlin/Heidelberg, Germany, 2016.
3. Bruni, E.; Jensen, A.P.; Angelidaki, I. Steam treatment of digested biofibers for increasing biogas production. *Bioresour. Technol.* **2010**, *101*, 7668–7671.
4. Sun, Y.; Cheng, J. Hydrolysis of lignocellulosic materials for ethanol production: A review. *Bioresour. Technol.* **2002**, *83*, 1–11.
5. Pandey, A. *Handbook of Plant-Based Biofuels*; CRC Press: Boca Raton, FL, USA, 2008.
6. Maitan-Alfenas, G.P.; Visser, E.M.; Guimarães, V.M. Enzymatic hydrolysis of lignocellulosic biomass: Converting food waste in valuable products. *Curr. Opin. Food Sci.* **2015**, *1*, 44–49.
7. Christy, P.M.; Gopinath, L.; Divya, D. A review on anaerobic decomposition and enhancement of biogas production through enzymes and microorganisms. *Renew. Sustain. Energy Rev.* **2014**, *34*, 167–173.
8. Romano, R.T.; Zhang, R.; Teter, S.; McGarvey, J.A. The effect of enzyme addition on anaerobic digestion of Jose Tall Wheat Grass. *Bioresour. Technol.* **2009**, *100*, 4564–4571.
9. Malayil, S.; Chanakya, H. Fungal Enzyme Cocktail Treatment of Biomass for Higher Biogas Production from Leaf Litter. *Procedia Environ. Sci.* **2016**, *35*, 826–832.
10. Quiñones, T. S.; Plöchl, M.; Budde, J.; Heiermann, M. Results of Batch Anaerobic Digestion Test–Effect of Enzyme Addition. *Agric. Eng. Int. CIGR J.* **2012**, *14*, 38–50.
11. Triolo, J.M.; Sommer, S.G.; Møller, H.B.; Weisbjerg, M.R.; Jiang, X.Y. A new algorithm to characterize biodegradability of biomass during anaerobic digestion: Influence of lignin concentration on methane production potential. *Bioresour. Technol.* **2011**, *102*, 9395–9402.

12. Koch, K.; Drewes, J.E. Alternative approach to estimate the hydrolysis rate constant of particulate material from batch data. *Appl. Energy* **2014**, *120*, 11–15.
13. Vavilin, V.; Rytov, S.; Lokshina, L. A description of hydrolysis kinetics in anaerobic degradation of particulate organic matter. *Bioresour. Technol.* **1996**, *56*, 229–237.
14. Angelidaki, I.; Alves, M.; Bolzonella, D.; Borzacconi, L.; Campos, J.L.; Guwy, A.J.; Kalyuzhnyi, S.; Jenicek, P.; Van Lier, J.B. Defining the biomethane potential (BMP) of solid organic wastes and energy crops: A proposed protocol for batch assays. *Water Sci. Technol.* **2009**, *59*, 927–934.
15. VDI—The Association of German Engineers. Vergärung organischer Stoffe. Substratcharakterisierung, Probenahme, Stoffdatenerhebung, Gärversuche; Beuth Verlag, Berlin, Germany, 2006.
16. Macé, S.; Bolzonella, D.; Cecchi, F.; Mata-Álvarez, J. Comparison of the biodegradability of the grey fraction of municipal solid waste of Barcelona in mesophilic and thermophilic conditions. *Water Sci. Technol.* **2003**, *48*, 21–28.
17. Eastman, J.A.; Ferguson, J.F. Solubilization of Particulate Organic Carbon during the Acid Phase of Anaerobic Digestion. *J. (Water Pollut. Control Fed.)* **1981**, *53*, 352–366.
18. APHA; Water Environment Federation; American Water Works Association. Standard Methods for the Examination of Water and Wastewater; American Public Health Association, Washington, DC, USA, 1998.
19. Bioprocess Control. *AMPTS II Light Automatic Methane Potential Test System Operation and Maintenance Manual*; Bioprocess Control, Lund, Sweden, 2016.
20. Darmana, D.; Henket, R.; Deen, N.G.; Kuipers, J. Detailed modelling of hydrodynamics, mass transfer and chemical reactions in a bubble column using a discrete bubble model: Chemisorption of $CO_2$ into NaOH solution, numerical and experimental study. *Chem. Eng. Sci.* **2007**, *62*, 2556–2575.
21. Tchobanoglous, G.; Burton, F. L.; Stensel, H. D. *Wastewater Engineering Treatment and Reuse*; McGraw-Hill Education: Boston, MA, USA, 2003.
22. Gali, A.; Benabdallah, T.; Astals, S.; Mata-Alvarez, J. Modified version of ADM1 model for agro-waste application. *Bioresour. Technol.* **2009**, *100*, 2783–2790.
23. Batstone, D.; Keller, J.; Angelidaki, I.; Kalyuzhnyi, S.; Pavlostathis, S.; Rozzi, A.; Sanders, W.; Siegrist, H.; Vavilin, V. The IWA Anaerobic Digestion Model No 1 (ADM1). *Water Sci. Technol.* **2002**, *45*, 65–73.
24. Reichert, P. *Aquasim 2.0-User Manual*; Swiss Federal Institute for Environmental Science and Technology: Dubendorf, Switzerland, 1998.


© 2019 by the authors. Licensee MDPI, Basel, Switzerland. This article is an open access article distributed under the terms and conditions of the Creative Commons Attribution (CC BY) license (http://creativecommons.org/licenses/by/4.0/).

## Article 4:

# Influences of temperature and feed particle content on granular sludge bed anaerobic digestion.

Tassew FA, Bergland WH, Dinamarca C, Bakke R. Influences of temperature and feed particle content on granular sludge bed anaerobic digestion. Submitted to the journal: Biomass and bioenergy.

# Influences of temperature and substrate particle content on granular sludge bed anaerobic digestion

Fasil A. Tassew*, Wenche Hennie Bergland, Carlos Dinamarca, Rune Bakke

*University of South-Eastern Norway, Department of Process, Energy and Environmental Technology Kjølnes ring 56, NO 3918 Porsgrunn, Norway*

**Abstract**

Influences of temperature (25-35 °C) and substrate particulate content (3.0-9.4 g TSS/L) on granular sludge bed anaerobic digestion (AD) were analysed in lab-scale reactors using manure as substrate and through modelling. Two particle levels were tested using raw (RF) and centrifuged (CF) swine manure slurries, fed into a 1.3 L lab-scale up-flow anaerobic sludge bed reactor (UASB) at temperatures of 25 °C and 35 °C. Biogas production increased with temperature in both high and low particle content substrates, however, the temperature effect was stronger on high particle content substrate. RF and CF produced comparable amount of biogas at 25 °C, suggesting that biogas at this temperature came mainly from digestion of small particles and soluble components present in similar quantities in both substrates. At 35 °C, RF showed significantly higher biogas production than CF, which was attributed to increased (temperature dependent) disintegration of larger solid particulates. ADM1 based modelling was carried out by separating particulates into fast and slow disintegrating fractions and introducing temperature dependent disintegration constants. Simulations gave a better fit for the experimental data than the conventional ADM1 model.

*Keywords:* ADM1, Anaerobic digestion, Particulate disintegration, Temperature

*Corresponding author
*Email address:* fasil.a.tassew@usn.no (Fasil A. Tassew)

*Preprint submitted to Biomass and Bioenergy* *June 21, 2019*

## 1. Introduction

UASB reactors are normally used for treatment of low suspended solids substrates such as industrial wastewater. Their attributes, such as low cost, high efficiency and low footprint, makes them attractive also for treatment of particle rich substrates such as sludge and manure slurries that are available in large quantities worldwide [1]. Solids accumulation and granular sludge floatation leading to losses of biomass are known challenges in the treatment of high-suspended solid wastewater [2], but high AD efficiency has also been reported for particle rich substrates [3]. Traditionally, CSTR reactors have been used to treat particle rich substrates such as manure slurries but due to drawbacks such as long hydraulic retention time (HRT) and large reactor volume requirement, high-rate AD reactors have become more popular. High-rate reactors are characterized by long sludge retention time (SRT), short HRT and efficient degradation of organic substances. Long SRT is achieved because of microbial aggregation phenomena to form granular sludge bed that stay in reactors for relatively long time. The use of high-rate reactors, however, has its own drawbacks with regard to particle rich substrates. Accumulation of solid particles in the sludge bed has been considered a problem [4]. Moreover, the interaction of solid particles with microorganisms in the sludge bed as well as the extent of contribution of solid particulates to biogas production are not clear. Due to these reasons, high-rate reactors have been mostly used for treatment of substrates with low solid content, mostly industrial wastes. Nevertheless, Bergland et al. [3] showed that particle rich substrates (swine manure slurry) could also be treated using high-rate lab-scale UASB reactors. Solid particulates are thought to undergo disintegration and hydrolysis before the rest of the anaerobic digestion process take place. Some researchers treat disintegration and hydrolysis as a single step while others do not. In this paper, we will treat them as distinct steps. The rate-limiting step in AD of particle rich substrates is usually disintegration/hydrolysis. Solid particulates disintegrate relatively slowly and tend to accumulate, making it challenging to adopt high-rate reactors for particle

rich substrates. The aim of this study is to contribute to the development of high-rate reactors for particle rich substrates. For this, it is important to understand how the suspended solids content influences granular sludge bed AD by identifying disintegration and hydrolysis patterns of particulates and their dependence on temperature.

### *1.1. Particle disintegration and hydrolysis*

Disintegration is a physical and biological process where complex composite substrates are progressively broken apart before hydrolysis takes place, whereas, hydrolysis is a biological enzymatic mediated process where biopolymers are broken into their respective monomers. Both steps are extracellular processes [5]. Particulate carbohydrates, proteins and lipids as well as inert materials are produced by disintegration of composite substrates. Microbes release enzymes that hydrolyse these biopolymers into smaller components and, given that polymers can hold particles together, hydrolysis contributes to disintegration making it difficult to distinguish the two steps. Carbohydrates are hydrolysed into monosaccharides, proteins into amino acids and lipids into long chain fatty acids (LCFA) [6]. Disintegration and hydrolysis are often modelled with first order kinetics with respect to reactor particle content, as a single step or two, such as in ADM1 [5]. However, AD experiments with high inoculum-to-substrate ratio resulted in relatively high hydrolysis rates, indicating that microorganisms play a role in the hydrolysis rate. For simple substrates (i.e. substrates with high proportion of soluble biodegradable components), first order kinetics is enough to characterize hydrolysis process. For complex substrates, the presence of solids and less biodegradable components makes bioavailability an important factor in determining the hydrolysis kinetics. Since first order kinetics does not consider microbial influence, it's fitness for complex substrates has been questioned. Surface-based kinetics are developed that consider available surface area of particulates for enzymatic action [7]. Inhibition of hydrolysis may occur in substrates with very high solid content (solid state AD) likely due to diffusion limitation [8]. In addition, hydrolysis could be inhibited by high concentra-

tions of LCFA, $H_2$ and $NH_3$ (Vavilin et al. [6] ). In this article, we intend to demonstrate that first order disintegration and hydrolysis kinetics can accurately model anaerobic digestion of complex substrates by classifying complex particulates into fast and slow disintegrating sections. We have demonstrated the effectiveness of this approach in batch anaerobic reactors (manuscript submitted to journal).

### *1.2. Temperature effect on particle hydrolysis*

Various authors have studied temperature effect on biogas production. Their findings indicate that there is positive correlation between temperature and biogas production. Increase in temperature leads to increase in microorganisms maximum substrate utilization rate as well as specific growth rate [9]. Anaerobic digestion is classified into three categories based on temperature. The categories are psychrophilic (<20 °C), mesophilic (20-42 °C) and thermophilic (42-60 °C). PsychrophilicAD is probably the least studied of the three categories. The psychrophilic reaction rates are slow and the microbial growth is limited. In addition, hydrolysis of suspended solid is near zero [10]. As a result, application of low temperature AD is restricted to very low strength wastewater with little or no suspended solids. Nevertheless, Lettinga et al. [10] showed that expanded granular sludge bed reactor (EGSB) might be feasible for soluble pre-acidified wastewater at temperatures of 5-10 °C. On the other hand, mesophilic AD provides optimum conditions and stable process for biogas production. As a result, large-scale anaerobic digesters often run on operational temperatures in the mesophilic range. Wide ranges of microorganisms thrive in the mesophilic temperature range with the optimum temperature often cited as 35 °C. Microbial diversity in turn contributes to the stability and shock tolerance of the anaerobic process. Thermophilic anaerobic digestion has benefits such as higher biogas production and better digestate quality [11]. However, it is less stable than the mesophilic AD due to high risk of ammonia or VFA inhibition. In addition, it is highly sensitive to temperature fluctuations (Unlike thermophilic microorganisms, mesophilic microorganisms may tolerate fluctuations of up to

±3 °C). When removal of pathogens from the digestate is a requirement, thermophilic AD is the best option as the high operating temperature kills most of the microorganisms present in the digestate. High temperature could also contributes to higher solid disintegration and hydrolysis (solid removal) compared to mesophilic AD [12]. In general, temperature increase leads to increase in the hydrolysis rate [13]. If enzyme concentration is not rate limiting, hydrolysis rate as a function of temperature is described by the Arrhenius equation as follows:

$$K_h = K_\infty e^{\frac{-\Delta E}{RT}} \quad (1)$$

Where, $K_h$ is hydrolysis rate constant, $K_\infty$ is specific rate constant in $d^{-1}$, $\Delta E$ is activation energy in $Jmol^{-1}$, T is temperature in K and R is ideal gas constant in $Jmol^{-1}K^{-1}$.

*1.3. Effect of temperature change in anaerobic digestion*

Temperature has strong influence in anaerobic digestion. It plays a major role in microbial growth, enzymatic activity, kinetics and conversion processes and consequently in biogas yield and composition. All the steps of anaerobic digestion are directly or indirectly affected by digestion temperature. Temperature variation within anaerobic digesters is typically not recommended due to difficulties associated with adaptation of microbial community and overall stability of the digestion process. The microbial community is comprised of various types of bacteria and Archea. They have different optimum temperatures for growth rate and activity. For example, activity and growth rate of hydrolytic bacteria increases with increasing temperature (well beyond the mesophilic range). This is considered a benefit because hydrolysis is often the rate limiting step, however, this benefit is negated by decline in the growth rate and activity of methanogens (Archea) leading to accumulation of volatile fatty acids (VFA) and process failure. Increase in temperature could also affect the digestion of specific type of substrates. It was shown that digestion of substrates rich with protein, such as cattle waste, are negatively affected due to increased

ammonia inhibition [14]. Free Ammonia concentration ($NH_3$) increases due to a shift in $NH_3/NH_4^+$ equilibrium in its favour as temperature rises.

$$NH_{3\,(aq)} + H_2O_{(l)} \rightleftharpoons {NH_4}^+{}_{(aq)} + {OH}^-{}_{(aq)}$$

There are indications that temperature change within a given range affects microbial activity and biogas production. The activity and growth rate of microorganisms increases by up to 50 % within the mesophilic range for every 10 °C increase in temperature [15]. Change in temperature also affects the physical and chemical properties of produced biogas as well as other components in the reactor. The solubility of biogas components, especially $CH_4$, in the reactor liquid mixture is an important aspect. Biogas plants that run at low temperature release effluents with higher content of dissolved $CH_4$ compared to biogas plants that run at high temperature. The dissolved $CH_4$ in the effluent is then released to the atmosphere as a greenhouse gas, which is a bad outcome from environmental and economical standpoint. In this article, we are investigating effect of temperature variation on anaerobic digestion of particle rich and particle "free" substrates by varying temperature between 25 °C and 35 °C. This will enable us to understand how biogas production and reactor stability is affected by temperature variation. In addition, it provides insight into how particulate disintegration and hydrolysis are affected by temperature.

## 2. Materials and methods

### *2.1. Samples*

Swine manure slurry was collected from a swine production farm in Porsgrunn, Norway. Two sets of substrate samples were prepared. The first sample was directly taken from a storage pit (called "Raw feed or RF"). The second sample was prepared by centrifuging the RF sample and only taking the liquid part (called "Centrifuged feed or CF"), thereby reducing the total and suspended solid contents. Centrifugation was carried out using a centrifuge

(Beckman J-25, with JA-10 rotor) at 10,000 RPM for 15 minutes and discarding the settled solids. All prepared samples were kept in a refrigerator at 4 °C until they were transferred into the feed container of the reactor.

*2.2. Sample analysis*

Influent and effluent samples were regularly analysed during the course of the experiment. Total solids (TS), total suspended solids (TSS), volatile solids (VS) and volatile suspended solids (VSS) were determined in accordance with American public health association standard method APHA 2540 [16]. Total and soluble COD (chemical oxygen demand) of influent and effluent samples were analysed using test kits and Spectrophotometric method in accordance with APHA standard method 5220 D. Feed and effluent pH were measured using Beckman 300 pH meter equipped with Sentix-82 pH electrode. Ammonium–Nitrogen content ($NH_4^+ - N$) was measured according to APHA 4500-$NH_3$. Both COD and $NH_4^+ - N$ concentrations were measured using commercially available Merck test kits and Spectroquant Pharo 300 spectrophotometer (Darmstadt, Germany). Volatile fatty acids (VFA) were analysed using gas chromatography (Hewlett Packard 6890) with a flame ionisation detector and a capillary column (FFAP 30 m, inner diameter 0.250 mm, film 0.25 µm). The oven was programmed to go from 100 °C, hold for one minute, to 180 °C at a rate of 30 °C/min, and then to 230 °C at a rate of 100 °C/min. The carrier gas used was helium at 245 mL/min. The injector and detector temperatures were set to 200 and 250 °C, respectively.

*2.3. Reactor and experimental procedure*

The UASB lab-scale reactor dimensions were 85 cm height and 4.4 cm internal diameter giving 1.3 L total volume. A mixture of granular sludge (0.5 L) obtained from various industries was used as inoculum. The reactor had been running using swine manure samples (both raw and centrifuged) for over a year prior to the start of the experiment. The up-flow velocity was set to 1.75 m/h, hydraulic retention time was 3.8 d and organic loading rate was 6.5 and

175 4.5 $gL^{-1}d^{-1}$ for RF and CF samples respectively. The reactor was equipped with heater temperature controls (±0.5 °C) and online biogas flow measurement. Data was logged online with LabVIEW software (Fig. 1). The reactor started at 35 °C, fed RF and run for 11 days before the temperature was lowered to 25 °C. After 15 days at 25 °C, CF was introduced and the experiment continued 180 at 25 °C for another 18 days before the temperature was raised back to 35 °C and run for 15 days (Table 1).

Table 1: Experimental design showing duration, temperature and feed types used during the experiment.

| Experiment | Time (d) | Temperature (°C) | Substrate |
|---|---|---|---|
| Phase 1 | 0-11 | 35 | RF |
| Phase 2 | 11-26 | 25 | RF |
| Phase 3 | 26-45 | 25 | CF |
| Phase 4 | 45-60 | 35 | CF |

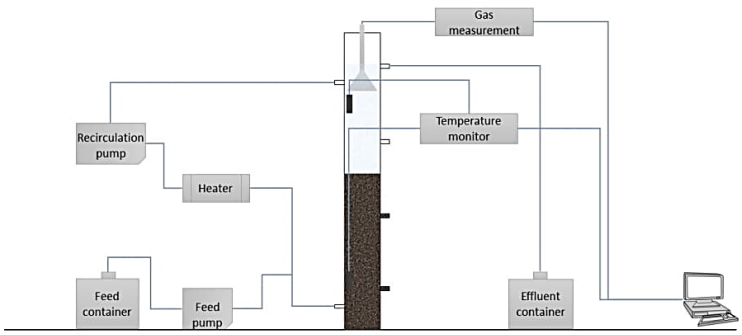


**Fig. 1.** Schematic diagram of applied UASB reactor setup.

*2.4. ADM1 simulation*

The modelling was based on the standard ADM1 implemented in Aquasim software [5, 17], only modified by splitting substrate particulates in two fractions, one easily and one slowly disintegrating, and making first order disintegration of these particle fractions temperature dependent. Rate expressions for disintegration of fast and slow fraction of the composite substrates are given as:

$$\frac{dXc1}{dt} = K_{dis1}Xc1 \tag{2}$$

$$\frac{dXc2}{dt} = K_{dis2}Xc2 \tag{3}$$

Where $\frac{dXc1}{dt}$ and $\frac{dXc2}{dt}$ are disintegration rates for fast and slow fractions in kg $CODm^{-3}d^{-1}$, Xc1 and Xc2 are fast and slow disintegrating fractions of the complex particulate respectively and $K_{dis1}$ and $K_{dis2}$ are rate constants for fast and slow disintegrating fractions respectively. Dependency of $K_{dis}$ values on temperature were based on Eq. (4).

$$K_{dis} = K_{dis,ref}e^{\left[\frac{-Ea}{R}\right]\left[\frac{1}{T}-\frac{1}{T_{ref}}\right]} \tag{4}$$

Where, Ea is activation energy in $Jmol^{-1}$, R is gas constant in $Jmol^{-1}K^{-1}$ and $T_{ref}$ is reference temperature in K. Activation energy was estimated from literature data on energy requirement for mechanical disintegration of solid substrates such as straws. According to Krátký and Jirout [15], the energy requirement to disintegrate straws to sizes less than 10 mm is 29 kWh/t (104.4 kJ/kg). In addition, Kunov-Kruse et al. [18] showed that the activation energy of cellulose hydrolysis is 96.4 ± 4.1 kJ/mol. Since straw, which is composed of upto 50 % cellulose, is one of the main sources of particulates in manure substrates, it is reasonable to base the estimate of Ea from these data. We used Ea of 90 kJ/mol for fast disintegrating and 130 kJ/mol for slow disintegrating particles (corresponding to $K_{dis}$ of 0.03 - 0.05 and 0.17 at 25 and 35 °C respectively). Gali et al. [19] showed that $K_{dis}$ for swine manure samples at 35 °C is around

0.17 $d^{-1}$ which we used as a reference $K_{dis}$ and T values. Input composite materials (Xc1 and Xc2) were determined based on the ratio between total and soluble COD values ($COD_{total}$ and $COD_{soluble}$) as shown in Eq. (5-7). Yields for the disintegration of complex materials for swine manure ADM1 modeling by Mata-Alvarez et al. [19] were used with modification to account for fast and slow disintegrating components (Table 2 & 3 ).

$$Xc = Xc1 + Xc2 \tag{5}$$

$$Xc1 = \frac{COD_{soluble}}{COD_{total}} Xc \tag{6}$$

$$Xc2 = 1 - \frac{COD_{soluble}}{COD_{total}} Xc \tag{7}$$

Two modes of simulations were carried out. In Mode 1, first order disintegration kinetics was used without classification of particulates into fast and slow disintegrating sections. In Mode 2, particulates were classified into fast and slow disintegrating. Fig. 2 illustrates the two modes of simulations employed.

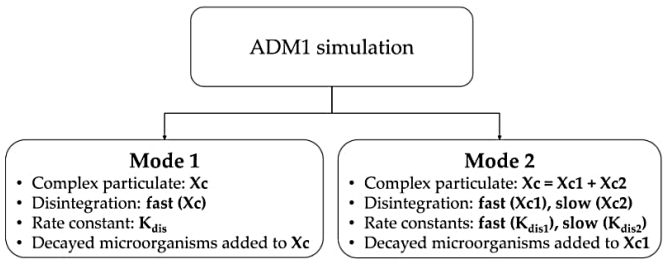


**Fig. 2.** ADM1 simulation scheme for Mode 1 and 2 simulations.

Table 2: Model settings for fast and slow disintegration parameters classified into fast and slow.

| Variable | Yield from disintegration | Value | |
|---|---|---|---|
| | | model | ADM1 |
| f_ch_xc1 | carbohydrates from complex particulates (fast) | 0.2305 | 0.2 |
| f_ch_xc2 | carbohydrates from complex particulates (slow) | 0.2305 | |
| f_li_xc1 | lipids from complex particulates (fast) | 0.0805 | 0.25 |
| f_li_xc2 | lipids from complex particulates (slow) | 0.0805 | |
| f_pr_xc1 | proteins from complex particulates (fast) | 0.101 | 0.2 |
| f_pr_xc2 | proteins from complex particulates (slow) | 0.101 | |
| f_SI_xc1 | soluble inerts from complex particulates (fast) | 0.0715 | 0.1 |
| f_SI_xc2 | soluble inerts from complex particulates (slow) | 0.0715 | |
| f_XI_xc1 | particulate inerts from complex particulates (fast) | 0.0165 | 0.25 |
| f_XI_xc2 | particulate inerts from complex particulates (slow) | 0.0165 | |

Table 3: Model settings for yield for acidogenesis.

| Variable | Yield from degradation | Value | |
|---|---|---|---|
| | | model | ADM1 |
| f_ac_aa | acetate from amino acid | 0.4 | 0.4 |
| f_ac_su | acetate from sugar | 0.41 | 0.41 |
| f_bu_aa | butyrate from amino acid | 0.26 | 0.26 |
| f_bu_su | butyrate from monosaccharide | 0.13 | 0.13 |
| f_fa_li | LCFAs from lipids | 0.95 | 0.95 |
| f_h2_aa | hydrogen from amino acid | 0.06 | 0.06 |
| f_h2_su | hydrogen from monosaccharide | 0.19 | 0.19 |
| f_pro_aa | propionate from amino acid | 0.08 | 0.05 |
| f_pro_su | propionate from monosaccharide | 0.27 | 0.27 |
| f_va_aa | valerate from amino acid | 0.23 | 0.23 |

Table 4: Model settings for input parameters.

| Variable | Description and unit | Value |
|---|---|---|
| input_Qin_dyn | feed flow rate ($m^3/d$) | $3.38 \times 10^{-4}$ |
| input_S_fa_in | long chain fatty acids ($kg\,CODm^{-3}$) | 2 |
| input_S_aa_in | amino acids ($kg\,CODm^{-3}$) | 2.83 |
| input_S_IC_in | total inorganic carbon (M) | 0.2 |
| input_S_IN_in | total inorganic nitrogen (M) | 0.2 |
| input_S_I_in | soluble inert COD ($kg\,CODm^{-3}$) | 2.3 |
| input_S_su_in | monosaccharides ($kg\,CODm^{-3}$) | 3.6 |
| input_X_I_in | particulate inerts ($kg\,CODm^{-3}$) | 2.7 |

## 3. Result and discussion

### *3.1. Biogas production*

The experiment was carried out in four phases based on substrate type and the temperature, all temperature and substrate changes were abrupt (Table 1). In Phase 1, with RF at 35 °C, biogas production rate increased from the start till the sixth day (Fig. 3), followed by stable 3.7 - 3.9 L/d production. An immediate decrease in biogas production rate was observed in Phase 2, from day 11, when the temperature was reduced to 25 °C (from 3.9 L/d to 1.4 L/d). However, it gradually increased for 10 d and stabilized around 2.5 L/d until the end of Phase 2.

The biogas production rate did not noticeably decrease from Phase 2 to Phase 3 at day 26 when RF was replaced by CF (at 25 °C ) even though $COD_{total}$ of CF was significantly lower than that of RF. Furthermore, biogas production rate was more stable in Phase 3 compared to Phase 2. In Phase four, where CF was used at 35 °C, the biogas production rate increased but with significant fluctuations and an average (11 %) less than the stable production in Phase 1. From Phase 1 to 2, the biogas production decreased roughly by 42 %. The decrease can be explained by temperature decline (10 °C within a

matter of few hours), which affects rate of hydrolysis as well as reaction kinetics. Solubility of Methane and other gases also increases as temperature decreases resulting in lower amount of biogas in the gas phase. The decline in biogas production seemed to recover in two steps with the first one being a sharp increase that lasted for few hours followed by gradual increase that stabilized towards the end of Phase 2. Effluent $VFA_{total}$ before and immediately after temperature decrease were 0.54 g/L (80 % acetate) and 1.6 g/L (62 % acetate) respectively, suggesting both a negative effect on acetoclastic methanogenesis and acetogenesis. Concentration of $VFA_{total}$ in the effluent increased to 2.3 g/L after few days in Phase 2 and seemed to stabilize at that concentration. Since methanogens are sensitive to temperature changes, process instability (VFA accumulation) during temperature decline is expected. However, the decrease in the proportion of oxidized acids indicates that it may also affect the oxidation of propionic acid to acetate and/or an increase in hydrolysis rate.

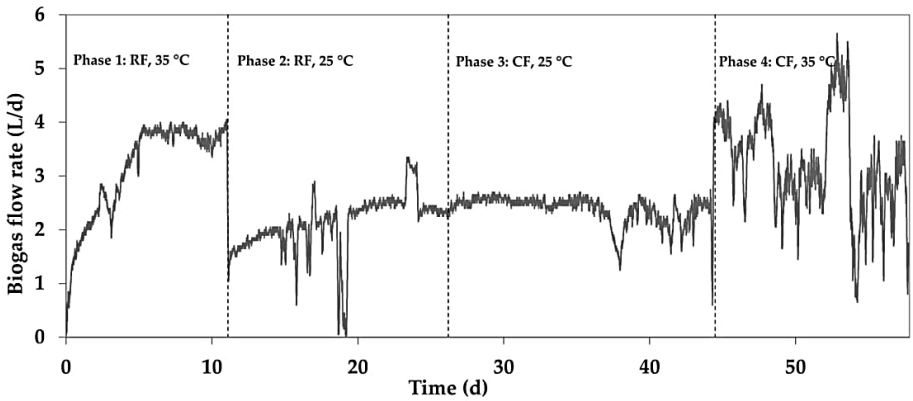


**Fig. 3.** Biogas flow rate during transitions between phases.

Gradual increase in biogas production was also observed in Phase 2. Kim et al. [20] observed similar trend. They observed recovery of biogas production rate with no lasting damage to the performance after initial decline due to sharp temperature decrease (temperature shock). However, their observed biogas yield decline was less pronounced than what we have observed (17% decline from 35 to

25 °C compared to 42% decline in our study). The reason for gradual increase in biogas production may be linked to gradual microbial adaptation to temperature change. In addition, solid particulates entrapped in the granular sludge may have been slowly disintegrated and hydrolysed contributing to the increase in biogas production throughout Phase 2. However, disintegration and hydrolysis of solid particulates at 25 °C does not seem to be carried out to an appreciable degree. In Phase 3, even with the decrease in $COD_{total}$ and solid content of the feed, the biogas production rate did not decrease in any appreciable way compared to Phase 2 (Table 5). Experimental results of total and suspended solid contents from influent and effluent samples showed that most of feed solid content ended up in the effluent. In fact, the percentage of solids was higher in the effluent of centrifuged sample than raw sample (Table 7). This is, perhaps, because solid particles in centrifuged sample are relatively smaller than those in the raw sample, which help most of solid particulates avoid entrapment in the sludge bed and wash out to the effluent before any degradation occurs. As a result, it is reasonable to assume that the biogas produced in Phase 3 must have come primarily from the digestion of soluble components.

Biogas production in Phase 4 showed the most fluctuation. However, experimental analysis of influent and effluent samples seems to indicate that the process was still stable with effluent $VFA_{total}$ of 0.17 g/L, pH of 8.1, 51 % $COD_{total}$ removal and 62 % $COD_{soluble}$ removal on average. When the temperature was increased from 25 °C to 35 °C at day 45, there was fast decline in the biogas production followed quickly by a sharp increase. During transition from 25 °C to 35 °C in Phase 1, the production rate also showed fast decline followed by quick recovery. This indicates that regardless of whether the temperature was increased or decreased, there seemed to be a decline in biogas production rate after rapid change in reactor temperature. However, the rate quickly recovers.

### *3.2. Methane yield and solid removal efficiency*

Methane yields were higher for CF than RF and increased with temperature (Table 6). Influent and effluent analysis show that temperature affects digestion

Table 5: Average biogas flow rate of RF and CF samples.

| Substrate | Average biogas flow rate (L/d) | | | | | |
|---|---|---|---|---|---|---|
| | Experimental | | Simulation | | | |
| | | | Mode 1 | | Mode 2 | |
| | 25 °C | 35 °C | 25 °C | 35 °C | 25 °C | 35 °C |
| RF | 2.1±0.5 | 3.7±0.2 | 2.7±0.3 | 2.6±0.6 | 2.5±0.4 | 3.0±0.9 |
| CF | 2.4±0.2 | 3.3±0.9 | 2.4±0.1 | 2.5±0.1 | 2.8±0.0 | 4.7±0.8 |

of both suspended and dissolved solids. At 25 °C, 50 % of the RF total suspended solids (TSS) were removed while 68 % was removed at 35 °C (Table 8). For dissolved solids (TDS), the removals were 7.8 % and 9.1 % at 25 °C and 35 °C, respectively. Little or negative TSS and 30 % TDS removals were observed for CF. Effluent $COD_{soluble}$ measurements show that the difference in biogas production between RF and CF was due to digestion of feed particulate content.

Table 6: Average methane yield of RF and CF samples.

| Substrate | Methane yield | | | | | |
|---|---|---|---|---|---|---|
| | L $CH_4$/g VSS | | L $CH_4$/g $COD_{total}$ | | $COD_{CH_4}$/g $COD_{total}$ | |
| | 25 °C | 35 °C | 25 °C | 35 °C | 25 °C | 35 °C |
| RF | 0.41 | 0.71 | 0.16 | 0.29 | 0.46 | 0.72 |
| CF | 0.76 | 1.06 | 0.26 | 0.37 | 0.74 | 0.92 |

Table 7: Feed and effluent analysis of samples from reactor fed raw and centrifuged manure.

| Property | RF | Effluent average | | CF | Effluent average | |
|---|---|---|---|---|---|---|
| | | 25 °C | 35 °C | | 25 °C | 35 °C |
| TS (g/L) | 17±3 | 12 | 10 | 12±0.4 | 10 | 8.7 |
| VS (g/L) | 10±2 | 5.3 | 4.2 | 6±1 | 4.6 | 3.2 |
| TSS (g/L) | 9±4 | 4.7 | 3.0 | 3±0.4 | 3.5 | 2.5 |
| VSS (g/L) | 7±3 | 4.3 | 2.9 | 3±0.3 | 3.2 | 2.3 |
| TDS (g/L) | 8±1 | 7.1 | 7.0 | 9±0.5 | 6.7 | 6.2 |
| VDS (g/L) | 3±0.4 | 1.0 | 1.3 | 3±0.4 | 1.4 | 0.9 |
| $COD_{total}$ (g/L) | 24±2 | 14 | 6.7 | 17±0.2 | 9.8 | 8.0 |
| $COD_{soluble}$ (g/L) | 15±2 | 6.5 | 3.3 | 13±0.2 | 6.3 | 4.0 |
| $NH_4^+ - N$ (g/L) | 1.9 | 1.9 | 1.5 | 1.7±0.1 | 1.9 | 1.8 |
| pH | 7±0.2 | 8.1 | 8.4 | 7±0.3 | 8.2 | 8.1 |
| Acetic acid (g/L) | 4±1 | 1.1 | 0.4 | 3±0.1 | 1.0 | 0.2 |
| Propionic acid (g/L) | 1±0.7 | 0.7 | 0.1 | 1±0.3 | 1.0 | 0.0 |
| $VFA_{total}$ (g/L) | 6±1 | 1.9 | 0.5 | 6±2 | 2.0 | 0.2 |

Table 8: Removal efficiencies of the reactor (based on g/L measurements in Table 7).

| Property | Average removal (%) | | | |
|---|---|---|---|---|
| | Raw feed | | Centrifuged feed | |
| | 25 °C | 35 °C | 25 °C | 35 °C |
| TS | 31 | 42 | 17 | 29 |
| VS | 47 | 58 | 23 | 47 |
| TSS | 50 | 68 | -16 | 16 |
| VSS | 42 | 61 | -19 | 17 |
| TDS | 8 | 9 | 28 | 33 |
| VDS | 60 | 48 | 58 | 73 |
| $COD_{total}$ | 44 | 73 | 43 | 54 |
| $COD_{soluble}$ | 58 | 79 | 50 | 68 |
| $VFA_{total}$ | 70 | 91 | 67 | 97 |

*3.3. Simulation results*

Comparison of the two modes of simulations revealed that classification of particles into fast and slow disintegrating fractions (Mode 2) leads to a better representation of the experimental data compared to Mode 1 simulation across all four phases of the experiment (Fig. 5 & 6). Application of the same simulation approaches on batch reactors also revealed Mode 2 simulation lead to a better fit to experimental observations (manuscript submited to journal). Mode 1 simulation assumes all particulates possess fast disintegration potential. Whereas Mode 2 assumes a fraction of the particulates disintegrate at a slower rate based on Eq. (4). The result from Mode 1 simulation revealed that the rate of methane production was consistently lower than the experimental data. In the batch test experiments we observed that Mode 1 simulation overestimate the rate of methane production, which was expected considering that more particulates have higher disintegration rate which means more production of methane. Our initial explanation for this was accumulation of VFA but pH data did not support it. However, data from biomass concentration (Fig. 4) showed that the growth of acetate (Xac) and fatty acid (Xfa) degrading organisms decline quite fast in Mode 1 simulation likely affecting the rate of methane production.

Mode 2 simulation showed a more efficient particulate removal and sensitivity to changes in temperature and particulate content than Mode 1 simulation (Fig. 7 & 8). In both modes of simulations, particulates accumulate regardless of whether they are fast or slow disintegrating, this continued until the start of Phase 3 when CF was introduced. During Phases 1 and 2 the rate of addition of particulates into the reactor was faster than the rate of disintegration and hydrolysis. After Phase 2, the particulate content started to decline. At the start of Phase 3 the particulates that were let into the reactor during Phases 1 and 2 had been in the reactor for several days, meaning even slow disintegrating portions of the particulates would have been starting to disintegrate. The particulate content of CF is much lower than that of RF, leading to slower rate of addition of particulates into the reactor. A combination of these factors have contributed to the decline in the particulate content in the latter two Phases of

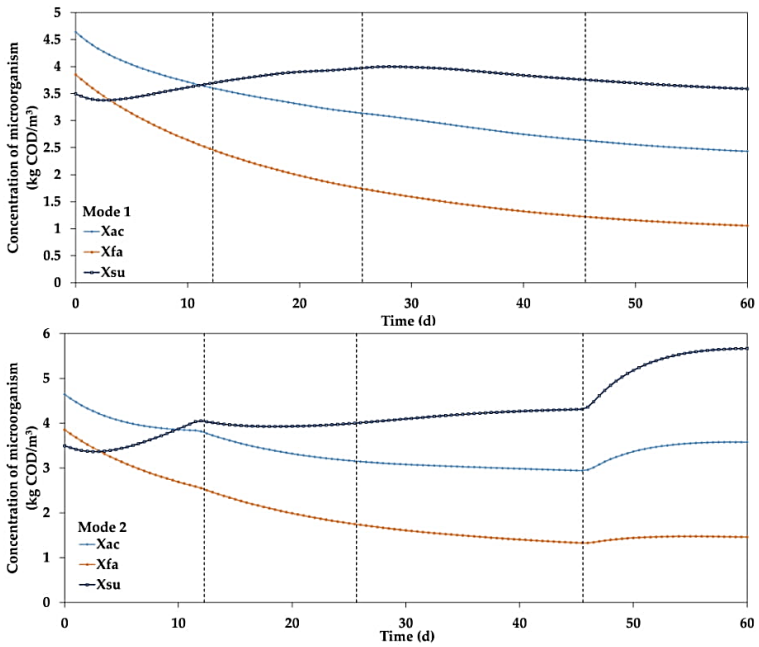


**Fig. 4.** Biomass concentration in the reactor during Mode 1 and Mode 2 simulations.

the experiment. However, in Mode 1 simulation, the decline in particulate content was short, after initial decline during early in Phase 3, particulate content seemed to stay constant. By contrast, Mode 2 showed a considerable decline in particulate content which continued until the end of the experiment.

Sensitivity analysis and parameter estimation were carried out on Ea values in Mode 2 simulation (Since $K_{dis}$ is used as a formula variable, we could not use it for sensitivity analysis, we used Ea instead, from which the sensitivity of $K_{dis}$ is deduced). Sensitivity analysis which combines identifiability and uncertainty analysis is used to check if model parameters can be uniquely determined from available data and to estimate the uncertainty of the parameter estimates [21]. The sensitivity function of biogas production with respect to Ea values is shown in Appendix A. Parameter estimation of Ea revealed values of 51444 and 150000 $Jmol^{-1}$ for $Ea_1$ and $Ea_2$ respectively, comparison of the simulation before and

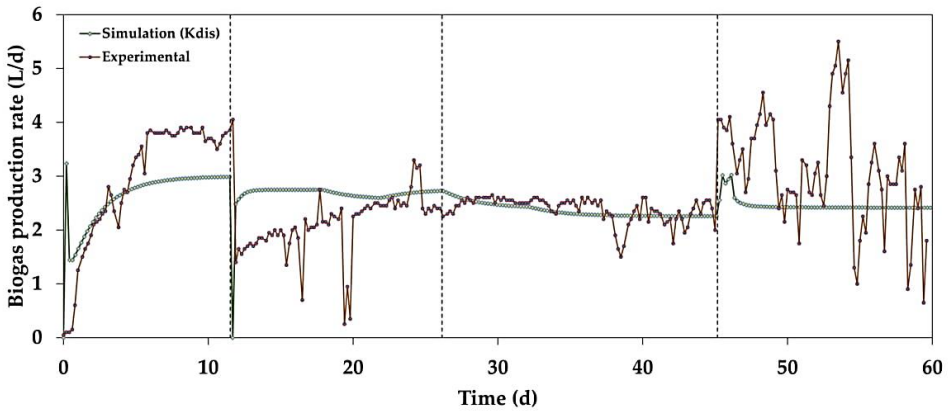


**Fig. 5.** Biogas flow rate when $K_{dis}$ and Xc are used (Mode 1 simulation).

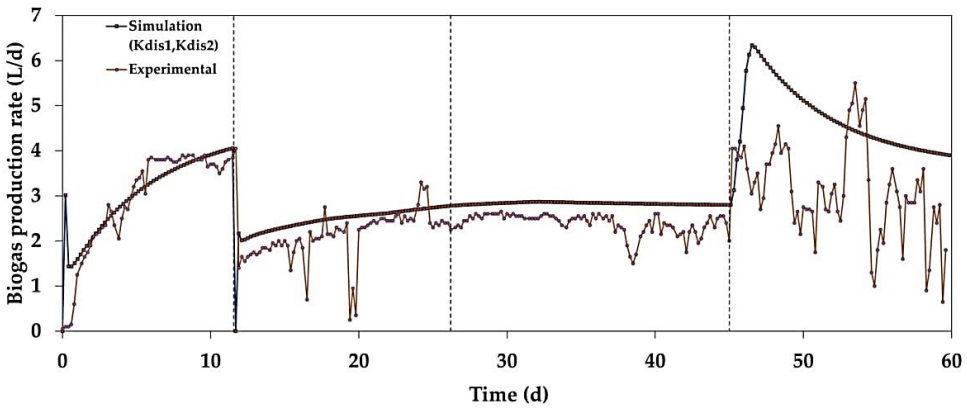


**Fig. 6.** Biogas flow rate when $K_{dis1}$, $K_{dis2}$, Xc1 and Xc2 are used (Mode 2 simulation).

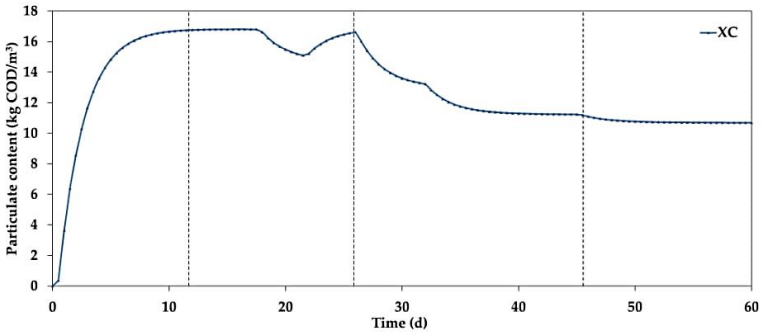


**Fig. 7.** Particulate content in Mode 1 simulation.

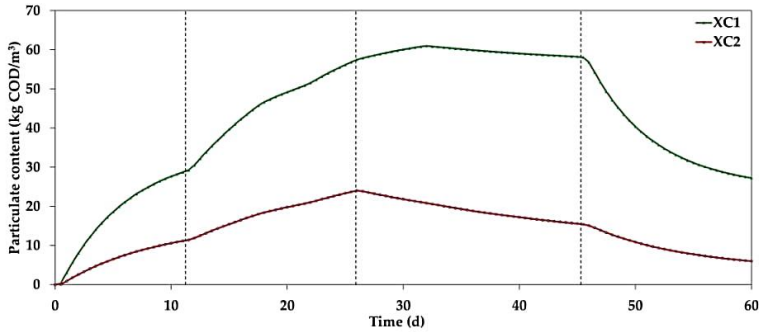


**Fig. 8.** Particulate content in Mode 2 simulation.

after the implementation of estimated parameters is presented in Appendix B.

## 4. Conclusions

We have carried out anaerobic digestion experiments using lab-scale UASB reactor on two sets of samples with varying level of suspended solids and digestion temperature. Our goals were to examine influences of temperature and particulate content on sludge bed anaerobic digestion. Based on the experiments and simulations carried out and the results obtained, we have made the following conclusions:

- Increase in temperature increased the overall biogas production in both high and low particulate content substrates but the temperature effect was stronger on high particle content substrates.
- Disintegration and hydrolysis of suspended solids were significantly enhanced by temperature increase from 25 to 35 °C.
- Methane yield were significantly higher for low particulate sample (CF) than high particulate sample (RF) at both 25 and 35 °C.
- Particulate and COD removal efficiencies were improved at higher temperature. $COD_{total}$ removal efficiency improved from 44 % at 25 °C to 73 % at 35 °C for high particulate substrate and from 43 % at 25 °C to 54 % at 35 °C for low particulate substrate. $COD_{soluble}$ removal efficiencies were also improved at higher temperatures but they were approximately similar for both high and low particulate substrates.
- Classifying particulates into fast and slow disintegrating and applying temperature dependent disintegration constant values ($K_{dis}$) fit the experimental data better than the traditional ADM1 method of simulation.

**Acknowledgement**

The authors would like to thank Dr. Dag Øvrebø for his invaluable help during sample collection process.

**Funding**

This research was part of a PhD project funded by Interreg BioGas2020.

**Conflict of interest**

The authors declare no conflict of interest.

## Appendix A. Sensitivity function of biogas production

The absolute-relative sensitivity function was used in Aquasim software to measure the absolute change in y for 100 % change in p. In this case, y is biogas production and p is parameter $Ea_1$ or $Ea_2$. It was calculated according to the following equation.

$$\text{Absolute} - \text{Relative sensitivity function} = \mathrm{p}\frac{\partial \mathrm{y}}{\partial \mathrm{p}} \tag{A.1}$$

In the tables below, the sensitivity function (SensAR) is expressed in: root mean square (r(av($\text{SensAR}^2$))) and mean absolute sensitivity (av(| SensAR |)) and for error contributions as: (av(| ErrCont |)) . `S_CH4`, `S_CO2` and `S_H2` are concentrations of $CH_4$, $CO_2$ and $H_2$ respectively.

Table A1: Variables ranked based on sensitivity to $Ea_1$ and $Ea_2$ in the headspace.

| **Parameter** | r(av(SensAR$^2$)) | | av(\| SensAR \|) | | av(\| ErrCont \|) | |
|---|---|---|---|---|---|---|
| | $Ea_1$ | $Ea_2$ | $Ea_1$ | $Ea_2$ | $Ea_1$ | $Ea_2$ |
| S_CH4 | 0.286 | 0.163 | 0.085 | 0.068 | 0 | 0 |
| S_CO2 | 0.004 | 0.003 | 0.001 | 0.001 | 0 | 0 |
| S_H2 | 0 | 0 | 0 | 0 | 0 | 0 |

Table A2: Variables ranked based on sensitivity to $Ea_1$ and $Ea_2$ in the bulk reactor.

| **Parameter** | r(av(SensAR$^2$)) | | av(\| SensAR \|) | | av(\| ErrCont \|) | |
|---|---|---|---|---|---|---|
| | $Ea_1$ | $Ea_2$ | $Ea_1$ | $Ea_2$ | $Ea_1$ | $Ea_2$ |
| S_CH4 | 0.233 | 0.085 | 0.025 | 0.016 | 0 | 0 |
| S_CO2 | 0.005 | 0.003 | 0.001 | 0.001 | 0 | 0 |
| S_H2 | 0 | 0 | 0 | 0 | 0 | 0 |
| **Other parameters** | | | | | | |
| Xc1 | 75.9 | 71.5 | 31.5 | 34.8 | 0 | 0 |
| Xc2 | 15.6 | 12.5 | 10.6 | 7.6 | 0 | 0 |

## Appendix B. Simulation before and after parameter estimation

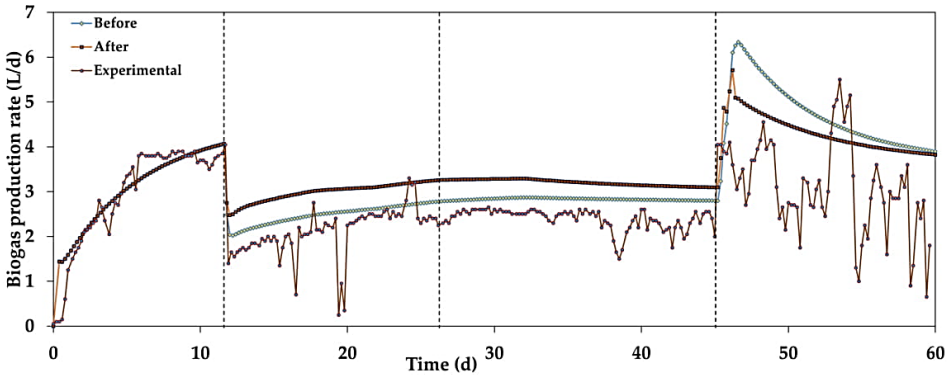


**Fig. B1.** Comparison of the simulation before and after the implementation of parameter estimation.

## References

[1] FAO, Nitrogen inputs to agricultural soils from livestock manure. new statistics, Tech. Rep. Rome, Italy, FAO (2018).

[2] G. Zeeman, W. T. Sanders, K. Y. Wang, G. Lettinga, Anaerobic treatment of complex wastewater and waste activated sludge—application of an upflow anaerobic solid removal (uasr) reactor for the removal and prehydrolysis of suspended cod, Water science and technology 35 (10) (1997) 121–128 (1997).

[3] W. H. Bergland, C. Dinamarca, M. Toradzadegan, A. S. R. Nordgård, I. Bakke, R. Bakke, High rate manure supernatant digestion, water research 76 (2015) 1–9 (2015).

[4] N. Mahmoud, G. Zeeman, H. Gijzen, G. Lettinga, Solids removal in upflow anaerobic reactors, a review, Bioresource technology 90 (1) (2003) 1–9 (2003).

[5] D. J. Batstone, J. Keller, I. Angelidaki, S. Kalyuzhnyi, S. Pavlostathis, A. Rozzi, W. Sanders, H. Siegrist, V. Vavilin, The iwa anaerobic digestion model no 1 (adm1), Water Science and Technology 45 (10) (2002) 65–73 (2002).

[6] V. A. Vavilin, B. Fernandez, J. Palatsi, X. Flotats, Hydrolysis kinetics in anaerobic degradation of particulate organic material: An overview, Waste Management 28 (6) (2008) 939–951 (2008). arXiv:bit.20858, doi:10.1016/j.wasman.2007.03.028.

[7] V. A. Vavilin, S. V. Rytov, L. Y. Lokshina, A description of hydrolysis kinetics in anaerobic degradation of particulate organic matter, Bioresource Technology 56 (2–3) (1996) 229–237 (1996). doi:10.1016/0960-8524(96)00034-X.

[8] E. A. Cazier, E. Trably, J. P. Steyer, R. Escudie, Biomass hydrolysis inhibition at high hydrogen partial pressure in solid-state anaerobic digestion, Bioresource Technology 190 (2015) 106–113 (2015). doi:10.1016/j.biortech.2015.04.055.
URL http://dx.doi.org/10.1016/j.biortech.2015.04.055

[9] C. Lin, T. Noike, K. Sato, J. Matsumoto, Temperature characteristics of the methanogenesis process in anaerobic digestion, Water Science and Technology 19 (1-2) (1987) 299–300 (1987).

[10] G. Lettinga, S. Rebac, G. Zeeman, Challenge of psychrophilic anaerobic wastewater treatment, TRENDS in Biotechnology 19 (9) (2001) 363–370 (2001).

[11] H. Ge, P. D. Jensen, D. J. Batstone, Relative kinetics of anaerobic digestion under thermophilic and mesophilic conditions, Water Science and Technology 64 (4) (2011) 848–853 (2011).

[12] Y. Z. Chi, Y. Y. Li, M. Ji, H. Qiang, H. W. Deng, Y. P. Wu, Mesophilic and thermophilic digestion of thickened waste activated sludge: A comparative

study, in: Advanced Materials Research, Vol. 113, Trans Tech Publ, 2010, pp. 450–458 (2010).

[13] A. Veeken, B. Hamelers, Effect of temperature on hydrolysis rates of selected biowaste components, Bioresource technology 69 (3) (1999) 249–254 (1999).

[14] A. G. Hashimoto, Ammonia inhibition of methanogenesis from cattle wastes, Agricultural Wastes 17 (4) (1986) 241–261 (1986). doi:10.1016/0141-4607(86)90133-2.

[15] T. J. Lukáš KRÁTKÝ, The effect of mechanical disintegration on the biodegradability of wheat strawle, inżynieria i aparatura chemiczna 52 (3) (2013) 202–203 (2013).

[16] A. P. H. Association, A. W. W. Association, Standard methods for the examination of water and wastewater, American public health association, 1989 (1989).

[17] P. Reichert, Aquasim a tool for simulation and data analysis of aquatic systems, Water Science and Technology 30 (2) (1994) 21 (1994).

[18] A. J. Kunov-Kruse, A. Riisager, S. Saravanamurugan, R. W. Berg, S. B. Kristensen, R. Fehrmann, Revisiting the Brønsted acid catalysed hydrolysis kinetics of polymeric carbohydrates in ionic liquids by in situ ATR-FTIR spectroscopy, Green Chemistry 15 (10) (2013) 2843–2848 (2013). doi:10.1039/c3gc41174e.

[19] A. Galí, T. Benabdallah, S. Astals, J. Mata-Alvarez, Modified version of ADM1 model for agro-waste application, Bioresource Technology 100 (11) (2009) 2783–2790 (2009). doi:10.1016/j.biortech.2008.12.052.
URL http://dx.doi.org/10.1016/j.biortech.2008.12.052

[20] K. J. Chae, A. Jang, S. K. Yim, I. S. Kim, The effects of digestion temperature and temperature shock on the biogas yields from the mesophilic

anaerobic digestion of swine manure, Bioresource Technology 99 (1) (2008) 1–6 (2008). doi:10.1016/j.biortech.2006.11.063.

[21] P. Reichert, Aquasim 2.0-user manual, computer program for the identification and simulaion of aquatic systems, Switzerland: Swiss Federal Institute for Environmental Science and Technology (EWAG) (1998).

## Conference poster:

# Image analysis to measure settling characteristics of granular sludge.

Fasil a. Tassew, Wenche Bergland, Carlos Dinamarca and Rune Bakke

Presented to: Granular sludge conference, IWA biofilms, Delft, Netherlands (2018)

University College of Southeast Norway

the international water association

# Image analysis to measure settling characteristics of granular sludge

F.A.Tassew*, W.H.Bergland, C. Dinamarca, R.Bakke

Department of Process, Energy and Environmental Technology
University College of Southeast Norway
Kjølnes ring 56
3918 Porsgrunn
Norway
fasil.a.tassew@usn.no

## Introduction

Granule characteristics may change with time and growth conditions. It is important to monitor such changes, especially settling behavior to avoid biomass loss. The objective of this paper is to establish a method that uses microscopic image analysis as a tool to monitor morphology and use this to estimate settling velocity of granules.

## Material and Methods

Five samples were used: two from industries and three from lab reactors ('Top', 'Middle', 'Bottom'). Images of at least 200 granules were taken using a stereomicroscope. Image processing was used to generate data about perimeter (P), area and shape factor (SF) of granules (equations 1 - 4). Equivalent diameter ($D_g$) of granules were calculated and used to estimate theoretical settling velocity of granules ($V_t$). A high-speed camera (50 fps) and a settling column were used to measure experimental settling velocity.

*Figure 1. Shape factor measurement examples showing centroid and eight radii for each granule, with increasing shape factor left to right.*

$$D_g = \frac{P}{\pi}\left[\frac{1}{1+\sqrt{\frac{2\pi SF}{P}}}\right] \quad (1) \qquad V_t = 0.781 f_w \left[\frac{D_g^{1.6}(\delta_g - \delta_f)}{\delta_g^{0.4}\mu_f^{0.6}}\right]^{0.714} \quad (2)$$

$$SF = \sqrt{\frac{1}{N-1}\sum_{i=1}^{N}|A_i - A_{mean}|^2} \quad (3) \qquad A_{mean} = \frac{1}{N}\sum_{i=1}^{N} A_i \quad (4)$$

$A_{mean}$ average distance from centroid to perimeter
$A_i$ distance from centroid to perimeter
$f_w$ correction factor for wall effect
$N$ number of distances measured
$g$ notation for granule
$f$ notation for fluid
$\mu$ viscosity
$\delta$ density

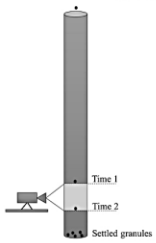


*Figure 2. Settling column and camera setup*

## Result and discussions

*All samples show different size distributions, but similar pattern.*

*Industry-2 and Top (from the lab reactor) have the most similar size distributions, while Industry-1 has much larger granules than the other samples.*

*Granule size increased from top to bottom in the lab scale reactor.*

| Sample | δ (Kg/m³) | Value | Mean | Median | St.Dv |
|---|---|---|---|---|---|
| Industry-1 | 1015 | Measured | 62 | 62 | 12 |
| | | Calculated | 59 | 59 | 19 |
| Top | 1075 | Measured | 45 | 43 | 12 |
| | | Calculated | 46 | 44 | 13 |
| Middle | 1075 | Measured | 59 | 52 | 23 |
| | | Calculated | 57 | 58 | 17 |
| Bottom | 1070 | Measured | 68 | 60 | 24 |
| | | Calculated | 63 | 60 | 16 |
| Industry-2 | 1070 | Measured | 63 | 58 | 19 |
| | | Calculated | 67 | 58 | 29 |

*Table 1. Theoretical and experimental settling velocities and densities of granules.*

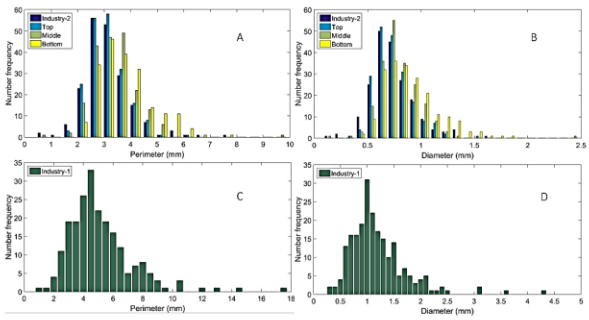


*Figure 3. Size distribution of granules based on perimeter and diameter: A and B shows granules from lab reactor and Industry-2 while C and D shows Industry-1 granules.*

- *The Top sample has the lowest calculated and measured settling velocity values. Both Industry samples and Bottom have settling velocities near 60 m/h.*
- *Settling velocity variations are best calculated for the Top sample while the calculations overestimate variations in the industry samples and underestimates in the Bottom and Middle samples.*
- *The relative errors between theoretical and experimental mean settling velocities are less than 8.5 % for all samples.*
- *Measured and calculated values increased with increasing Reynolds number.*
- *Agreement between the measured and calculated values are weaker at higher Re values*

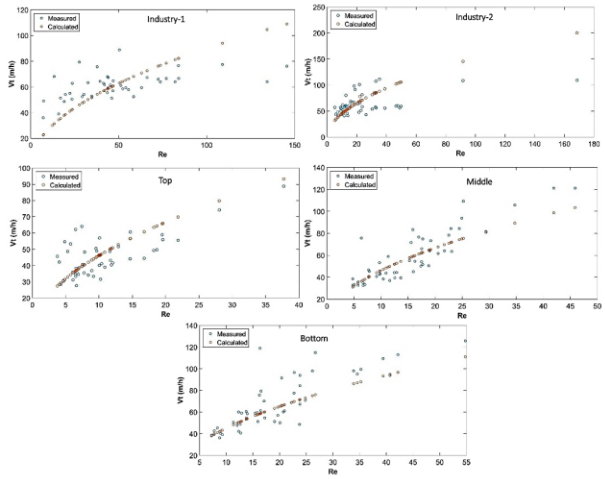


*Figure 4. Comparison of theoretical and experimental settling velocities of granules with respect to Reynolds number.*

## Conclusions

Based on the above findings the following conclusions were made:

- Granules' settling velocity depends on shape in addition to size and density.
- A shape factor and equivalent diameter, both measured by analysis of images from a stereomicroscope, can be used to calculate settling velocities of granule samples comparable to measured velocities.
- This method can be an efficient way to monitor settling velocity variations.

## References

Ahn, Y.-H. and Speece, R. E. (2003). Settleability assessment protocol for anaerobic granular sludge and its application. Water SA, 29(4):419–426.

Alpenaar, A. and granular Sludge, A. (1994). Characterization and Factors Affecting Its Functioning. PhD thesis, PhD Thesis, Wageningen University, The Netherlands.

Alves, M., Cavaleiro, A. J., Ferreira, E. C., Amaral, A. L., Mota, M., da Motta, M., Vivier, H., and Pons, M.-N. (2000). Characterisation by image analysis of anaerobic sludge under shock conditions. Water science and technology, 41(12):207–214.

Arsenijevi´c, Z. L., Grbav˘ci´c, Ž., Gari´c-Grulovi´c, R., and Bošković-Vragolovi´c, N. (2010). Wall effects on the velocities of a single sphere settling in a stagnant and counter-current fluid and rising in a co-current fluid. Powder Technology, 203(2):237–242.

Ataide, C., Pereira, F., and Barrozo, M. (1999). Wall effects on the terminal velocity of spherical particles in newtonian and nonnewtonian fluids. Brazilian Journal of Chemical Engineering, 16(4):387–394.

Bellouti, M., Alves, M., Novais, J., and Mota, M. (1997). Flocs vs granules: differentiation by fractal dimension. Water Research, 31(5):1227– 1231.

Acknowledgement: This work is part of a PhD project and supported by Interreg Biogas2020 project. The authors would like to thank Samee Maharjan for helping with image analysis and Joachim Lundberg for providing high speed digital camera.

Interreg Öresund-Kattegat-Skagerrak European Regional Development Fund — EUROPEAN UNION — BioGas2020

# Appendix A: Matlab code for image preprocessing

This Matlab code prepares the image file for further processing.

```
I= imread('image.jpg');

I= rgb2gray(I);

I2 = imadjust(I);

level = graythresh(I2);

bw = im2bw(I2,level);

bw = bwareaopen(bw, 50);

imshow(bw)

cc = bwconncomp(bw, 4)

cc.NumObjects
```

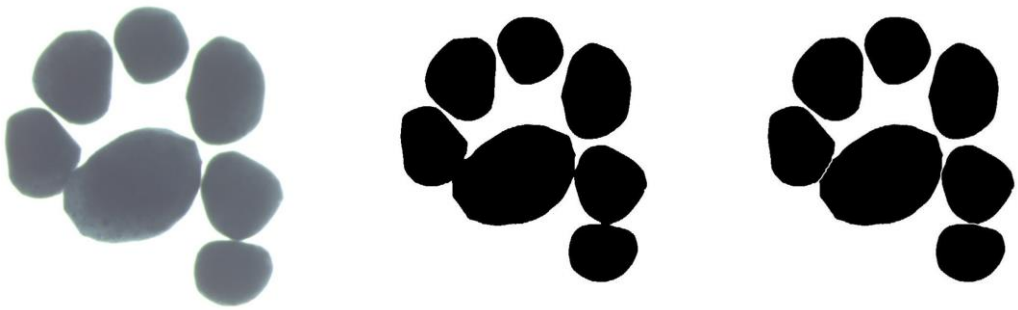

**Figure A.1: An example of the progression of the granule image from original to preprocessed file.**

# Appendix B: Matlab code for image processing

After image preprocessing the Matlab code below generates data about perimeter, shape factor, and area from the preprocessed file. (See Figure A.2 )

```
rgbImage = imread('preprocessed_image.jpg');

grayImage = rgb2gray(rgbImage);

fontSize =12;

subplot(2, 2, 1);

imshow(grayImage);

title('Original Image', 'fontSize', fontSize);

    % chage to binary

thresholdValue = 200;

binaryImage = grayImage < thresholdValue;

    % Do a "hole fill" to get rid of any background pixels inside the object.

binaryImage = imfill(binaryImage, 'holes');

    % Display the binary image.

subplot(2, 2, 1);

imagesc(binaryImage);

colormap(gray);

title('Binary Image', 'fontSize', fontSize);

    % Label each object so we can make measurements of it
```

```
[labeledImage, numberOfRegions] = bwlabel(binaryImage, 8);

subplot(2, 2, 2);

coloredLabels = label2rgb(labeledImage, 'hsv', 'k', 'shuffle');

        % pseudo random color labels

imshow(coloredLabels);

title('Labeled Binary Image', 'fontSize', fontSize);

        % locate the centroid of the object

measurements = regionprops(binaryImage, 'Centroid','Area','Perimeter');

        % 'Centroid' – 1–by–Q vector that specifies the center of mass of the region.

Perimeterinmm = ([measurements.Perimeter])*(8.54/686);

        % the correction factor for perimeterinmm depends on the  image pixel size

          in this case (686)  and calibrated distance the image represents in this case

           it is 8.54 mm.

        % mm/1198 pixels

Areainmm2 = ([measurements.Area])*((8.54/686).^2);

centroids = [measurements.Centroid];

centroidx = centroids(1:2:end);

centroidy = centroids(2:2:end);

        % Plot the centroids of each object

subplot(2, 2, 3);
```

```
imshow(binaryImage);
title('Centroid Locations', 'fontSize', fontSize);
hold on
for k = 1 : numberOfRegions
  plot(centroidx(k), centroidy(k), 'b*');
end
        % Define object boundaries
boundaries = bwboundaries(binaryImage);
numberOfBoundaries = size(boundaries, 1);
for k = 1 : numberOfBoundaries
  thisBoundary = boundaries{k};
  boundaryx = thisBoundary(:, 2);
  boundaryy = thisBoundary(:, 1);
  plot(boundaryx, boundaryy, 'r–', 'LineWidth', 1);
            % compute distances from boundaries to edge.
  allDistances = sqrt(((boundaryx – centroidx(k))*(8.54/686)).^2 + ((boundaryy – centroidy(k))*(8.54/686)).^2);
          % depending on image dimension 8.54/686 is a correction factor for pixels
          to mm conversion: allDistances = sqrt(((boundaryx – centroidx(k))*(
          8.54/686)).^2 + ((boundaryy – centroidy(k))*( 8.54/686)).^2);
  STDV(k) = std(allDistances);
```

```
    AVDIST(k) = mean(allDistances);

            % Find farthest point, max distance.

    [maxDistance(k), indexOfMax] = max(allDistances);

            % Drawline

    x1 =  centroidx(k);

    y1 =  centroidy(k);

    x2 = boundaryx(indexOfMax);

    y2 = boundaryy(indexOfMax);

    line([x1, x2], [y1, y2], 'Color', [1 0 1], 'LineWidth', 1);

end

ShapeFactor = num2cell(STDV);

aaa=[Perimeterinmm, Areainmm2, AVDIST, STDV];

xlswrite('PSD from Matlab_brgrd.xlsx',transpose(ShapeFactor),'266a','A1');

xlswrite('PSD from Matlab_brgrd.xlsx',transpose(Perimeterinmm),'266a','B1');

xlswrite('PSD from Matlab_brgrd.xlsx',transpose(Areainmm2),'266a','C1');

hold off;
```

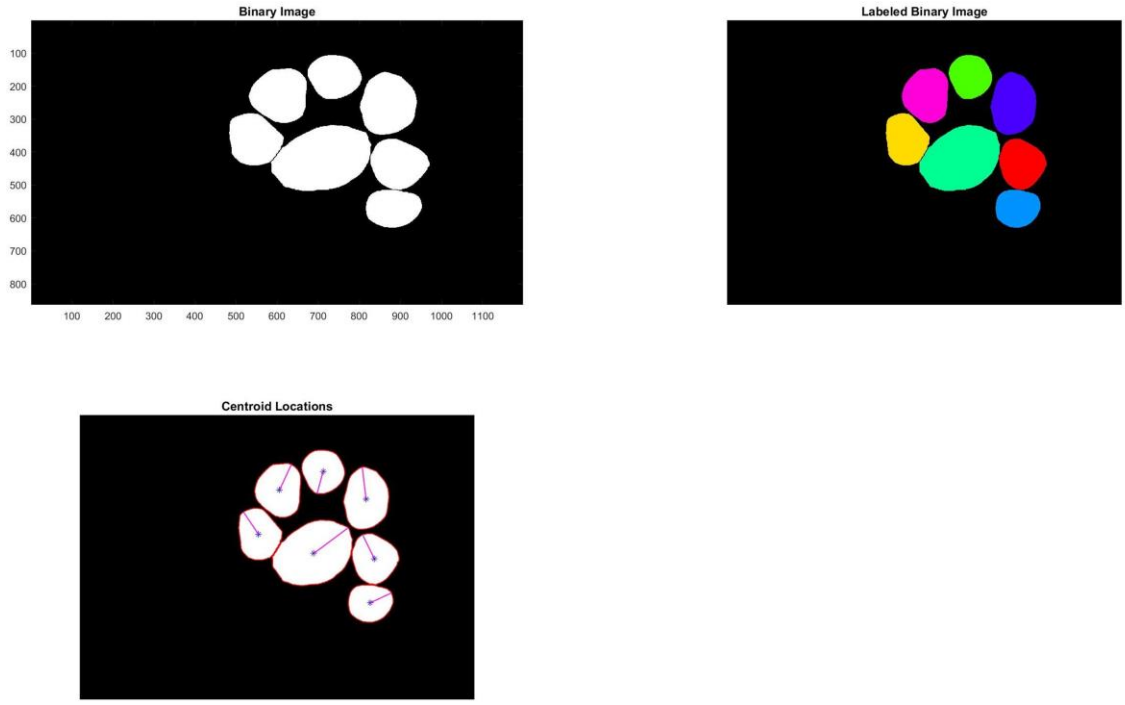


**Figure A.2: Visualising data generation from preprocessed images using Matlab code.**

Doctoral dissertation no. 56
**2020**

—

**Capabilities of anaerobic granular sludge bed process for the treatment of particle-rich substrates**

Dissertation for the degree of Ph.D

—

Fasil Ayelegn Tassew

—

ISBN: 978-82-7206-542-2 (print)
ISBN: 978-82-7206-543-9 (online)

usn.no